

## Curriculum Vitae

**Lisa Marie Leung**

Ph.D. Candidate

University of Maryland, Baltimore

[lisaleung6@gmail.com](mailto:lisaleung6@gmail.com)

**Date:** June 22, 2017

---

### EDUCATION

---

**Ph.D., Molecular Microbiology & Immunology**, University of Maryland, Baltimore, Baltimore, MD, 2012-2017

**B.A., Biology**, St. Mary's College of Maryland, St. Mary's City, MD, 2000-2004

---

### PUBLICATIONS

---

Trudeau, M. C., **L. M. Leung**, E. Roti Roti, and G. A. Robinson. 2011. hERG1a N-terminal eag domain-containing polypeptides regulate homomeric hERG1b and heteromeric hERG1a/hERG1b channels: A possible mechanism for Long QT syndrome. *The Journal of General Physiology*. 138 (6): 581.

Liu, Y-Y., C. E. Chandler, **L. M. Leung**, C. L. McElheny, R. T. Mettus, R. M. Q. Shanks, J-H. Liu, D. R. Goodlett, R. K. Ernst, and Y. Doi. 2017. Structural Modifications of Lipopolysaccharide Conferred by *mcr-1* in Drug-Resistant Gram-Negative ESKAPE Pathogens. *Antimicrobial Agents and Chemotherapy*. doi: AAC.00580-17.

[May 2017 accepted for publication to *Scientific Reports*] **Leung, L. M.**, W. E. Fondrie, Y. Doi, J. K. Johnson, D. K. Strickland, R. K. Ernst, and D. R. Goodlett. Identification of the ESKAPE pathogens by mass spectrometric analysis of microbial membrane glycolipids.

[June 2017 accepted for publication to *The Journal of Antimicrobial Chemotherapy*] **Leung, L. M.**, V. S. Cooper, Q. Guo, M. P. Pacey, C. L. McElheny, R. T. Mettus, D. A. Rasko, D. R. Goodlett, R. K. Ernst, and Y. Doi. Structural modifications of lipopolysaccharide in colistin-resistant, KPC-producing *Klebsiella pneumoniae*.

[April 2017 submitted for publication to the *International Journal of Mass Spectrometry*] Liang, T., T. Schneider, S. H. Yoon, B. L. Oyler, **L. M. Leung**, G. Yen, Y. Huang, R. K. Ernst, E. Nilsson, and D. R. Goodlett. Performance Characterization of Surface Acoustic Wave Nebulization for Lipid A Mass Spectrometric Analysis.

---

## PENDING PUBLICATIONS

---

[Manuscript to be submitted to *The Journal of Experimental Medicine*] Crawford, M. A., D. J. Fisher, **L. M. Leung**, S. Lomonaco, M. W. Allard, C. Lascols, A. Cannatelli, T. Giani, G. M. Rosso, Y. Doi, M. W. Allard, S. K. Sharma, E. Khan, D. R. Goodlett, R. K. Ernst, and M. A. Hughes. CXC Chemokines Exhibit Antimicrobial Activity against Multidrug-Resistant Gram-Negative Pathogens.

[Manuscript in preparation] **Leung, L. M.**, C. L. McElheny, Y. Doi, D. R. Goodlett, and R. K. Ernst. Characterization of *Acinetobacter* spp. Isolates from a Large Cohort of Patients and Colistin Resistance Monitoring Following Colistimethate Treatment.

---

## PRESENTATIONS

---

**Leung, L. M.**, D. R. Goodlett, and R. K. Ernst. Characterization of LPS modifications in select antibiotic-resistant Gram-negative bacteria using Surface Acoustic Wave Nebulization Mass Spectrometry. Poster presented at: American Society for Mass Spectrometry 63<sup>rd</sup> Annual Conference; 2014 Jun 15-19; Baltimore, MD.

**Leung, L. M.**, D. R. Goodlett, and R. K. Ernst. Zero passage analysis of *Escherichia coli* from complex biological fluids by MALDI-TOF mass spectrometry. Poster presented at: The 2015 Mid-Atlantic Microbial Pathogenesis Meeting; 2015 Jan 25-27; Wintergreen, VA.

**Leung, L. M.**, T. Liang, M. Wilson, S. H. Yoon, R. Ernst, and D. Goodlett. A Cartesian Product Approach to Lipid A Structure Identification. Poster presented at: American Society for Mass Spectrometry 64<sup>rd</sup> Annual Conference; 2015 May 31-Jun 4; St. Louis, MO.

**Leung, L. M.**, D. R. Goodlett, and R. K. Ernst. Zero passage analysis of *Escherichia coli* from complex biological fluids by MALDI-TOF mass spectrometry. Talk presented at: The 9<sup>th</sup> Summer Workshop on Mass Spectrometry in Biotechnology and Medicine; 2015 July 5-11; Dubrovnik, Croatia.

**Leung, L. M.**, B. L. Oyler, D. R. Goodlett, and R. K. Ernst. Structural characterization of lipid biomarkers from *Staphylococcus aureus* following microextraction for mass spectrometric phenotyping. Poster presented at: American Society for Mass Spectrometry 65<sup>th</sup> Annual Conference; 2016 Jun 5-9; San Antonio, TX.

**Leung, L. M.**, W. E. Fondrie, D. R. Goodlett, and R. K. Ernst. Identification of the ESKAPE Pathogens by Mass Spectrometric Analysis of Microbial Membrane Glycolipids. Poster presented at: The 2017 Mid-Atlantic Microbial Pathogenesis Meeting; 2017 Feb 12-14; Wintergreen, VA.

**Leung, L. M.,** W. E. Fondrie, D. R. Goodlett, and R. K. Ernst. Identification of the ESKAPE Pathogens by Mass Spectrometric Analysis of Microbial Membrane Glycolipids. Poster talk presented at: American Society for Microbiology ASM Microbe 2017; 2017 Jun 1-5; New Orleans, LA.

---

## **PATENTS**

---

**Provisional Patent,** Author on a pending application, US application 62/281,523 entitled “Diagnostic Identification of Bacterial Species Directly from Blood Culture Bottles Using MALDI-TOF Mass Spectrometry”; Date of filing: January 26, 2016.

---

## **RESEARCH AND PROFESSIONAL EXPERIENCE**

---

**GRADUATE RESEARCH ASSISTANT** August 2012 – June 2017

**Molecular Microbiology & Immunology**

**University of Maryland Graduate Program in Life Sciences**

“Microbial Membrane Glycolipids as Diagnostic Markers of Infection”

*Advisors: David Goodlett, Ph.D. and Robert Ernst, Ph.D.*

- Develop and optimize lipid extraction and purification methodologies for mass spectrometric analysis
- Acquire mass spectra from glycolipids extracted from numerous microorganisms in the development of a glycolipid mass spectral database with a focus on the ESKAPE pathogens and top microorganisms implicated in bacteremia and UTI
- Adapt a software platform to identify and characterize unknown pathogens by comparison of their glycolipid mass spectral profiles to those within the reference database

**LAB RESEARCH TECHNICIAN** August 2004 – August 2013

**Department of Physiology**

**University of Maryland School of Medicine**

*PI: Matthew Trudeau, Ph.D.*

- Managed the organization of the lab including ordering equipment and supplies; bookkeeping; preparation of media, gels, buffers, and solutions
- Performed a variety of molecular biology techniques including plasmid subcloning (PCR, digestion, ligation, transformation), DNA/protein extraction from bacterial and mammalian cells, and quantitative and qualitative analysis of proteins via SDS-PAGE and Western blot
- Harvested oocytes from *Xenopus laevis* (African clawed frog) for RNA microinjection and electrophysiological recordings

**UNDERGRADUATE DISSERTATION** Summer 2003 – Spring 2004

**Department of Biology**

**St. Mary's College of Maryland**

“Host Determination of *Escherichia coli* by Antibiotic Resistance Analysis”

*Mentor: Jeffrey Byrd, Ph.D.*

- Isolated *E. coli* from environmental samples in order to determine the source of fecal coliform pollution by comparison of antibiotic resistance profiles to a library of *E. coli* from known sources
- Conducted discriminant analyses of these profiles, a complex, multivariate statistical method that determines patterns within large data sets

---

## AWARDS AND HONORS

---

**ASM Student and Post Doctoral Award**, American Society for Microbiology travel award for my ASM Microbe abstract and gave a poster talk and poster presentation at ASM Microbe 2017; Date of presentations: June 4, 2017

**Graduate Translational Research Award**, Outstanding translational research from the UMB Office of Technology Transfer at the 39<sup>th</sup> Annual Graduate Research Conference, an internal conference featuring presentations from students and postdocs from all graduate programs; Date of presentation: March 13, 2017

**Travel Award**, American Society for Mass Spectrometry travel award from the Washington-Baltimore Mass Spectrometry Discussion Group for my ASMS abstract and gave an oral presentation at the annual post-ASMS WBMSDG meeting; Date of presentation: June 13, 2016

**Outstanding Presentation Award**, Best oral presentation at the 38<sup>th</sup> Annual Graduate Research Conference, an internal conference featuring presentations from students and postdocs from all graduate programs; Date of presentation: March 25, 2016

**Presentation Winner**, Best oral and poster presentations at the 9<sup>th</sup> Mass Spectrometry in Biotechnology and Medicine Summer School, an MS training event with approximately 60 participants; Dates presented: July 5-11, 2015

---

## SOCIETY MEMBERSHIPS

---

**American Society for Microbiology**, National, Student Member 2015-present

**American Society for Microbiology Maryland Branch**, Local, Student Member 2012-present

**American Society for Mass Spectrometry**, National, Student Member 2014-present

---

## TEACHING EXPERIENCE

---

**Trained all new members of Dr. Trudeau's Lab, Dept. of Physiology, University of Maryland School of Medicine**

- Trained five students, two postdocs, and another lab tech in all the molecular biology techniques as Dr. Trudeau's lab manager

**Spent three semesters as a Teaching Assistant for "Principles of Biology Lab", the introductory lab course for biology majors, St. Mary's College of Maryland**

- Conducted lab, wrote and graded quizzes, prepped experiments, and provided individual guidance to students during lab as an undergraduate student

---

## **UNIVERSITY SERVICE**

---

**Organized student-led comprehensive exam preparation for junior graduate students for two semesters**

- Determined outline for the month-long study program leading up to the exam, administered weekly mock exams, and recruited senior students to participate in mock exams

**Organized the Microbial Pathogenesis Journal Club for two semesters, student-organized weekly meetings with program faculty, staff and students to discuss recent publications in the field**

- Scheduled presenters and recruited representatives from life science companies for sponsorships

## **Abstract**

**Title of Dissertation:** Microbial Membrane Glycolipids as Diagnostic Markers During Infection

**Lisa Marie Leung, Doctor of Philosophy, 2017**

**Dissertation Directed by:** Robert K. Ernst, Professor, Department of Microbial Pathogenesis, School of Dentistry -and- David R. Goodlett, Professor, Department of Pharmaceutical Sciences, School of Pharmacy

The worldwide impacts of infectious diseases drive the development of novel diagnostics and therapeutics to combat them. Rapid and accurate diagnoses of bacterial infections enable clinicians to quickly initiate targeted antimicrobial chemotherapy, reducing patient morbidity and mortality. The advent of a mass spectrometry-based platform targeting bacterial proteins represents a new and promising technology that simplifies the clinical workflow and reduces time and cost from conventional methodologies. The approach makes identifications via unique protein mass spectra by comparison against a reference database of spectra from known sources. A wealth of research regarding essential glycolipids, which are found in abundance in microbial membranes, has revealed tremendous structural diversity among these molecules that is species- and often intraspecies-specific in response to environmental signals. This thesis introduces a novel diagnostic platform that takes advantage of this specificity to identify the ESKAPE pathogens via their unique glycolipid mass spectral fingerprint in a manner

similar to MS protein phenotyping. Importantly, differentiation on the basis of colistin susceptibility is demonstrated in select Gram-negative bacteria and conferred by the recently discovered plasmid-mediated *mcr-1* gene. The platform also detects and identifies organisms directly from patient specimens illustrating the potential for this platform to be culture-free. These capabilities offer significant advantages over protein typing, and the glycolipid library exists on the same instrumentation suggesting that the two approaches could complement each other offering an additively more powerful diagnostic platform.

Microbial Membrane Glycolipids as Diagnostic Markers During Infection

by  
Lisa M. Leung

Dissertation submitted to the Faculty of the Graduate School of the  
University of Maryland, Baltimore in partial fulfillment  
of the requirements for the degree of  
Doctor of Philosophy  
2017

## **PREFACE**

Herein I present my thesis research conducted for the past four years in the labs of Drs. Robert Ernst and David Goodlett. Truly though, the topic of the research represents the professional culmination of the last 18 years I have spent as a scientist, which began in my undergraduate. Then, I determined the source of fecal coliform bacteria in environmental samples by antibiotic resistance profiling, resistance profiles being unique between human, agricultural and wildlife sources. And today, I continue to investigate unique characteristics of microorganisms that allow us to identify them. In the work presented here, I develop and validate a novel diagnostic platform that utilizes mass spectrometric analysis of microbial membrane glycolipids as a means to identify bacteria during infection. The discovery that the complex glycolipids that reside in bacterial membranes are unique was hypothesized by Drs. Ernst and Goodlett over years of observation in elucidating the structures of lipopolysaccharide in Gram-negative organisms. Given my experience and interest in public health, I was fortunate to become the first person in their labs to investigate this hypothesis under my two co-advisors. I believe my work, under their guidance, provides definitive proof-of-concept of this novel platform that may one day, with continued work, have a real impact in the clinical microbiology laboratory.

To my mother, Beverley, and my aunt, Linda, who became the first in our family to go to college and went on to become a medical doctor and a college professor respectively, for showing me how to succeed as a woman in science.

## ACKNOWLEDGEMENTS

There are many people without which this work would not have been possible.

First and foremost, I would like to thank my thesis advisors, Dr. Goodlett and Dr. Ernst, who have been unrelenting in their support of me. I couldn't have asked for more student-focused mentors than Bob and Dave. They've given me many opportunities to learn, conference and collaborate. They have challenged me to become a better scientist and especially a better science writer, reading countless manuscript drafts, grant proposal drafts and conference abstracts. They have given me independence to conduct my own research and make my own decisions yet advice and guidance when I needed it. They have also been very emotionally supportive of me when I would struggle with the stresses of graduate school. Their mentorship gave me more than I could adequately express my gratitude for here. I look forward to our continued personal and professional relationship throughout the rest of my career.

I would like to thank the members of the Ernst and Goodlett labs for all their help. This dissertation would very much not have been possible without their scientific input and friendship. I would especially like to thank Will Fondrie for his above-and-beyond bioinformatics help on my flagship first author publication; Dr. Sung Hwan Yoon and Ben Oyler for help with mass spectrometric analyses and critical reading of my manuscripts; Tao Liang for collaborative efforts based on our similar research projects that allowed me to become a co-author on one of his publications; and, Dr. Alison Scott for all the professional advice and help navigating conferences. I would also like to thank my fellow students in my year for talking me down from many ledges over the past five years and being my companions and friends through this whole process. I am particularly thankful for Dr. Beth French and Dr. Jeff Freiberg who took the qualifying exam at the same time as me for study and emotional support during arguably the worse time in a graduate student's life.

I would like to thank my committee members for their valuable input and useful discussions during our committee meetings. I would especially like to thank my committee member, Dr. Mark Shirliff, for being one of my dissertation readers, for letting me rotate in his lab, and for serving as a reference during my post graduate job search. I would also like to thank my collaborators, Dr. Molly Hughes of the University of Virginia, Dr. J. Kristie Johnson of the University of Maryland Medical Center, and in particular Dr. Yohei Doi of the University of Pittsburgh for consultations and contribution of clinical strains and who is co-author on all of my three accepted publications during my time as a student.

Finally, I want to thank the Molecular Microbiology & Immunology program chair Dr. Bret Hassel, former chair Dr. Nick Carbonetti, and program coordinator June Green. The people in this program are friendly and truly student-oriented. They were happy to offer extra help and advice and were always patient with me. I would also like

to thank the MMI program itself and the University of Maryland Graduate School. I appreciate the program's rigor and the school's progressiveness: it was a great environment to prepare for the next phase of my professional career.

Thank to everyone for making this an amazing and valuable experience.

# TABLE OF CONTENTS

<b>PREFACE</b> .....	<b>iii</b>
<b>DEDICATION</b> .....	<b>iv</b>
<b>ACKNOWLEDGEMENTS</b> .....	<b>v</b>
<b>TABLE OF CONTENTS</b> .....	<b>vii</b>
<b>LIST OF TABLES</b> .....	<b>x</b>
<b>LIST OF FIGURES</b> .....	<b>xi</b>
<b>LIST OF ABBREVIATIONS</b> .....	<b>xiv</b>
<b>CHAPTER ONE: Mass Spectrometry-based Diagnostics for the Clinical Laboratory</b> .....	<b>1</b>
Abstract .....	1
The global impact of infectious disease.....	2
A guide to current diagnostics in the clinical laboratory .....	3
Mass spectrometry: A revolution in clinical diagnosis.....	13
MS-based clinical diagnostics – The last ten years .....	26
Final remarks and future directions .....	35
<b>CHAPTER TWO: Identification of the ESKAPE pathogens by mass spectrometric analysis of microbial membrane glycolipids</b> .....	<b>36</b>
Abstract .....	36
Introduction.....	37
Results.....	40
Glycolipid mass spectral library construction.....	40
Lipid extraction and MALDI-TOF-MS reproducibility .....	52
Species-specific signature ions differentiate all ESKAPE pathogens .....	55
Detection of antimicrobial resistance.....	60
Identification from polymicrobial mixtures.....	66
Direct identification from blood culture .....	68
Discussion.....	71
Materials and Methods.....	75

<b>CHAPTER THREE: Structural modification of lipopolysaccharide in colistin-resistant, KPC-producing <i>Klebsiella pneumoniae</i> .....</b>	<b>80</b>
Synopsis .....	80
Background .....	81
Methods .....	82
Results .....	85
Characteristics of clinical cases associated with colistin-resistant <i>K. pneumoniae</i> ..	85
Overview of the colistin-susceptible and resistant <i>K. pneumoniae</i> strains .....	87
Genetic changes consistent with colistin resistance .....	90
Identification of Ara4N addition to lipid A isolated from <i>K. pneumoniae</i> LPS .....	90
Discussion .....	97
<b>CHAPTER FOUR: Characterization of <i>Acinetobacter</i> spp. Isolates from a Large Cohort of Patients and Colistin Resistance Monitoring Following Colistimethate Treatment .....</b>	<b>100</b>
Abstract .....	100
Introduction .....	101
Results .....	103
Overview of <i>Acinetobacter</i> clinical isolates in this study .....	103
MIC determination of study isolates .....	106
Colistin susceptibility determination by MALDI-TOF .....	106
Susceptibility correlation between MIC methods and LA modification of <i>A. baumannii</i> LPS .....	110
Comparison of <i>Acinetobacter</i> isolates by MALDI-TOF .....	110
Discussion .....	113
Materials and Methods .....	116
<b>CHAPTER FIVE: Structural Modification of Lipopolysaccharide Conferred by <i>mcr-1</i> in Gram-Negative ESKAPE Pathogens .....</b>	<b>119</b>
Abstract .....	119
Introduction .....	120
Results .....	122
<i>mcr-1</i> confers colistin resistance in <i>E. coli</i> , <i>K. pneumoniae</i> and <i>A. baumannii</i> and reduced susceptibility in <i>P. aeruginosa</i> .....	122
Lipid A is modified by the addition of phosphoethanolamine in all species examined .....	124

Discussion.....	138
Methods.....	140
<b>CHAPTER SIX: Concluding Remarks.....</b>	<b>143</b>
The MS Glycolipidomic Library: A novel diagnostic platform .....	143
Introduction.....	143
The MS glycolipid library identified the ESKAPE pathogens .....	143
Colistin resistance is detected by glycolipid mass spectra.....	144
Feasibility studies for the potential development of the glycolipid library .....	145
Library module: Culture-free .....	146
Library module: Fungi .....	152
Future directions .....	155
Sample preparation, processing and analysis.....	155
Structural analyses .....	156
Computational model development .....	157
<b>REFERENCES.....</b>	<b>159</b>

## LIST OF TABLES

Table 2.1. List of all ESKAPE pathogen strains used in this study.....	43
Table 2.2. List of species, strains and mass spectra in Biotyper glycolipid library.....	49
Table 2.3. Similarity scores for small heat map dot product comparison.....	57
Table 2.4. MALDI Biotyper results for identifying <i>K. pneumoniae</i> and <i>A. baumannii</i> ..	65
Table 3.1. Characteristics and outcomes of patients with carbapenem and colistin-resistant <i>K. pneumoniae</i> .....	86
Table 3.2. Colistin MICs, lipid A modification and <i>mgrB</i> , <i>pmrAB</i> , <i>phoPQ</i> loci.....	88
Table 5.1. Minimum inhibitory concentrations of <i>mcr-I</i> -positive strains used in the study. .....	123
Table 5.2. <i>m/z</i> proposed structure assignments.....	129
Table 6.1. List of species isolated from urine.....	150
Table 6.2. List of fungal species in the glycolipid library.....	153

## LIST OF FIGURES

Figure 1.1. A clinical strategy for bacterial identification. ....	5
Figure 1.2. Overview of the typical workflow of the clinical laboratory. ....	12
Figure 1.3. Schematic representation of a MALDI-TOF mass spectrometer. ....	17
Figure 1.4. Present and future applications of MS in the clinical laboratory. ....	25
Figure 1.5. General structure and key features of Gram-positive and negative bacterial membranes. ....	30
Figure 1.6. Schematic representation of Gram-negative bacterial membrane and general structure of the essential glycolipid LPS. ....	31
Figure 1.7. Chemical structures of lipid A from different Gram-negative organisms. ....	32
Figure 2.1. Strategy for glycolipid-based mass spectrometry platform for pathogen identification. ....	42
Figure 2.2. Variability determination for <i>P. aeruginosa</i> . ....	53
Figure 2.3. Representative mass spectra from ESKAPE pathogens. ....	54
Figure 2.4. Dot product analysis of mass spectra for differentiation of ESKAPE pathogens. ....	56
Figure 2.5. MALDI-TOF MS of <i>K. pneumoniae</i> grown at different temperatures. ....	58
Figure 2.6. Dot product analysis with hierarchical clustering for multiple replicates per ESKAPE pathogen. ....	59
Figure 2.7. Consensus mass spectra of colistin-resistant and colistin-susceptible <i>A. baumannii</i> and <i>K. pneumoniae</i> . ....	62
Figure 2.8. MALDI-TOF-MS of <i>A. baumannii</i> and <i>K. pneumoniae</i> with differential colistin resistance. ....	63
Figure 2.9. Dot product scores between library consensus spectra and test spectra partitioned by colistin resistance. ....	64
Figure 2.10. Mass spectrum from a mixed sample of <i>S. aureus</i> NRS384, <i>K. pneumoniae</i> TBE818, and <i>P. aeruginosa</i> BE399. ....	67
Figure 2.11. Detection of <i>S. aureus</i> and <i>K. pneumoniae</i> from blood culture. ....	69
Figure 2.12. Mass spectra from <i>S. aureus</i> confirming mass shift in blood culture. ....	70

Figure 3.1. Genome-based phylogeny of the <i>K. pneumoniae</i> strains. ....	89
Figure 3.2. MALDI-TOF MS of <i>K. pneumoniae</i> with differential colistin susceptibility.	92
Figure 3.3. Lipid A structures with corresponding <i>m/z</i> values found in <i>K. pneumoniae</i> clinical isolates.....	93
Figure 3.4. Tandem mass spectrometry (MS <sup>2</sup> ) of <i>K. pneumoniae</i> A3 showing fragment ions of <i>m/z</i> 1955 and 1971. ....	94
Figure 3.5. Structures of <i>m/z</i> 1955 lipid A and fragment ions at <i>m/z</i> 1824, 1744, 1727, 1596, and 1580.....	95
Figure 3.6. Structures of <i>m/z</i> 1971 lipid A and fragment ions at <i>m/z</i> 1840, 1760, 1743, 1612, and 1596.....	96
Figure 4.1. Classification scheme according to identifications and MIC/MS determinations of clinical isolates collected during the course of this study.....	105
Figure 4.2. Lipid A structures of “signature” ions with corresponding <i>m/z</i> values.....	108
Figure 4.3. MALDI-TOF MS of <i>A. baumannii</i> with differential colistin susceptibility collected within-patient.....	109
Figure 4.4. MALDI-TOF MS comparison of representative <i>A. baumannii</i> complex isolates.....	112
Figure 5.1. MS analysis of strain <i>E. coli</i> YD626, WT and expressing <i>mcr-1</i> . ....	125
Figure 5.2. MS analysis of <i>E. coli</i> strains expressing <i>mcr-1</i> and <i>K. pneumoniae</i> strains expressing <i>mcr-1</i> . ....	126
Figure 5.3. MS analysis of <i>E. coli</i> strains and <i>K. pneumoniae</i> strains containing empty plasmid.....	128
Figure 5.4. MS analysis of <i>K. pneumoniae</i> strain ATCC 13883, WT and expressing <i>mcr-1</i> .....	131
Figure 5.5. MS analysis of <i>A. baumannii</i> strain SM1536, WT and expressing <i>mcr-1</i> ..	133
Figure 5.6. MS analysis of <i>A. baumannii</i> strains expressing <i>mcr-1</i> and <i>P. aeruginosa</i> strains expressing <i>mcr-1</i> . ....	134
Figure 5.7. MS analysis of <i>A. baumannii</i> strains and <i>P. aeruginosa</i> strains containing empty plasmid pMQ124. ....	135
Figure 5.8. MS analysis of <i>P. aeruginosa</i> strain 8542455, WT and expressing <i>mcr-1</i> ..	137

Figure 6.1. MALDI-TOF MS of <i>E. coli</i> W3110 lipid A in different blood types and blood culture bottles.....	148
Figure 6.2. Direct specimen analysis of microbial glycolipids from urine.....	151
Figure 6.3. Mass spectra from representative yeast species in the fungal library. ....	154

## LIST OF ABBREVIATIONS

<b>AMK</b>	Amikacin
<b>AMU</b>	Atomic mass units
<b>AR</b>	Antimicrobial resistance
<b>Ara4N</b>	4-amino-4-deoxy-L-arabinopyranose
<b>AST</b>	Antimicrobial susceptibility testing
<b>BAL</b>	Bronchoalveolar lavage
<b>BC</b>	Blood culture
<b>BSI</b>	Bloodstream infection
<b>CAMP</b>	Cationic antimicrobial peptide
<b>CDC</b>	Centers for Disease Control and Prevention
<b>CFU</b>	Colony forming unit
<b>CHCA</b>	$\alpha$ -Cyano-4-hydroxycinnamic acid
<b>CI</b>	Chemical ionization
<b>CID</b>	Collision-induced dissociation
<b>CL</b>	Cardiolipin
<b>CLSI</b>	Clinical & Laboratory Standards Institute
<b>CML</b>	Clinical microbiology laboratory
<b>CMS</b>	Colistimethate sodium
<b>CRE</b>	Carbapenem-resistant Enterobacteriaceae
<b>Da</b>	Dalton
<b>DAG</b>	Diacylglycerol
<b>DART</b>	Direct analysis in real time mass spectrometry
<b>DNA</b>	Deoxyribonucleic acid
<b>DOR</b>	Doripenem
<b>DOX</b>	Doxycyline
<b>EI</b>	Electron ionization
<b>ELISA</b>	Enzyme-linked immunosorbent assay
<b>ERT</b>	Ertapenem
<b>ESBL</b>	Extended-spectrum $\beta$ -lactamase
<b>ESI</b>	Electrospray ionization mass spectrometry
<b>ESKAPE</b>	<i>Enterococcus faecium</i> , <i>Staphylococcus aureus</i> , <i>Klebsiella pneumoniae</i> , <i>Acinetobacter baumannii</i> , <i>Pseudomonas aeruginosa</i> , and <i>Enterobacter</i> spp.
<b>EUCAST</b>	European Committee on Antimicrobial Susceptibility Testing
<b>FAB</b>	Fast atom bombardment mass spectrometry
<b>FDA</b>	Food and Drug Administration
<b>FEP</b>	Cefepime

<b>GATK</b>	Genome Analysis Toolkit
<b>GC</b>	Gas chromatography
<b>GEN</b>	Gentamicin
<b>GLC</b>	Gas-liquid chromatography
<b>GTRCAT</b>	Generalized time-reversible model
<b>HAI</b>	Hospital-acquired infection
<b>HGAP</b>	Hierarchical genome assembly process
<b>HiTMS</b>	Hierarchical tandem mass spectrometry
<b>HPLC</b>	High-performance liquid chromatography
<b>ICU</b>	Intensive care unit
<b>ID</b>	Infectious diseases
<b>ID</b>	Identification
<b>ISO</b>	International Organization for Standardization
<b>IVD</b>	<i>In vitro</i> diagnostic
<b>JP</b>	Jackson-Pratt drain
<b>KE</b>	Kinetic energy
<b>KPC</b>	<i>Klebsiella pneumoniae</i> carbapenemase
<b>LA</b>	Lipid A
<b>L-Ara4N</b>	4-amino-4-deoxy-L-arabinose
<b>LB</b>	Lysogeny broth
<b>LOD</b>	Limit of detection
<b>LOS</b>	Lipooligosaccharide
<b>LPS</b>	Lipopolysaccharide
<b>LTA</b>	Lipoteichoic acid
<b>MALDI</b>	Matrix-assisted laser desorption/ionization mass spectrometry
<b>MBT</b>	MALDI Biotyper
<b>MCP</b>	Multi-channel plate
<b>MCR</b>	Mobilized colistin resistance gene
<b>MEM</b>	Meropenem
<b>MIC</b>	Minimum inhibitory concentration
<b>MLST</b>	Multi-locus sequence typing
<b>MP</b>	Monophosphate
<b>MRSA</b>	Methicillin-resistant <i>Staphylococcus aureus</i>
<b>MS</b>	Mass spectrometry
<b>MSSA</b>	Methicillin-sensitive <i>Staphylococcus aureus</i>
<b>MSP</b>	Main SPectra
<b>MW</b>	Molecular weight
<b><i>m/z</i></b>	Mass-to-charge ratio
<b>NGS</b>	Next generation sequencing
<b>NICU</b>	Neonatal intensive care unit

<b>OC</b>	OffLine Classification
<b>PA</b>	Phosphatidic acid
<b>PAMP</b>	Pathogen-associated molecular pattern
<b>PC</b>	Phosphatidylcholine
<b>PCR</b>	Polymerase chain reaction
<b>PDR</b>	Pandrug resistance
<b>PE</b>	Phosphatidylethanolamine
<b>PEtN</b>	Phosphoethanolamine
<b>PFGE</b>	Pulsed-field gel electrophoresis
<b>PG</b>	Phosphatidylglycerol
<b>PI</b>	Phosphatidylinositol
<b>PL</b>	Phospholipid
<b>PNA-FISH</b>	Peptide-nucleic acid fluorescence <i>in situ</i> hybridization
<b>POC</b>	Point-of-care
<b>PS-MS</b>	Paper spray mass spectrometry
<b>Pt</b>	Patient
<b>Py-GC</b>	Pyrolysis-gas chromatography mass spectrometry
<b>QTOF</b>	Quadrupole time-of-flight
<b>REIMS</b>	Rapid evaporative ionization mass spectrometry
<b>RNA</b>	Ribonucleic acid
<b>rRNA/rDNA</b>	Ribosomal RNA
<b>RTC</b>	Real Time Classification
<b>RT-PCR</b>	Real-time PCR
<b>RUO</b>	Research use only
<b>SAWN</b>	Surface acoustic wave nebulization mass spectrometry
<b>SNIP</b>	Sensitive Nonlinear Iterative Peak
<b>SNP</b>	Single nucleotide polymorphism
<b>SNR</b>	Signal-to-noise ratio
<b>ST</b>	Sequence type
<b>TA</b>	Teichoic acid
<b>TAT</b>	Turnaround time
<b>TGC</b>	Tigecycline
<b>TLR4</b>	Toll-like receptor 4
<b>TOB</b>	Tobramycin
<b>TOF</b>	Time-of-flight
<b>TZP</b>	Piperacillin-tazobactam
<b>UMMC</b>	University of Maryland Medical Center
<b>UTI</b>	Urinary tract infection
<b>UVPD</b>	Ultraviolet photodissociation
<b>VAP</b>	Ventilator-associated pneumonia

<b>VRE</b>	Vancomycin-resistant enterococci
<b>WGS</b>	Whole genome sequencing
<b>WHO</b>	World Health Organization
<b>WT</b>	Wild-type
<b>XDR</b>	Extensive drug resistance

# **CHAPTER ONE: Mass Spectrometry-based Diagnostics for the Clinical Laboratory**

## **Abstract**

The global health impact of infectious diseases has always driven development of novel diagnostics and therapeutics to combat it. Basic research to understand microbes and their differences has given rise to the utilization of those unique features to make more rapid diagnoses. Work to develop diagnostic tools over the past century has resulted in notable milestones: microscopy and culture techniques has formed the backbone of the clinical microbiology lab for the last 50 years; molecular biology-based technologies offer unprecedented improvements in accuracy and precision; and more recently, advancements in biotechnology and bioinformatics have opened new fields to make significant contributions in the analysis of limited patient material. Among those, mass spectrometry (MS) has emerged as an important and increasingly indispensable tool. In this chapter, an overview of clinical diagnostics is presented with an emphasis on the development of MS-based technologies starting with the early work with MS as a diagnostic; MS phenotyping using microbial proteins in depth, which represents the most promising implementation to date; and, the latest efforts being explored with regard to novel biomarkers, instrumentation, and analytics. Finally, how these different MS approaches, used in combination, will further enhance the scope and capability of these platforms and the impact in the clinical microbiology laboratory will be discussed.

## **The global impact of infectious disease**

Infectious diseases are an ongoing global health threat (1). Among the estimated 58.8 million deaths that occur per year, 32% (~15 million) can be attributed to infectious diseases (ID) (2). According to the World Health Organization's (WHO) World Health Statistics (3), this burden falls disproportionately on the developing world with infectious diseases as an especially overwhelming contributor to child mortality. The WHO's Universal Health Coverage Initiative (4) finds a direct correlation between health burdens of selected ID indicators, such as effective tuberculosis treatment incidence, and access to health care facilities and personnel where diagnoses can be made and prompt therapies initiated. According to the Centers for Disease Control and Prevention's (CDC) National Center for Health Statistics (5), septicemia continues to be among the leading causes of hospitalization and death in the United States. Furthermore, early and aggressive treatment significantly enhances survival rates of patients in particular for cases involving antibiotic-resistant infections (6–8). Finally, both the WHO and CDC recognize the serious threat posed by antibiotic-resistant bacteria, estimated to have caused over 2 million illnesses and 23,000 deaths overall (9, 10). It is therefore reasonable to conclude that successful diagnosis and treatment of infection is essential to address the substantial health and economic impacts of ID. Therefore, the development of more rapid and accurate diagnostics are urgently needed to further improve outcomes and direct treatments for patients worldwide.

## **A guide to current diagnostics in the clinical laboratory**

**Microbiological culture.** When a patient is suspected of having a bacterial infection, determination of the infectious agent is typically made by phenotypic characterization. Microscopy followed by microbiological culture is the current gold standard in the clinical laboratory (11, 12). Direct examination of clinical specimens by microscopy to determine cell morphology (*i.e.* cocci *v.* bacilli) and a Gram stain (a technique first published in 1884) to differentiate Gram-positive and negative bacteria are performed (13). The pathogen is then cultured on a variety of different media to isolate single colonies followed by determination of phenotypic characteristics (*e.g.* motility), enzymology (*e.g.* catalase activity), and metabolic restrictions (*e.g.* glucose fermentation) thus allowing a primary identification. **Figure 1.1** shows the standard workflow for incoming microbial specimens in a typical clinical microbiology laboratory (CML). Notice that for some organisms, specifically the Gram-negative Enterobacteriaceae, there are still multiple potential candidates at the end of this screening pipeline. Expansion of culture-based diagnostic technologies has also introduced antimicrobial susceptibility testing (AST), monitoring of bacterial growth inhibition in the presence of a spectrum of different antibiotics at a range of strategic concentrations. The resistance profiles are used not only for further characterization but to guide definitive antimicrobial chemotherapy (12). AST is accomplished through disk diffusion testing, agar/broth dilution assays, and/or Etest (14). It is worth noting that automated platforms such as the Becton Dickinson Phoenix, bioMérieux VITEK2, and Biolog OmniLog exist for phenotypic and antimicrobial susceptibility testing (15, 16). Additionally, the BacterioScan 216Dx UTI System utilizes microfluidic and laser light scattering technologies to analyze smaller sample volumes

vastly reducing turnaround time (TAT) with comparable accuracy (17). These platforms, while streamlining the phenotyping process, require cultivation; therefore, there remains a need for more rapid diagnostics, particularly in instances such as septicemia where rapid appropriate intervention significantly improves morbidity and mortality.



**Figure 1.1. A clinical strategy for bacterial identification.** Schematic diagram depicting the typical pipeline for identification of a causative agent by phenotypic characterization. Diagram was created based on conversations with and information provided by Dr. J. Kristie Johnson, Chief Pathologist at the University of Maryland Medical Center.

**Molecular diagnostics.** Nucleic acid-based technologies are common and effective diagnostic tools. Hybridization methods function by specially designed probes that target complementary sequences in the microbial genome and yield a fluorescence-positive result by microscopy. Multiple micro- and macro-arrays containing a selection of specific genetic markers are now available (18). The species specificity of 16S ribosomal RNA genes has given rise to the adjunctive laboratory test using peptide nucleic acid (PNA) fluorescence *in situ* hybridization (FISH); this involves PNA probes, DNA mimics that hybridize with high specificity to their 16S rRNA targets (19). Additionally, pulsed-field gel electrophoresis (PFGE), a technique in which genomic DNA is digested by restriction enzymes and DNA fragments separated on agarose to generate a DNA fingerprint, provides epidemiological typing, highly valuable when handling multiple isolates as in an outbreak scenario (20). These nucleic acid-based approaches have vastly improved sensitivity and specificity over culture-based platforms though are limited to organisms for which probes have been engineered (21).

To overcome this limitation, direct sequencing of patient samples is now the more widely used. This involves extraction of genomic DNA from the sample followed by amplification and purification by PCR and Sanger sequencing of specific genes – usually the 16S ribosomal RNA genes but also virulence or antibiotic resistance genes such as the *tuf* and *mecA* genes (for *Staphylococcus aureus*). For specific organisms, including *Mycobacterium tuberculosis* and *Chlamydia trachomatis*, specialized PCR kits are required at additional time and expense (22–24). Multi-locus sequence typing (MLST), amplification and sequencing of internal fragments from a panel of housekeeping genes has epidemiological applications similar to PFGE and is used primarily for a global

phylogenetic analysis to determine the clonal lineage of an outbreak strain (25). Regardless, the rationale is the same: oligonucleotide primers target sequences to amplify specified genes for sequencing, which will provide a species (and perhaps even a sub-species) identification. However, it is important to note some important limitations: some genetic profiles have limited classifying power and may only provide genus level identifications; high sensitivity may lead to false positives from commensal contaminants or probe mismatching; small permissible reaction volumes compared to conventional methods may result in false negatives in infections where bacterial density is low (*e.g.* bacteremia). Ultimately, molecular diagnostic analysis from monomicrobial culture is still recommended to improve yield and avoid discordant results from mixed infections, which can extend time-to-diagnosis; importantly, all of these assays require prior knowledge of what one is looking for; and finally, protocols are costly, time-consuming, and require substantial laboratory facilities and personnel without any viable paths for automation as yet (22, 23).

**Implications of high-throughput sequencing.** Next generation sequencing (NGS) technologies permit whole bacterial genome sequencing, which provides the most comprehensive genetic information available and has enabled culture-free DNA sequencing, even from single cells (26). Commercial platforms including the miSeq (Illumina), Ion Torrent (Life Technologies), and 454 GS Junior (Roche) are increasingly compact and high throughput (27). Each utilizes slightly different sequencing technology; however, all involve random fragmentation of the genome, sequestration of DNA templates with universal adapters and primers and massively parallel sequencing by several rounds of amplification with specialized nucleotides that emit a photometric, colorimetric, or

electrometric signal upon incorporation. These methods yield far shorter reads yet provide far deeper sequence coverage and vastly more sequence data in a shorter time than traditional Sanger sequencing. Why these platforms have not extensively integrated into CMLs is somewhat unclear although issues such as high instrumentation and reagent costs, high technician skill requirements, a high bioinformatics burden, and a need for streamlining processing particularly regarding data analysis on the multiple platforms are associated with this platform. Also, the presence of a gene as identified by sequencing does not necessarily mean it is expressed by the bacteria.

Presently, NGS technologies are most applicable in epidemiological studies in which clinical specimens are all routed through a fully-equipped core laboratory for determination of outbreak origin and containment and prevention strategies. Following the bioterror attack in 2001 where letters were laced with *Bacillus anthracis* spores, the initial investigation struggled to gain valuable forensic information to lead to a potential source. In 2011, Rasko et al. (28) were able to determine sequence variants despite high genetic homogeneity by comparative analyses of whole genomes from outbreak and reference strains, as well as correlate an observed phenotype (reduced sporulation) with the unique genetic backgrounds of the outbreak strains. Rohde et al. (29) and Rasko et al. (30), in a highly collaborative global effort, were able to undertake rapid whole genome sequencing of isolates from patients in the 2011 outbreak of *Escherichia coli* in Germany. The strains were determined to be serotype O104:H4, a rare Shiga toxin-expressing enteroaggregative *E. coli*. Additionally, they identified novel virulence genes that may have contributed to the overall higher incidence of hemolytic-uremic syndrome associated with this outbreak. Sherry et al. (31) conducted a pilot study using NGS of whole genomes of multi-drug

resistant *E. coli* isolates and found all originated from the same neonatal intensive care unit (NICU) as well as identified important antibiotic resistance genes including *bla*<sub>CTX-M-15</sub>, which encodes the extended-spectrum  $\beta$ -lactamase (ESBL) conferring resistance to  $\beta$ -lactam antibiotics.

**Point-of-care assays.** Point-of-care (POC) tests, quite simply, are performed at the site of patient care (*e.g.* a hospital or physician's office). These are immunology or serology-based assays that, unlike classical microbiological testing, rely on testing of the patient rather than the microbe to identify the infectious agent. As such, they have become a valuable alternative in certain instances: their simplified workflow does not require highly trained personnel, the fact that they are culture-independent ensures faster delivery of results for initiation of focused therapy *in lieu* of pending culture-dependent results, they potentially lower nosocomial transmission (by indicating patients for isolation more rapidly), or they are highly useful in instances when organisms are uncultivable (18, 32). Some examples include: a rapid test for pneumonia by detecting C-polysaccharide in the cell wall of *Streptococcus pneumoniae* (33); a *Legionella* urinary antigen test for detection of lipopolysaccharide of *Legionella*, a fastidious organism (34); a malaria test that targets histidine-rich protein 2 of *Plasmodium falciparum* (32); a serologic (detects antibodies against the invading organism rather than the organism itself) assay that measures IgG levels against *Helicobacter pylori* by ELISA (35); and, antepartum detection of *Streptococcus agalactiae* in pregnant women, which exemplifies the use of a novel, handheld real-time (RT)-PCR POC device (36). However, these tests suffer from several major setbacks, most importantly low sensitivity in immunoassays; loss of specificity when the antigen presents in the host without infection as in commensal colonization, a prior

cured infection or chronic exposure in endemic areas; the fact that the etiological agent will be missed if it's not what the assay was expressly designed to find; and, cross-reactivity or, conversely, lack of detection due to a patient's immune compromised status for serological tests (32).

**Figure 1.2** provides a schematic representation of the techniques described in detail in the previous sections.

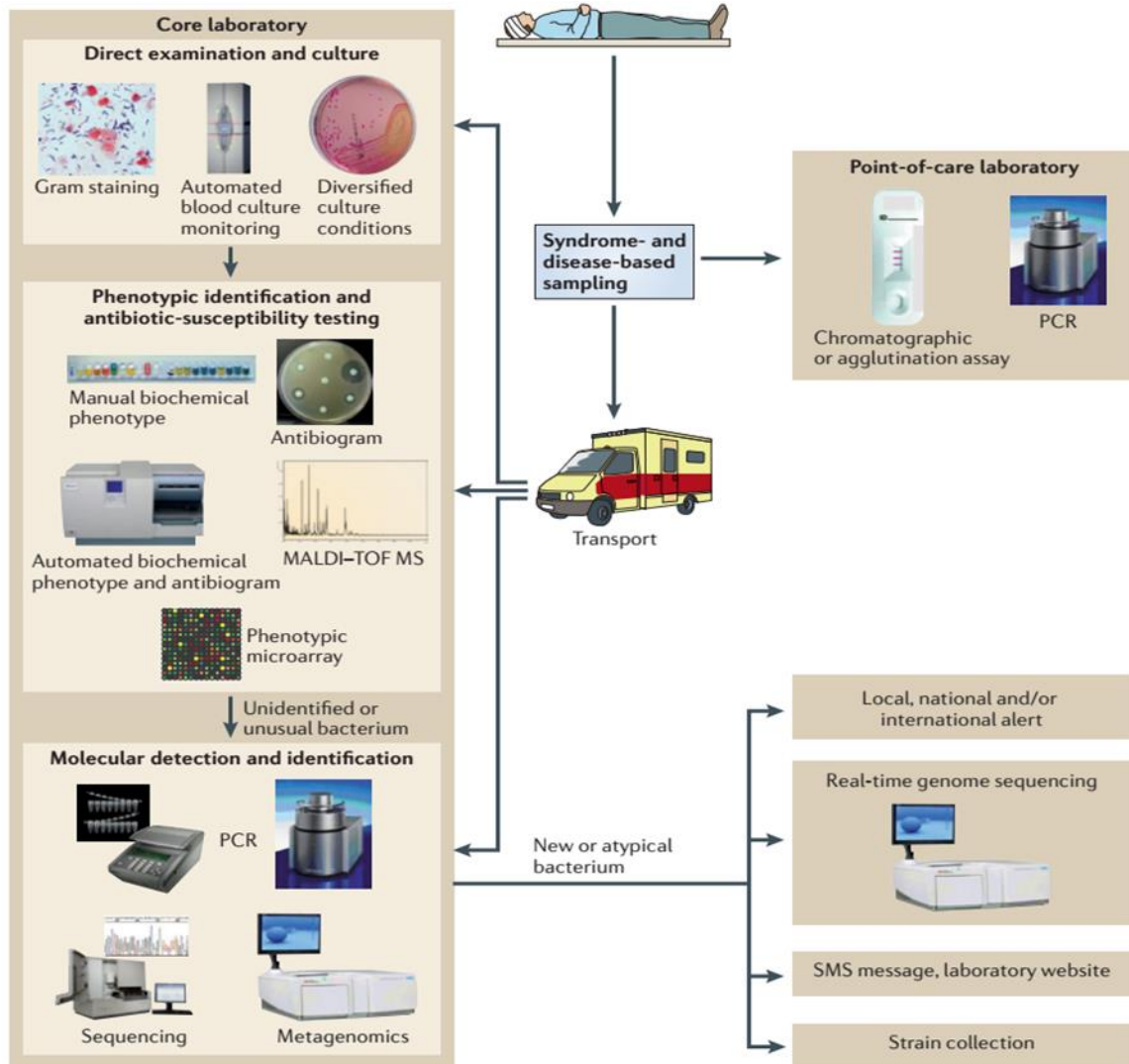


**Figure 1.2. Overview of the typical workflow of the clinical laboratory.** Schematic diagram describes the different routes for specimen processing in the clinical microbiology laboratory from conventional methods like Gram stain and culture to those involving phenotypic and biochemical testing to molecular-based detection exemplified by sequencing of PCR-amplified genes to POC assays that screen for specific antigens. More advanced, rapid technologies involving whole genome sequencing or MS fingerprinting are becoming popular and are poised to overtake conventional methodologies. *Reprinted by permission from Macmillan Publishers Ltd: Nature Reviews Microbiology (18), Copyright 2013.*

## **Mass spectrometry: A revolution in clinical diagnosis**

**The early years.** The principle of mass spectrometry (MS) is simple: it is an analytical technique for determining the mass of individual ions in a sample with a readout or spectrum of ions indicating the measured mass-to-charge ratios ( $m/z$ , where  $m$  is the mass and  $z$  is the number of elemental charges of the ion) and intensities. Individual mass spectra can provide an abundance of information on molecular structure, function, and sample composition. Mass spectrometry now represents a revolutionary shift in microbiological diagnostics but work to develop the technology for those purposes has been undertaken for decades. Originally, a study by Reiner (*Nature*, 1965) (37) first proposed that different bacteria produced unique fingerprints when analyzed by pyrolysis-gas chromatography (Py-GC). Chromatograms of Gram-positive, Gram-negative and Mycobacteria were found to be different with variations in both ion intensities and retention times (37). Subsequently, Simmonds (*Appl. Microbiol.*, 1970) analyzed the pyrolysis products of this study by MS: he identified the small organic molecules that were breakdown products from the pyrolysis step (in which samples are induced to the gas phase by extremely high temperatures,  $\sim 500^{\circ}\text{C}$ ) and determined them to be a complex mixture of microbial proteins, carbohydrates, nucleic acids, lipids, and porphyrins (38). From this, two studies by collaborators combined these approaches, utilizing Py-GC-MS to closely replicate the results of the previous two studies (39, 40); they proposed that a mass spectral fingerprint, rather than a gas chromatogram, offered a more qualitative and quantitative differentiation. Despite overcoming significant defects in reproducibility, this technique is based on relative intensities of low molecular weight ( $<300$  amu) chemical constituents, resulting in multiple molecular species contributing to each ion and substantial overlap between mass

spectra from different organisms. Numerous studies, as well as advances in the technology continued to refine the technique from the 1970's through the 1990's. Anhalt and Fenselau (41) employed direct insertion of lyophilized (freeze-dried) bacteria into the mass spectrometer to see a larger spectrum of products and a milder pyrolysis step to observe less fragmented biomolecules including phospholipids (PL) and ubiquinones. They were the first to suggest MS fingerprinting to diagnose infection by the species-specific membrane composition of PL. Multiple studies followed utilizing combinations of GC, gas-liquid chromatography (GLC), high-performance liquid chromatography (HPLC), and GC-MS. To bypass pyrolysis entirely, "soft" desorption techniques such as fast atom bombardment (FAB)-MS, electron impact (EI)-MS, and chemical ionization (CI)-MS were developed, which allowed examination of whole PL, fatty acids, and even short-chain fatty acid metabolites (42–45). Cole and Enke (46) and Smith et al. (47) employed tandem MS (MS/MS) to analyze PL by FAB-MS and electrospray ionization (ESI)-MS, respectively, in which collision with a neutral gas is used to fragment molecular ions into their product ions, allowing more structural detail and information to be contributed to the PL profiles. The observations that PL could be evaluated by both the polar head groups, as well as variation in the length and composition of the fatty acids, fueled the investigations into use of PLs for microbial differentiation. Ultimately, problems with low reproducibility between sample and spectral replicates, low variability between microorganisms, and the need for more simplified sample preparation left researchers in search of a new biomarker (48).

**Use of MALDI-TOF mass spectrometry in diagnostics.** The first suggestion of proteins for MS profiling of bacteria was introduced in 1994 from protein extracts of lysed cells (49) followed closely by two studies using direct examination of whole cells (48, 50), and represent the most broadly efficacious and validated use of mass spectrometry for microbial diagnostics. Since the 1980's, newly discovered methods permitted the design of mass spectrometers for the analysis of large and polar bioactive molecules (51). MS-based proteomics and protein phenotyping take advantage of so-called “softer” ionization techniques, which refers to ionization that results in less fragmentation of the desired analyte. Most research and commercial typing platforms are based on a MALDI-TOF-MS platform due to its theoretically unlimited mass range (necessary for large biomolecules, like proteins), its comparative ease of use (and potential for automation), and its capability for high throughput analysis (obviously highly sought after for a diagnostic laboratory). These techniques are addressed in more detail in this chapter (**Figure 1.3**) (52).

Matrix-assisted laser desorption/ionization time-of-flight mass spectrometry describes the ionization method (MALDI) and mass analyzer (TOF) components of the instrument. MALDI is the result of work done by Michael Karas, Franz Hillenkamp, and Koichi Tanaka in the 1980's and is typified by the use of a MALDI matrix for generation of ions (53, 54). Matrices are highly energy-absorbent mono- or polycyclic hydrocarbon rings; they facilitate efficient ion generation at lower laser irradiation thresholds allowing ionization of large, more thermally labile biomolecules, and multiple types are available dependent on the molecule to be ionized (*i.e.* proteins, peptides, nucleic acids, lipids, etc.). For this analysis, samples are embedded within the matrix on a target plate, allowed to co-crystallize, and irradiated by a laser within a strong vacuum. Energy absorption and

excitation of matrix molecules causes sublimation of the solid state sample into gas molecules that rise in a plume from the target surface. In what is likely a separate yet nearly simultaneous event, random collisional forces cause energy transfer from the matrix molecules to the analyte that results in ionization of the analyte. As ions, they can now enter the instrument and are manipulated by carefully calibrated and controlled voltage fields (55). Mass-to-charge ratios of ions are determined by the TOF analyzer. Gaseous ions at the source are accelerated by a fixed potential applied to the target plate shortly following ionization. The kinetic energy imparted to the ions can be expressed by the equation:  $KE = (1/2)mv^2$ , where KE=kinetic energy, m=mass, and v=velocity. At this point, the ions enter the flight tube, and, as can be seen in the expressed equation, the velocity at which each ion travels through the flight tube is related to its mass. Therefore, measurement of the time taken for an ion to travel the flight path before being detected by the detector can be used to derive a molecule's mass (56).

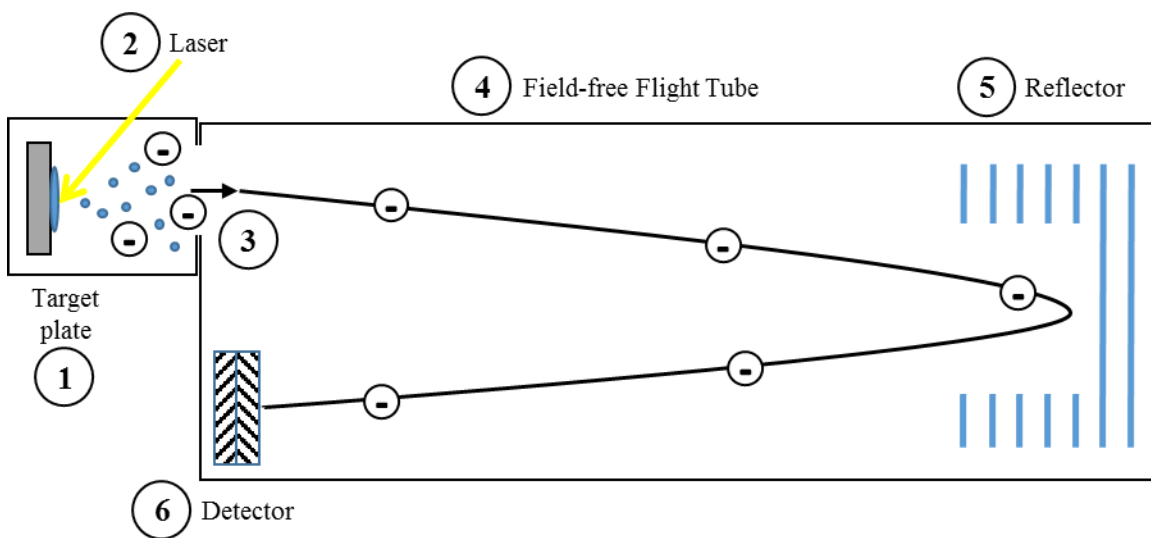


**Figure 1.3. Schematic representation of a MALDI-TOF mass spectrometer. 1)** Samples embedded within an absorbing matrix and allowed to dry on a target plate are placed in the ion source and the instrument is pumped down to high vacuum ( $10^{-3}$  torr). **2)** Pulsed laser irradiation on the surface of the sample generates plumes of gaseous phase ions within the source. **3)** Voltage applied to the target plate extracts ions into the mass analyzer giving them a fixed amount of kinetic energy (KE). **4)** As ions enter the flight tube, their velocities are determined by the KE imparted to them as well as their molecular masses such that lower molecular weight ions will travel at a greater velocity than higher ones. **5)** In reflectron TOF, a reflector corrects for energetic differences in ions: due to positional differences within the ion source, ions with equal masses may have slightly different kinetic energies and, therefore, travel at different velocities. The reflector, which is a series of concentric rings that generate an electric field of increasing voltages, corrects this: ions with higher KE will travel further into the reflector giving them longer flight paths. It also doubles the distance ions have to travel; both improve mass resolution. **6)** Ions are detected by a multi-channel plate (MCP), which amplifies the ion signal and establishes the time of flight from  $t_0$  (*i.e.* the laser pulse) from which the  $m/z$  value is derived.

**The basis of MS protein typing.** Mass spectrometric analysis of bacterial proteins and peptides to make an identification represents the most comprehensive technology available in the clinical laboratory; traditionally, multi-step combinations of direct microscopy, phenotypic characterization, gene sequencing results, and hybridization steps are used (57). The commercial protein phenotyping platforms rely on mass spectrometric analysis of whole bacterial cells or an extraction of bacterial proteins to generate a mass spectrum of proteins in the  $m/z$  range of 2 to 60 kDa, which were found to be comprised of mostly ribosomal proteins but also DNA-binding and heat shock proteins (58). These mass spectra were exhaustively determined to be unique in a species-specific manner, and an identification is made by comparison of the mass spectrum from the unknown sample against a reference database of mass spectra from known sources (59). There are several commercial platforms currently available: the most well-known are the MALDI Biotyper (Bruker Daltonics, Billerica MA) and the VITEK MS (bioMérieux S.A., France), which consist of a MALDI-TOF instrument, a mass spectral database of reference organisms, and a coupled software program for data processing and analysis. While they each have their own benefits and drawbacks, both display comparable accuracy, in general, and both have received partial approval for a portion of their library from the Food and Drug Administration (FDA) just within the last four years (60). These platforms, along with more specifics of their methodologies, are described in more detail below.

*MALDI Biotyper.* The MALDI Biotyper (MBT), developed by Bruker Daltonics, Inc., was introduced in 2011 (52) following work to validate its applications to both clinical laboratory identifications (61, 62) and identification of organisms relevant in biodefense (63). It was originally coupled to the Autoflex II MS instrument but is now based on the

Microflex CA MALDI-TOF system, a more compact benchtop model. Sample preparations require culture on solid media to obtain single colonies, which are smeared directly onto the target plate within matrix although they can also be overlaid with formic acid or subjected to an in-tube formic acid-ethanol extraction prior to spotting to improve spectral quality or to lyse biohazardous organisms prior to analysis. The MBT RTC (Real Time Classification) program operates as an automated data collection and analysis software: mass spectra are acquired from target spots, converted to mass lists, and compared by pattern matching of ion positions and intensities against an associated mass spectral reference database. A readout of the top ten most likely causative agents is generated, which is based on an assigned log score that reflects the confidence of the identification. Confidence scores range from 0 to 3, and the manufacturer's recommended score cutoffs denote a positive species identification (2.0 to 3.0), a positive genus/probable species identification (1.7 to 1.999), and an unreliable identification (0 to 1.699) although many studies have noted that relaxing of score thresholds to  $\geq 1.7$  affects specificity minimally (64, 65). Uniquely, the platform also includes the OC (Offline Classification) program, allowing users to expand the commercial database to include their own microbial entries. Acquired mass spectra are compiled into a Main SPectra (MSP), which is a projection of averaged mass spectra that can be manually compared against unknown spectra using this software. There is also the capability to conduct taxonomic analyses, so it is highly useful for researchers although it cannot be applied in the clinic. This has been the most extensively studied among the protein platforms with numerous publications assessing accuracy and precision as well as comparative analyses against traditional phenotypic methods, PCR-based sequencing approaches, as well as the other MALDI-TOF

platforms. Recent notable studies employ the most up-to-date instrumentation, software, and database iterations for evaluation of the current platform: Lévesque et al. (66) conducted a side-by-side comparison of the MBT versus the VITEK MS and determined accuracy rates of 86.4% for the Biotyper and 92.3% for the VITEK MS for correctly identifying a diverse range of 642 microorganisms and Deak et al. (67), in comparing the two platforms for the routine identification of 477 bacterial and yeast clinical isolates, found 93.7% and 93.9% positive species identification for the Biotyper and VITEK MS, respectively. The Biotyper has also received extensive study of direct specimen analysis, which has resulted in the incorporation of component platforms for identification of pathogens from blood and urine. Several studies have developed front-end preparation protocols for direct examination of blood culture bottles that boast accuracy approaching that of the direct colony method. This is mostly through removal of contaminant human cells and enrichment of microbial proteins either through gentle lysis of human cells by use of detergents (68, 69) or removal of them by differential centrifugation (64, 65, 70–72). Additional studies have assessed the efficacy of the commercial Sensityper kit (Bruker Daltonics, Billerica MA) for standardized sample processing (68, 73). Similarly, direct identifications in urine from urinary tract infection (UTI) patients, where bacterial loads are typically higher and there are far fewer contaminating cells, have been demonstrated by an initial low-speed centrifugation to remove leukocytes (74) or by diafiltration to remove salts (75).

*VITEK MS.* Work on this platform began in 1998 by AgnosTec: originally called SARAMIS and based on the AXIMA MALDI-TOF system (Shimadzu Corporation, Japan), it was acquired by bioMérieux and now comprises the VITEK MS clinical platform

and the RUO (research use only) platform VITEK MS Plus. Identification of an unknown sample relies on comparisons against mass spectra within a reference database, as with the Biotyper, although there are a few modifications to the standard pattern matching algorithm. First, some database entries are so-called SuperSpectra in which multiple spectral replicates are averaged to generate a consensus mass spectrum for comparison purposes. Secondly, select ions present in the SuperSpectra are placed in weighted matrix bins according to their uniqueness as determiners; in other words, ions with higher species specificity (*i.e.* ions that are found to be more indicative of a species) are assigned greater importance when making comparisons. (60) Marked improvements in identification rates for organisms are seen when identified via a SuperSpectra mass spectrum, and a number of studies have observed an association between the number of spectra used to build a super spectrum and positive identification rates using SuperSpectra. How these identifications are scored is also slightly different than the Biotyper: database comparison receives a confidence score between 0 and 99.9% without threshold cutoffs for a positive identification, rather a percent score that denotes the level of confidence that is then provided to the technician for final interpretation. Studies have found comparable and often increased sensitivity and specificity to the MALDI Biotyper although this platform suffers from a remarkably smaller but pathogen-targeted integrated reference library (though the number of FDA-approved database entries is larger) (67). The VITEX MS platform appears to be more functional and effective in studying certain microbial classes for which the depth of the database has been more thoroughly developed, such as yeasts (76) and mycobacteria (77). Recently, Zhou et al. (78) examined 181 isolates of the group viridans streptococci, which have proven to be an especial challenge for both platforms, and found

that the Bruker Biotyper and Vitek MS IVD systems correctly identified 88.4% and 98.9%, respectively.

*Current work and future directions.* Tremendous progress has been made to adapt the use of MS ion profiles of proteins and peptides for microbial identification. Work conducted over the last two decades has resulted in a highly simplified front-end sample preparation that is amenable for the CML; considerable validation of the sensitivity and specificity of current research and clinical platforms; and, expansion of the scope and depth of reference databases, which remains the primary hindrance to improvements in accuracy. Despite this, there remain significant limitations to this platform including a persistent inability to discern certain closely related species (*e.g. E. coli v. Shigella flexneri*) and an inability to reliably sub-speciate, so work continues to address these issues with innovative, alternative approaches. To overcome these limitations, McFarland et al. (79) employed a top-down strategy fragmenting proteins via tandem MS to generate a mass spectral fingerprint of fragment ions to aid in differentiation of *Salmonella enterica* serovars. Initially, they generated mass spectra of intact proteins to identify slight mass differences between subsets of ions and then used MS<sup>2</sup> to identify and sequence these selected markers to correlate these nonsynonymous mutations back to single nucleotide polymorphisms (SNPs) in the bacterial genome. Using a bottom-up approach, Gekenidis et al. (80) trypsinized proteins prior to analysis to generate a mass spectrum of bacterial peptides allowing widening of the *m/z* range of interest and increased interrogation of the resulting tryptic peptides from *Salmonella* subspecies. This increased the ability to identify biomarkers while use of high-intensity focused ultrasound aided in solubilization to expand the pool of cellular proteins in the analysis. Both proteomics strategies are based on the

concept that offering more ions for a mass spectral profile would lead to higher discriminatory power and that has been borne out by these studies' findings; however, they rely on direct infusion of samples via ESI, which requires alternate ionization to be coupled to the clinical platform that is not easily multiplexed and requires significantly more technical skill for inquiry and deconvolution of spectra. Alternately, elucidation of an antibiotic susceptibility profile, in addition to an identification would provide insight into how to treat an infection, so that has become an attractive option for study. Initially, studies by Burckhardt and Zimmerman (81), Hrabák et al. (82), and Sparbier et al. (83) were able to detect  $\beta$ -lactamase-producing, Gram-negative Enterobacteria by detection of  $\beta$ -lactam hydrolysis products by MS. Susceptible and resistant strains were incubated in the presence of antibiotics and culture supernatants were analyzed; in general, observed loss of  $\beta$ -lactam ions and a corresponding increase in hydrolyzed  $\beta$ -lactam ions agreed well with MIC determinations of resistance. Furthermore, addition of enzyme-specific inhibitors to the reaction led to suppression of this phenomenon allowing further identification of  $\beta$ -lactamase classes, *i.e.* penicillinases, carbapenemases, and metallo- $\beta$ -lactamases (83, 84). An interesting pair of studies addressed the main issue of the previous studies, namely, that this assay will only detect  $\beta$ -lactam-resistance: Sparbier et al. (85) and Jung et al. (86) used  $^{13}\text{C}$  isotopically-labeled lysine in the presence of antibiotics to distinguish methicillin-susceptible and resistant *S. aureus* and  $\beta$ -lactam, aminoglycoside, or fluoroquinolone-resistant *Pseudomonas aeruginosa*. This strategy is dependent on the premise that only resistant strains will undergo protein biosynthesis when antibiotic is present, and the incorporation of these "heavy" amino acids are readily detected as a mass shift of the protein ions in the spectrum. Data are acquired by MALDI-TOF, and the authors also

experimented with different data analysis algorithms for automated analyses of these labeled ions rendering these methods more adaptable to the clinic.

**Figure 1.4** summarizes the numerous techniques and clinical applications of MS discussed in the previous sections.

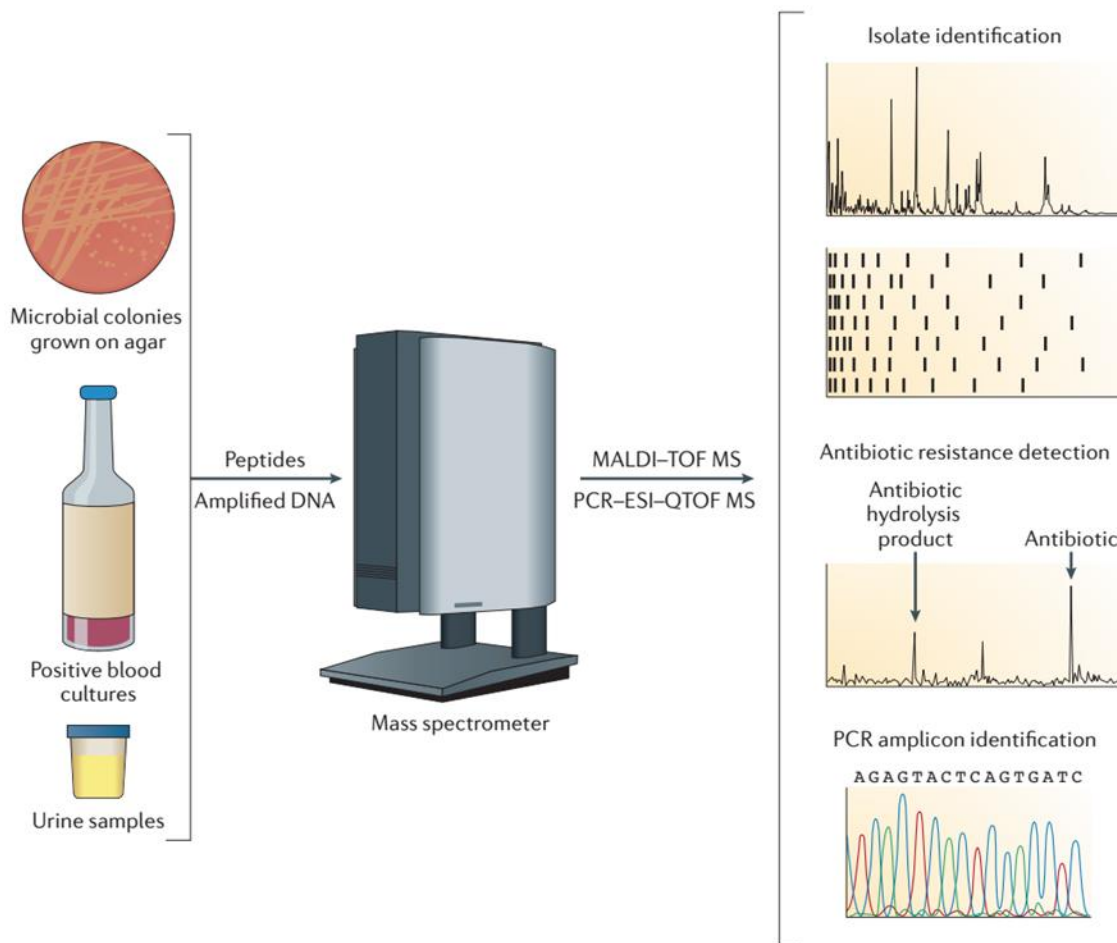


**Figure 1.4. Present and future applications of MS in the clinical laboratory.**

Schematic diagram showing the capabilities and applications of mass spectrometry in the clinical microbiology laboratory. Cultured organisms, blood cultures or urine specimens are analyzed by MALDI-TOF of bacterial proteins and peptides to determine identification and antibiotic-susceptibility or by ESI-QTOF of amplified DNA products for identification via characterization of PCR amplicons. *Reprinted by permission from Macmillan Publishers Ltd: Nature Reviews Microbiology (18), Copyright 2013.*

## **MS-based clinical diagnostics – The last ten years**

**The promise of –omics technologies.** This chapter has already introduced prior work to develop use of novel biomarkers for diagnostic purposes before the advent of protein profiling. Yet, work has continued on those fronts bolstered by new advancements in the field. It is worth mentioning the work of a few groups to develop and evaluate a novel approach coupling PCR to MS taking advantage of the high sensitivity of molecular methodologies and the ease of data interpretation of MS-based technologies (87, 88). PCR/ESI-MS amplifies broadly conserved bacterial genes, mainly ribosomal and housekeeping genes by multiplex PCR and specialized antibiotic resistance gene determinants with the resultant amplicons analyzed by MS to generate a nucleic acid fingerprint permitting identification by comparison against a database of genomic sequences of known organisms (**Figure 1.4**) (89). The technology is now commercially available, and comparative analysis of PCR/ESI-MS to MALDI-TOF-MS for protein phenotyping found comparable accuracy (90). Indisputably however, lipidomics, global analysis of structural lipids or lipid metabolites for characterization of healthy or pathologic conditions, represents the most rapidly emerging field with regard to clinical microbiology.

**Lipidomics in microbial diagnostics.** Bacterial membranes are composed of lipids of diverse structure and dynamic composition. As with eukaryotic membranes, the prokaryotic membrane is characterized by a bilayer of amphiphilic glycerophospholipids and membrane-associated proteins although there are marked variations in phospholipid (PL) composition (91). In *E. coli*, the prototypical microorganism for study, the predominant PLs are phosphatidylserine (PS), phosphatidylglycerol (PG), phosphatidylethanolamine (PE), and cardiolipin (CL, a diphosphatidylglycerol).

Proceeding work has found these general characteristics to hold true for a diversity of other microbes including *S. enterica* Typhimurium and *S. aureus* (92, 93) though differences in species composition and ratio are observed and form the basis for use of PL in diagnostic profiling. In contrast, the eukaryotic (host) membrane is comprised primarily of phosphatidylcholine (PC), phosphatidylinositol (PI), and phosphatidic acid (PA); PS and PE are also present, and PG and CL are found primarily in mitochondrial membranes (94, 95).

The earliest work investigating MS as a diagnostic focused on phospholipid and fatty acid fingerprinting as possible means of identifying microorganisms is described in detail in this work; and in fact, work continues today with incorporation of new and innovative technologies to overcome current limitations. Voorhees et al. (96) and Cody et al. (97) addressed issues of matrix interference in MALDI MS fatty acid (FA) profiling by use of a replacement matrix, CaO, or matrix-free ionization via an ambient (*i.e.* does not occur under vacuum) ionization method known as direct analysis in real-time (DART), respectively. To circumvent time-consuming preparation steps for MALDI MS analysis of intact PL, a pair of studies by Ishida et al. (98, 99) utilized an on-probe sample pretreatment with NaI for generation of characteristic PL profiles from whole bacterial cells to identify Gram-negative Enterobacteriaceae and Gram-positive *Bacillus subtilis*. This approach has obvious parallels to the on-plate formic acid overlay for direct analysis of bacterial cells for protein mass spectra. Finally, Hamid et al. (100) employed paper spray mass spectrometry (PS-MS) for bacterial discrimination: the technique involves a colony smear onto a solvent-wetted filter paper tip (held at the inlet of the mass spectrometer) to which a high voltage potential is applied causing ionization. This serves to bypass sample

extraction and preparation and the use of matrix. Despite this promising work in evaluating microbial PL profiles, this approach has always faced the same recurrent challenges: difficulties in reproducibility between strains within the same species or even between different strain replicates, differences resulting from culture or preparation conditions or inter-laboratory reproducibility, and difficulties in direct specimen analysis due to overlapping ions from eukaryotic phospholipids making quantitative analysis unreliable with both pathogen and host contributing ions to the PL profile. However, microbial membranes are highly complex offering a broad repertoire of other lipid and glycolipid species as potential markers of infection.

**A novel diagnostic biomarker: Microbial glycolipids.** Within the lipid class of molecules, there are a multitude of other, more complex glycosylated lipids found in microbial membranes that could be exploited for diagnostic discrimination as can be seen in **Figure 1.5**. The Gram-positive bacterial membrane is enclosed by a thick cell wall composed of peptidoglycan, dense layers of repeating polysaccharide matrices connected by short peptide linkages. Teichoic acid (TA), a peptidoglycan-associated sugar chain, and lipoteichoic acid (LTA), a membrane lipid-anchored TA, penetrate the cell wall and are unique components of Gram-positive bacteria (101, 102). Gram-negative bacteria are characterized by a double bilayer membrane in which lipopolysaccharide (LPS) comprises the outer leaflet of the outer membrane. (91) LPS has been extensively studied because of its function as the pathogen-associated molecular pattern (PAMP) recognized by Toll-like receptor 4 (TLR4) (103) and as the bacterial endotoxin chiefly responsible for initiating the systemic inflammation cascade that leads to septic shock during sepsis (104). LPS consists of a membrane lipid moiety known as lipid A (LA); a polysaccharide of arranged pentose,

hexose and heptose sugars called core polysaccharide connected to LA via an ester linkage; and, a chain of repeating ring polysaccharide units called O-polysaccharide (that may or may not be present, *i.e.* smooth or rough LPS, respectively) (**Figure 1.6**). The biosynthetic pathway has been determined due to considerable work by Raetz and colleagues (92, 105). This pathway is a tightly controlled process undertaken by conserved genes that have been identified in all Gram-negative organisms. LA is considered to be the principle component dictating endotoxicity and the most conserved: the general structure of lipid A consists of a  $\beta$ -1,4'-bis-phosphorylated,  $\beta$ -1',6-linked disaccharide glucosamine backbone substituted with 4 to 7 ester- and amide-linked fatty acyl chains (106) (**Figure 1.6**). However, there is also a tremendous amount of structural diversity that has been observed among LPS due to post-synthetic modifications, which have also been thoroughly determined by many groups to be a species-specific process (107–109). **Figure 1.7** shows the lipophilic anchor of LPS, lipid A (LA), from different organisms to highlight this diversity with special emphasis on the middle panel showing intraspecies diversity that is associated with different virulence phenotypes in strains of *P. aeruginosa* (110). These glycolipids are essential components of bacterial membranes, found in high abundance ( $\sim 10^6$  LPS molecules per bacterium), and are easily extracted and analyzed by MS; therefore, they represent attractive chemical fingerprints for study as a diagnostic marker.

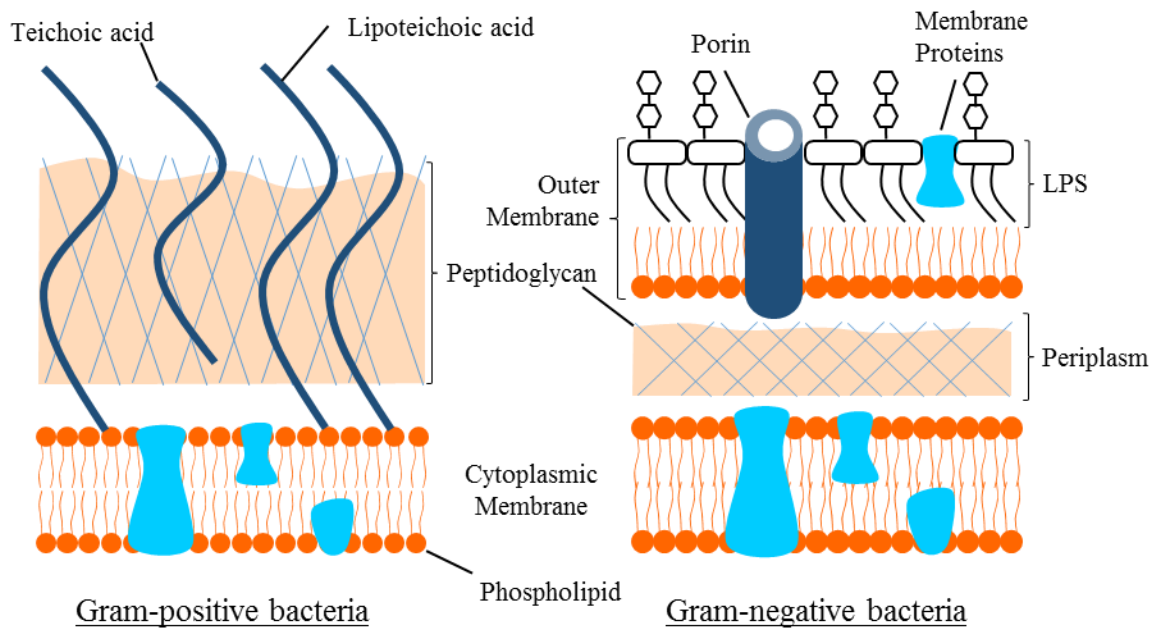


**Figure 1.5. General structure and key features of Gram-positive and negative bacterial membranes.**

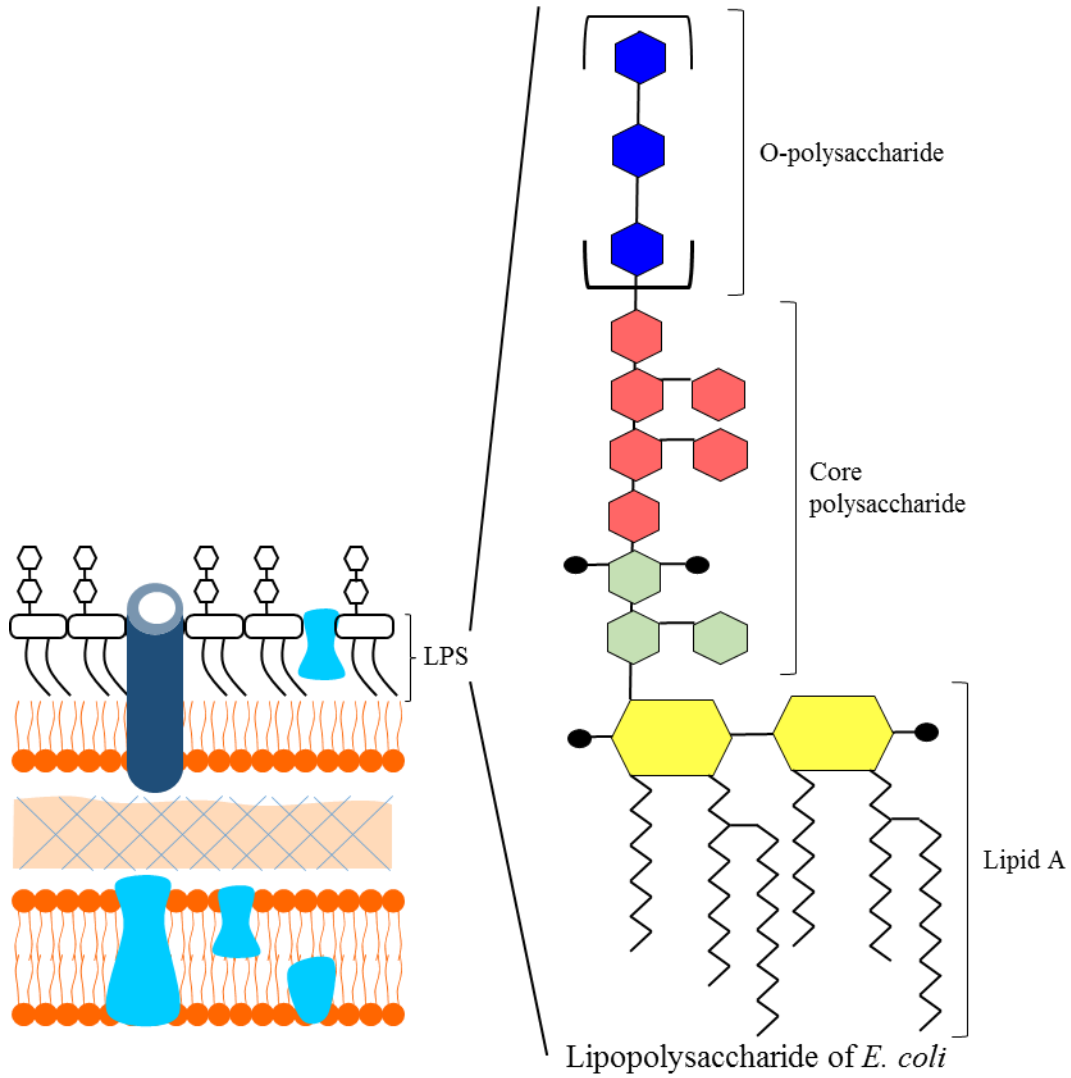


**Figure 1.6. Schematic representation of Gram-negative bacterial membrane and general structure of the essential glycolipid LPS.**

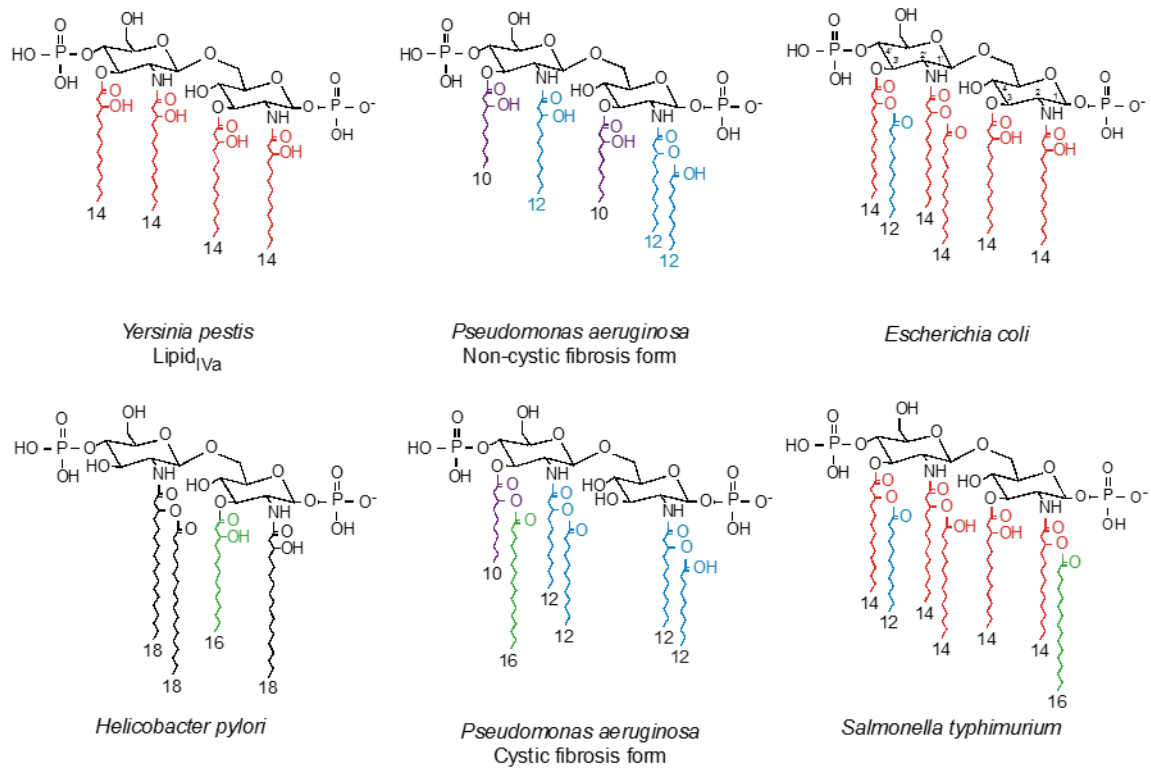


**Figure 1.7. Chemical structures of lipid A from different Gram-negative organisms.** Representative Gram-negative bacteria showing the diversity of LPS-derived lipid A. Structural diversity presents mostly as differences in fatty acyl chain length and composition as shown here but also as modifications to the terminal phosphate functional groups. *Reprinted by permission from Macmillan Publishers Ltd: Nature Reviews Microbiology* (110), Copyright 2005.

**Use of LPS and other membrane lipoglycans.** Due to variation in the length and composition of fatty acyl chains, Parker et al. (111) in 1982 showed extraction and analysis of the hydroxy fatty acids of LPS-derived LA by GLC could give an accurate estimation of the biomass of Gram-negative bacteria in soil samples; the study authors further proposed that the “patterns” of these hydroxyl fatty acids might also define community structure. Similarly, Uhlig et al. (112) in 2016, in detecting endotoxin in environmental samples via quantitation of 3-hydroxy fatty acids, also showed variations in 3-OH FA profiles from four Gram-negative organisms. However, exploration into this biomarker is mostly focused on the potential of MS examination of intact LPS or LA and is being investigated by multiple groups. Tremendous research has been devoted to determination of LPS structure in the characterization of the LPS synthesis pathway and as it relates to pathogenesis and host immunity, and it is through this work that it was first proposed that the uniqueness of LPS might be exploited for diagnostic purposes. Larrouy-Maumus et al. (113) reported direct detection of LA from whole cells and proposed it as a potential means of identifying Gram-negative bacteria. Others have reported detection of LA via rapid evaporative ionization mass spectrometry (REIMS) of select colonies (114, 115), an ambient ionization method involving electrical current applied directly to the surface of an analyte (in this case a colony) at the inlet of the mass analyzer, coupled to multivariate statistical analyses for the identification of clinically relevant bacterial and fungal species. Our work has contributed significantly to development of this platform as well. Leung et al. (116) conducted a proof of concept study in which a library of 50 microbial species was built for the identification of the ESKAPE (*Enterococcus faecium*, *Staphylococcus aureus*, *Klebsiella pneumoniae*, *Acinetobacter baumannii*, *Pseudomonas aeruginosa*, and

*Enterobacter* spp.) pathogens. This entailed generation of mass spectra of intact LA, as well as Gram-positive bacterial and fungal mass profiles. Pathogen identifications were made via adaptations to the Bruker MBT protein-based software, as well as exploration of a novel computational algorithm for identification. This was further validated by two subsequent studies ((117); Leung *et al.* 2017, *manuscript in preparation*) that correlate structural modifications of LA visualized by MS with resistance to colistin as determined by MIC in *K. pneumoniae* and *A. baumannii*. Furthermore, two studies by Yoon *et al.* (118, 119) elucidated LA structures of *Salmonella minnesota* and *Francisella novicida* by surface acoustic wave nebulization (SAWN) MS and a hierarchical tandem MS (HiTMS) algorithm for automated structure assignment. This employs a softer ionization method than MALDI or ESI eliminating matrix effects as with the former or clogging of the capillary, which tends to occur with lipids and glycolipids in the latter, and high-throughput structural analysis that aids in rapid identification by glycolipid fingerprinting. Similarly, elucidation of LPS, lipooligosaccharide (LOS), and LA structures from a variety of microorganisms by ultraviolet photodissociation mass spectrometry (UVPD-MS) and development of a hierarchical method for *de novo* lipid A structure assignment known as UVliPiD has resulted in multiple publications from the Brodbelt group (120, 121). Although no explicit diagnostic platform is offered, this higher energy fragmentation results in a broader range of fragment ions and more precise structure determinations that would add significance to a library of mass spectral fingerprints by correlating them to well-defined LA structures.

## **Final remarks and future directions**

Numerous reviews have suggested that clinical laboratories are transitioning away from traditional culture-based phenotypic methods toward adoption of more rapid sequencing and biophysical techniques for microbial diagnostics. These novel platforms hold the promise of improving time-to-diagnosis and, thus, better directing patient support and therapy. While there is yet no approach that single-handedly addresses all the challenges faced in the clinical laboratory, great improvements have been made within the last two decades that have been the subject of this chapter. There will always be a need for physicians and clinicians to combine patient reporting and their medical and technical expertise with laboratory results to make a diagnosis. New genomic, proteomic, and lipidomic approaches already benefit from a more simplified workflow and less involvement of laboratory reagents and consumables, which also lower costs following initial investment in instrumentation. In the case of MS, the technology exemplifies this offering the highest simplicity and ease of use and lowest cost per sample as well as the potential for unified data analyses and outputs; all of this contributes to overall feasibility of implementation in a clinical or hospital setting. Protein profiling offers the most significant advance and is already being implemented in the clinic with great success, and recent work has extended proteomics as well as developments in fields like glycolipidomics that operate on the same principles and platforms. Advancements in MS platforms and applications have greatly expanded the capabilities of this technology and suggest combining the clinical power of these emerging methodologies into an additively more powerful platform.

## **CHAPTER TWO: Identification of the ESKAPE pathogens by mass spectrometric analysis of microbial membrane glycolipids**

### **Abstract**

Rapid diagnostics that enable identification of infectious agents improve patient outcomes, antimicrobial stewardship, and length of hospital stay. Current methods for pathogen detection in the clinical laboratory include biological culture, nucleic acid amplification, ribosomal protein characterization, and genome sequencing. Pathogen identification from single colonies by matrix-assisted laser desorption/ionization time-of-flight mass spectrometry (MALDI-TOF-MS) analysis of high abundance proteins is gaining popularity in clinical laboratories. Here, we present a novel and complementary approach that utilizes essential microbial glycolipids as chemical fingerprints for identification of individual bacterial species. Gram-positive and negative bacterial glycolipids were extracted using a single optimized protocol. Extracts of the clinically significant ESKAPE pathogens: *Enterococcus faecium*, *Staphylococcus aureus*, *Klebsiella pneumoniae*, *Acinetobacter baumannii*, *Pseudomonas aeruginosa*, and *Enterobacter* spp. were analyzed by MALDI-TOF-MS in negative ion mode to obtain glycolipid mass spectra. A library of glycolipid mass spectra from 50 microbial entries was developed that allowed bacterial speciation of the ESKAPE pathogens, as well as identification of pathogens directly from blood bottles without culture on solid medium and determination of antimicrobial peptide resistance. These results demonstrate that bacterial glycolipid mass spectra represent chemical barcodes that identify pathogens, potentially providing a useful alternative to existing diagnostics.

## **Introduction**

Infectious diseases pose an ongoing threat to public health. Rapid and accurate pathogen detection is needed to guide physicians in the treatment of infection to improve patient and economic outcomes (122). In the clinical laboratory, bacterial isolates are routinely identified by morphological and biochemical methods. Once the bacteria are identified, additional testing such as antibiotic susceptibility can be performed to guide definitive antibiotic treatment. Microbiological culture followed by biochemical identification of bacteria is the current gold standard for clinical diagnostics, but this strategy requires additional testing to detect closely related organisms, as with the Enterobacteriaceae (11). Nucleic acid amplification and sequencing of essential bacterial genes, such as the 16S rDNA, for bacterial identification offers increased accuracy; however, high sensitivity can result in false positives and it may not provide valuable sub-species information (22). Collectively, these methods are time intensive, require at least 24 hours of incubation of clinically obtained material, and often significantly increase the cost and burden of diagnostic laboratory support. Next generation sequencing of whole bacterial genomes is proposed as a culture-free alternative, but it is highly technical with regard to bioinformatic interpretation and is more costly compared to traditional methods (26).

To address some of the current challenges in bacterial identification, mass spectrometric analysis of bacterial proteins is emerging as the dominant technology in many clinical laboratories. Currently, there are two commercially available platforms, the Bruker MALDI Biotyper (52) and bioMérieux VITEK MS (76, 77). These platforms identify bacteria by comparison of a mass spectrum of bacterial proteins from an unknown species to a reference library of previously recorded mass spectra (52, 66, 76, 77). These

protein-based platforms have significant limitations, including: requirement for cell culture to obtain pure colonies, poor identification at the species level for closely related species (*e.g. Escherichia coli v. Shigella flexneri*), inability to identify pathogens directly from complex biological samples, and inability to identify antimicrobial resistance on the FDA-approved platform although Bruker has introduced a workflow for the identification of  $\beta$ -lactamases on the research use only (RUO) platform (62). To address the urgent need for novel technologies that can overcome these challenges and expand the ability to rapidly diagnose bacterial infections, we propose the use of highly abundant membrane glycolipids as another class of molecules to exploit for bacterial identification.

Bacterial membranes are composed of lipids of diverse structure and composition. Similar to eukaryotic cell membranes, microbial membranes are composed of a bilayer of amphiphilic glycerophospholipids. In Gram-negative bacteria, there are two distinct membranes separated by a periplasm, whereas in Gram-positive bacteria, the membrane is enclosed by a cell wall (123). Previously, use of bacterial membrane phospholipids had been proposed to phenotype bacteria (11). Specifically, analysis of fatty acids and membrane phospholipids by gas chromatography with flame ionization detection or mass spectrometry (MS) was explored with limited success. Because fatty acid profiles are not unique for each microbial species, species are differentiated via differences in ion intensities, which vary as a function of growth (46, 47, 124). This is further complicated by the fact that bacteria and mammalian hosts share some of the same phospholipids; consequently, direct analysis of patient specimens is not possible due to the inability to distinguish bacterial phospholipids from those of the host.

Alternatively, microbial membranes possess more complex, glycosylated lipids that are exclusive to bacterial cell membranes and thus are not produced by mammals. They are present in high abundance, approximately  $10^6$  molecules per bacterium, and are readily extracted from bacteria grown under laboratory conditions or directly from biological fluids. In Gram-negative bacteria, lipopolysaccharide (LPS) comprises the outer leaflet of the outer membrane. The general architecture consists of a lipophilic anchor moiety (lipid A), a core oligosaccharide of arranged hexoses, and an O-polysaccharide chain of repeating subunits. The endotoxin component, lipid A (LA), consists of a glucosamine disaccharide backbone flanked by terminal phosphate residues and fatty acyl chains that extend from the backbone (106). In contrast, Gram-positive bacteria have numerous cell wall glycans including cardiolipin and lipoteichoic acid (LTA), which is composed of a diacylglycerol (DAG) lipid that anchors in the membrane and a complex oligosaccharide that penetrates the cell wall (125). Examination of the literature suggests these bacterial glycolipids could provide species-specific mass spectral profiles due to their immense diversity in the arrangement of fatty acyl side chains and sugar-associated functional groups (102, 107). We thus hypothesized that these glycolipids represent novel chemical fingerprints that would enable identification of bacteria by MS in a manner similar to bacterial proteins.

To evaluate the diagnostic potential of these membrane glycolipids, we examined the ESKAPE pathogens: Gram-positive *Enterococcus faecium* and *Staphylococcus aureus* and Gram-negative *Klebsiella pneumoniae*, *Acinetobacter baumannii*, *Pseudomonas aeruginosa*, and *Enterobacter* spp., so named for their ability to escape antibiotic treatment. They are of considerable concern due to their prevalence in hospital-acquired infections (HAI) and acquisition of resistance to antibiotics such as polymyxins (126), a family of

cationic antimicrobial peptides (CAMPs) available as polymyxin B sulfate and colistin (polymyxin E). CAMPs bind negatively-charged LPS through electrostatic interactions with the terminal phosphate groups and insert in the bacterial membrane, disrupting permeabilization leading to cell death (127). Emergence of polymyxin resistance has been observed in the ESKAPE pathogens *K. pneumoniae* (128), *A. baumannii* (129), and *P. aeruginosa* (130). When analyzed by MS, we and others have shown that antimicrobial-resistant ESKAPE isolates are chemically distinct from their susceptible counterparts illustrating the potential of our approach to not only identify bacteria but also to improve antibiotic stewardship by reducing the use of broad spectrum antibiotics.

In this study, we utilize bacterial glycolipid extracts in a manner analogous to the protein-based platform to identify the ESKAPE pathogens by MALDI-TOF-MS. Using a single extraction protocol originally designed for LPS extraction, we were able to differentiate all ESKAPE pathogens by dot product analyses of their mass spectra. Furthermore, a glycolipid mass spectral library containing 50 unique microbial entries including the ESKAPE pathogens was built using the database and software package of the MALDI Biotyper, which is a platform currently in use in the clinical laboratory. Importantly for clinical use, the glycolipid-based method has an advantage over the protein-based approach: antimicrobial resistant strains could be distinguished from the related susceptible strains in tested cases. These results suggest developing MS glycolipid profiling as a diagnostic platform that could impact clinical practice.

## **Results**

**Glycolipid mass spectral library construction.** For generation of high-quality mass spectra for inclusion in the library, samples were grown in liquid culture and lipids

extracted as described by El Hamidi et al. (131). This small-scale ammonium isobutyrate extraction disrupts the membrane and liberates the glycolipids (LA, LTA, and DAG) from their polysaccharide constituents. To account for previously observed differences in glycolipid structure when growth temperature is altered, bacteria were grown at both 25°C and 37°C and their extracts were analyzed by MALDI-TOF-MS in negative ion mode over a limited mass range  $m/z$  1,000-2,400 using the matrix norharmane (132). The strategy that allowed for the generation of an optimized mass spectral library consisting of a minimum of twelve unique strains per ESKAPE pathogen is outlined in **Figure 2.1**. **Table 2.1** lists the individual strains used in this study. This process resulted in a mass spectral ESKAPE pathogen library of six unique species and an additional 44 non-ESKAPE pathogens used as decoys for further analyses (**Table 2.2**).

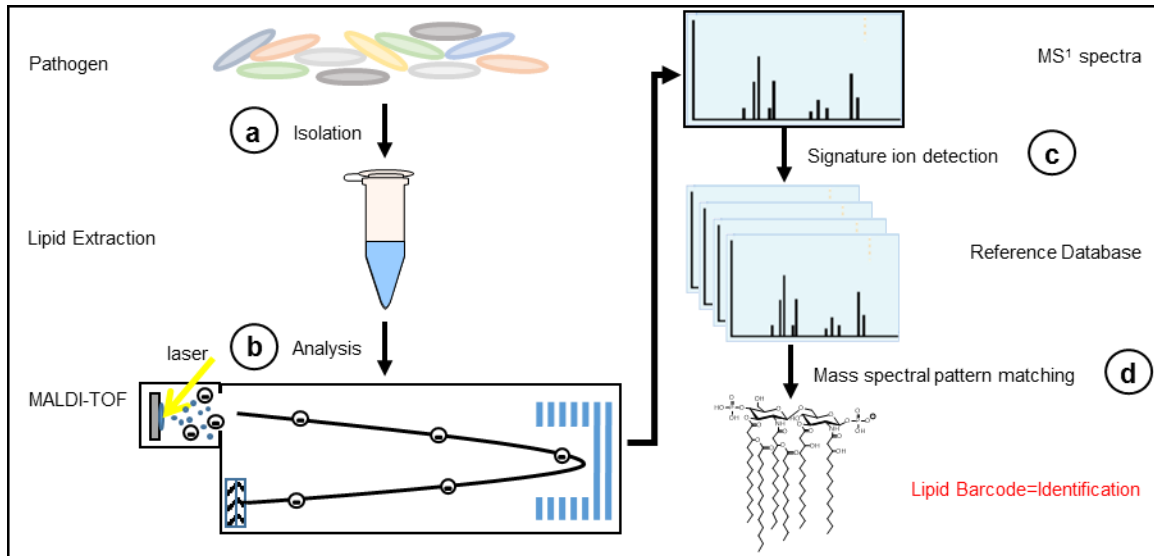


**Figure 2.1. Strategy for glycolipid-based mass spectrometry platform for pathogen identification.** (a) Microbes are isolated from pure culture or biological specimen and whole cell lipids are extracted by hot ammonium-isobutyrate (b) Lipid extracts are purified and analyzed by MALDI-TOF-MS (c) A mass spectrum of membrane glycolipids is acquired and compared against an extensive reference database of mass spectral profiles from known organisms via pattern-matching to (d) Generate a digital identification output and an assigned confidence score.

**Table 2.1. List of all ESKAPE pathogen strains used in this study.**

Organism	Strain name	Map assignment	MIC	Source/resistance	Origin
<i>Enterococcus faecium</i>	YD1	Ec1		ICU patient	Y. Doi
	YD2	Ec2		ICU patient	Y. Doi
	YD3	Ec3		ICU patient	Y. Doi
	YD4	Ec4		ICU patient	Y. Doi
	YD5	Ec5		ICU patient	Y. Doi
	YD6	Ec6		ICU patient	Y. Doi
	YD7	Ec7		ICU patient	Y. Doi
	YD8	Ec8		ICU patient	Y. Doi
	YD9	Ec9		ICU patient	Y. Doi
	YD10	Ec10		ICU patient	Y. Doi
	YD11			VRE	Y. Doi
	YD12			VRE	Y. Doi
<i>Staphylococcus aureus</i>	8325-4	S1		Methicillin susceptible	M. Shirtliff
	WT	S2		Methicillin susceptible	M. Shirtliff
	RN4220	S3		Methicillin susceptible	M. Shirtliff
	RN6390	S4		Methicillin susceptible	M. Shirtliff
	Seattle 1945	S5		Methicillin susceptible	M. Shirtliff
	M2	S6		Methicillin resistant	M. Shirtliff
	NRS123	S7		Methicillin resistant	M. Shirtliff
	NRS384	S8		Methicillin resistant	M. Shirtliff
	NRS385	S9		Methicillin resistant	M. Shirtliff
	NRS484	S10		Methicillin resistant	M. Shirtliff
	NRS72			Methicillin susceptible	M. Shirtliff
	M1			Methicillin susceptible	M. Shirtliff
	NRS22			Methicillin resistant	M. Shirtliff
	NRS382			Methicillin resistant	M. Shirtliff
	NRS1			Methicillin resistant	M. Shirtliff
	NRS100			Methicillin resistant	M. Shirtliff
	NRS387			Methicillin resistant	M. Shirtliff
DOH040			Methicillin resistant	Y. Doi	
DOH075			Methicillin resistant	Y. Doi	
<i>Klebsiella pneumoniae</i>	A2 Obscure	K1	0.38	Abdominal fluid	Y. Doi
	B3 Bright	K2	0.25	Foley drainage	Y. Doi
	C4	K3	0.38	JP drainage	Y. Doi
	D4	K4	0.38	Blood	Y. Doi
	TBE818	K5	0.5		Y. Doi
	A5	K6	>256	BAL	Y. Doi
	B6	K7	>256	Urine	Y. Doi
	C6	K8	16	Urine	Y. Doi
	F9	K9	8		Y. Doi
	I4	K10	16	Urine	Y. Doi
	TBE812		0.25		R. Ernst
	TBE815		0.25		R. Ernst
	TBE817		0.25		R. Ernst
	TBE821		0.13		R. Ernst
	TBE823		1		R. Ernst
	TBE847		1		R. Ernst
	B3 Obscure		0.25		Y. Doi
	B5		0.25		Y. Doi
	B8		0.25		Y. Doi
	E5		0.25		Y. Doi
	F2		0.25		Y. Doi
	F8		0.38		Y. Doi
	G7		0.38		Y. Doi
	H4 Bright		0.25		Y. Doi
	I1		0.25		Y. Doi
	A8-BL13802		S		M. Hughes

**Table 2.1 Continued**

Organism	Strain name	Map assignment	MIC	Source/resistance	Origin
<i>Klebsiella pneumoniae</i>	A9-BL12125		S		M. Hughes
	A11-BL12456		S		M. Hughes
	C8-KKBO-1		S		M. Hughes
	C9-KPB-1		S		M. Hughes
	TBE805		>64		R. Ernst
	TBE806		>128		R. Ernst
	TBE810		>256		R. Ernst
	TBE811		>256		R. Ernst
	TBE813		>64		R. Ernst
	TBE814		>256		R. Ernst
	TBE820		>64		R. Ernst
	TBE824		>256		R. Ernst
	TBE827		>256		R. Ernst
	B9		>256		Y. Doi
	C3		128		Y. Doi
	C5		128		Y. Doi
	C8		64		Y. Doi
	D1		16		Y. Doi
	D7		256	BAL	Y. Doi
	E6		8		Y. Doi
	F3		128		Y. Doi
	H5		64		Y. Doi
	I2		>256		Y. Doi
	A1-BL849		R		M. Hughes
	A2-BA3783		R		M. Hughes
	A3-BU19801		R		M. Hughes
	A4-BA2664		R		M. Hughes
	A5-BL8800		R		M. Hughes
	A6-BA2880		R		M. Hughes
	A7-MS84		R		M. Hughes
C14-KKBO-1 mut_1		R		M. Hughes	
C5-KKBO-4		R		M. Hughes	
C6-KPB-2		R		M. Hughes	
<i>Acinetobacter baumannii</i>	EAS011	A1	1	BAL	Y. Doi
	MWH019	A2	1	BAL	Y. Doi
	PM3757	A3	0.5	Urine	Y. Doi
	TBE0122	A4	2	BAL	R. Ernst
	YD14	A5	1	Sputum	Y. Doi
	EAS004	A6	>128	Sputum	Y. Doi
	SM1590	A7	4	Tracheal aspirate	Y. Doi
	PM3714	A8	16	Sputum	Y. Doi
	PM3839	A9	32	Sputum	Y. Doi
	PM3850	A10	64	Abscess	Y. Doi
	EAS001		0.5		Y. Doi
	EAS002		0.5		Y. Doi
	EAS005		0.5		Y. Doi
	EAS006		0.5		Y. Doi
	EAS008		0.5		Y. Doi
	EAS009		0.5		Y. Doi
	EAS010		1		Y. Doi
	EAS019		0.5		Y. Doi
	EAS025		0.5		Y. Doi
	EAS028		0.25		Y. Doi
	MWH001		0.5		Y. Doi
	MWH007		0.5		Y. Doi

**Table 2.1 Continued**

Organism	Strain name	Map assignment	MIC	Source/resistance	Origin
<i>Acinetobacter baumannii</i>	MWH008		0.5		Y. Doi
	MWH009		0.5		Y. Doi
	MWH011		0.5		Y. Doi
	MWH012		1		Y. Doi
	MWH013		0.5		Y. Doi
	MWH014		0.5		Y. Doi
	MWH021		1		Y. Doi
	MWH023		1		Y. Doi
	MWH031		0.5		Y. Doi
	SM1533		0.5		Y. Doi
	SM1534		0.5		Y. Doi
	SM1536		0.5		Y. Doi
	SM1537		0.5		Y. Doi
	SM1538		1		Y. Doi
	SM1539		0.5		Y. Doi
	SM1540		1		Y. Doi
	SM1544 # 1		1		Y. Doi
	SM1544 # 2		0.5		Y. Doi
	SM1545		0.5		Y. Doi
	SM1549		0.5		Y. Doi
	SM1551		0.5		Y. Doi
	SM1560		0.5		Y. Doi
	SM1561		1		Y. Doi
	SM1562		1		Y. Doi
	SM1565		0.5		Y. Doi
	SM1566		0.5		Y. Doi
	SM1567		0.5		Y. Doi
	SM1568		0.5		Y. Doi
	SM1569		0.5		Y. Doi
	SM1571		0.5		Y. Doi
	SM1572		0.5		Y. Doi
	SM1574		1		Y. Doi
	SM1577		0.5		Y. Doi
	SM1578		0.5		Y. Doi
	SM1579		1		Y. Doi
	SM1580		1		Y. Doi
	SM1584		1		Y. Doi
	SM1587		1		Y. Doi
	SM1594		0.5		Y. Doi
	SM1596		0.5		Y. Doi
	SM1599		0.5		Y. Doi
	SM1600		0.5		Y. Doi
	SM1601		0.5		Y. Doi
	SM1602		0.5		Y. Doi
	SM1603		0.5		Y. Doi
	SM1604		0.5		Y. Doi
	SM1607		0.5		Y. Doi
	SM1608		0.5		Y. Doi
	SM1610		0.5		Y. Doi
	SM1627		0.5		Y. Doi
	SM1629		0.5		Y. Doi
	SM1632		1		Y. Doi
	SM1636		0.5		Y. Doi
	SM1639		1		Y. Doi
	SM1645		0.5		Y. Doi
	SM1658		0.5		Y. Doi

**Table 2.1 Continued**

Organism	Strain name	Map assignment	MIC	Source/resistance	Origin
<i>Acinetobacter baumannii</i>	SM1660		1		Y. Doi
	SM1662		1		Y. Doi
	SM1665		0.5		Y. Doi
	SM1670		0.5		Y. Doi
	SM1672		0.5		Y. Doi
	SM1673		0.5		Y. Doi
	SM1675		0.5		Y. Doi
	SM1679		0.5		Y. Doi
	SM1680		0.5		Y. Doi
	SM1684		0.5		Y. Doi
	SM1685		0.5		Y. Doi
	SM1686		0.5		Y. Doi
	SM1687		0.5		Y. Doi
	SM1688		1		Y. Doi
	SM1689		1		Y. Doi
	PM3632		1		Y. Doi
	PM3636		2		Y. Doi
	PM3638		1		Y. Doi
	PM3640		1		Y. Doi
	PM3641		1		Y. Doi
	PM3642		0.5		Y. Doi
	PM3643		1		Y. Doi
	PM3647		1		Y. Doi
	PM3648		0.5		Y. Doi
	PM3651		1		Y. Doi
	PM3652		1		Y. Doi
	PM3654		0.5		Y. Doi
	PM3654a		0.5		Y. Doi
	PM3658		0.5		Y. Doi
	PM3661		1		Y. Doi
	PM3663		1		Y. Doi
	PM3664		1		Y. Doi
	PM3665		0.5		Y. Doi
	PM3667		1		Y. Doi
	PM3669		1		Y. Doi
	PM3672		1		Y. Doi
	PM3680		1		Y. Doi
	PM3682		1		Y. Doi
	PM3685		1		Y. Doi
	PM3693		1		Y. Doi
	PM3694		1		Y. Doi
	PM3696		1		Y. Doi
	PM3698		0.5		Y. Doi
	PM3700		1		Y. Doi
	PM3701		0.5		Y. Doi
	PM3716		1		Y. Doi
	PM3718		0.5		Y. Doi
	PM3719		1		Y. Doi
PM3720		0.5		Y. Doi	
PM3721		1		Y. Doi	
PM3722		1		Y. Doi	
PM3723		0.5		Y. Doi	
PM3724		0.5		Y. Doi	
PM3725		2		Y. Doi	
PM3726		0.5		Y. Doi	
PM3728		0.5		Y. Doi	

**Table 2.1 Continued**

Organism	Strain name	Map assignment	MIC	Source/resistance	Origin
<i>Acinetobacter baumannii</i>	PM3731		0.5		Y. Doi
	PM3735		0.5		Y. Doi
	PM3740		0.5		Y. Doi
	PM3741		0.5		Y. Doi
	PM3742		0.5		Y. Doi
	PM3743		0.5		Y. Doi
	PM3748		0.5		Y. Doi
	PM3749		0.5		Y. Doi
	PM3752		0.25		Y. Doi
	PM3753		0.25		Y. Doi
	PM3754		0.25		Y. Doi
	PM3762		0.5		Y. Doi
	PM3769		0.5		Y. Doi
	PM3776		0.5		Y. Doi
	PM3778		0.5		Y. Doi
	PM3786		0.5		Y. Doi
	PM3790		0.5		Y. Doi
	PM3793		0.5		Y. Doi
	PM3795		1		Y. Doi
	PM3796		1		Y. Doi
	PM3797		1		Y. Doi
	PM3798		0.5		Y. Doi
	PM3801		1		Y. Doi
	PM3802		1		Y. Doi
	PM3809		1		Y. Doi
	PM3811		1		Y. Doi
	PM3813		1		Y. Doi
	PM3817		0.5		Y. Doi
	PM3820		1		Y. Doi
	PM3821		1		Y. Doi
	PM3823		0.5		Y. Doi
	PM3824		0.5		Y. Doi
	PM3827		0.5		Y. Doi
	PM3828		0.5		Y. Doi
	PM3829		1		Y. Doi
	PM3831		0.5		Y. Doi
	PM3833		0.5		Y. Doi
	PM3834		0.5		Y. Doi
	PM3836		1		Y. Doi
	PM3844		1		Y. Doi
	PM3845		1		Y. Doi
	PM3848		1		Y. Doi
	PM3865		0.5		Y. Doi
	PM3892		0.5		Y. Doi
	PM3897		0.5		Y. Doi
	PM3898		1		Y. Doi
	PM3905		1		Y. Doi
PM3907		0.5		Y. Doi	
PM3908		1		Y. Doi	
PM3918		0.5		Y. Doi	
PM3929		0.5		Y. Doi	
PM3930		0.5		Y. Doi	
ATCC17978		1		Y. Doi	
TBE779		1		R. Ernst	
TBE1020		1		R. Ernst	
TBE1023		2		R. Ernst	

**Table 2.1 Continued**

Organism	Strain name	Map assignment	MIC	Source/resistance	Origin
<i>Acinetobacter baumannii</i>	TBE1025		2	Urine	R. Ernst
	TBE1029		2		R. Ernst
	TBE1015		>128		R. Ernst
	TBE1021		>256		R. Ernst
	TBE1027		>256		R. Ernst
	TBE1031		>256		R. Ernst
	EAS003		>128		Y. Doi
	SM1589		4		Y. Doi
	SM1591		4		Y. Doi
	SM1592		4		Y. Doi
	SM1622		4		Y. Doi
	SM1624		4		Y. Doi
	SM1637		64		Y. Doi
	SM1682		32		Y. Doi
	SM1683		32		Y. Doi
	PM3633		>128		Y. Doi
	PM3849		8		Y. Doi
	PM3855		>128		Y. Doi
	PM3859		32		Y. Doi
	PM3860		>128		Y. Doi
PM3911		8	Y. Doi		
PM3914		16	Y. Doi		
<i>Pseudomonas aeruginosa</i>	ATCC31482	P1			ATCC
	ATCC55734	P2			ATCC
	ATCC700888	P3			ATCC
	ATCC700829	P4			ATCC
	V022	P5			R. Ernst
	BE402	P6			R. Ernst
	YD15	P7			Y. Doi
	TRPA179	P8			Y. Doi
	ATCC47085	P9			ATCC
	PAO1	P10			R. Ernst
	ATCC43495				ATCC
	V015				R. Ernst
	V055				R. Ernst
	V093				R. Ernst
TRPA087				Y. Doi	
<i>Enterobacter cloacae</i>	FN2541	Eb1		ICU patient	J.K. Johnson
	FN2542	Eb2		ICU patient	J.K. Johnson
	FN2543	Eb3		ICU patient	J.K. Johnson
	YDC590	Eb4		Bronchial wash	Y. Doi
	YDC673	Eb5		Perigastric fluid	Y. Doi
	YDC665	Eb6		BAL	Y. Doi
	YDC470	Eb7			Y. Doi
	YDC482	Eb8			Y. Doi
	YDC541	Eb9			Y. Doi
	YDC612	Eb10		BAL	Y. Doi
	FN2532			ICU patient	J.K. Johnson
	YDC560-1				Y. Doi
	YDC611				Y. Doi

**Table 2.2. List of species, strains and mass spectra in Biotyper glycolipid library.**

Class	Organism	Strain	# replicates	Origin
Gram-negative bacteria	<i>Bordetella pertussis</i>	Wild-type	4	R. Ernst
	<i>Brucella abortus</i>	2308	2	R. Ernst
	<i>Brucella melitensis</i>	16M	1	R. Ernst
	<i>Brucella suis</i>	1330	1	R. Ernst
	<i>Burkholderia cenocepacia</i>	CEP0790	7	R. Ernst
		N3	2	R. Ernst
		ATCC 17759	6	ATCC
	<i>Burkholderia multivorans</i>	ATCC 17616	9	ATCC
	<i>Citrobacter</i> spp.	M12	1	Y. Doi
		M17	1	Y. Doi
		BL17316	8	M. Hughes
	<i>Enterobacter aerogenes</i>	ENF 10856	6	BD Biosciences
		ENF 11218	7	BD Biosciences
		ENF 11237	10	BD Biosciences
		YDC497	6	Y. Doi
	<i>Enterobacter sakazakii</i>	YD255	3	Y. Doi
		YD256	2	Y. Doi
	<i>Escherichia coli</i>	K12	46	R. Ernst
		ENF 18187	8	BD Biosciences
		ATCC 25922	2	ATCC
		YDC107	3	Y. Doi
		YD626	2	Y. Doi
	<i>Franciscella novicida</i>	U112	39	R. Ernst
	<i>Francisella tularensis holarctica</i>	LVS	2	R. Ernst
	<i>Klebsiella oxytoca</i>	ENF 3950	9	BD Biosciences
		ENF 4321	9	BD Biosciences
		ENF 11686	9	BD Biosciences
	<i>Legionella bozemanii</i>	4648	4	T. McNealy
	<i>Legionella pneumophila</i>	ATCC LA-1	3	ATCC
		ATCC Concord 3	3	ATCC
		ATCC Bloom 2	4	ATCC
		ATCC 33152	4	ATCC
		5099	3	T. McNealy
		4632	3	T. McNealy
	1782	3	T. McNealy	
	<i>Legionella wadsworthii</i>	5706	3	T. McNealy
	<i>Morganella morgannii</i>	YDC562	6	Y. Doi
		YDC700	6	Y. Doi
		YDC721	6	Y. Doi
		YDC723	5	Y. Doi
<i>Porphyromonas gingivalis</i>	W50	13	R. Ernst	
<i>Proteus mirabilis</i>	YDC672-1	8	R. Ernst	
	YDC714	6	Y. Doi	
	NO-051/03	6	Y. Doi	
	NO-051/03	6	M. Hughes	
<i>Providencia rettgeri</i>		9	Y. Doi	
<i>Providencia stuartii</i>	YDC737	8	Y. Doi	
	YDC672-2	6	Y. Doi	
	YD257	6	Y. Doi	
<i>Pseudomonas fluorescens</i>	ATCC BAA-477	6	R. Ernst	
<i>Pseudomonas fluorescens</i>	BE561	1	R. Ernst	
<i>Pseudomonas putida</i>	ATCC 700007	2	R. Ernst	
	6732-1	3	R. Ernst	
	ATCC 49128	1	R. Ernst	
	BE560	1	R. Ernst	
<i>Pseudomonas stutzeri</i>	TBE589	1	R. Ernst	

**Table 2.2 Continued**

Class	Organism	Strain	# replicates	Origin
Gram-negative bacteria	<i>Salmonella minnesota</i>	R595	10	R. Ernst
	<i>Salmonella typhimurium</i>	CS339	9	R. Ernst
	<i>Serratia marcescens</i>	SM3	13	Y. Doi
		SM4	10	Y. Doi
		SM5	10	Y. Doi
		SM8	1	Y. Doi
		SM11	10	Y. Doi
		SM12	10	Y. Doi
		SM13	7	Y. Doi
		YDC507	3	Y. Doi
		YDC563	4	Y. Doi
		YDC583	3	Y. Doi
		YDC591	3	Y. Doi
		YDC609	4	Y. Doi
		YDC629	3	Y. Doi
		YDC639	3	Y. Doi
YDC647	3	Y. Doi		
YDC719	3	Y. Doi		
	5	7	M. Hughes	
<i>Stenotrophomonas maltophilia</i>	CF2	5	R. Ernst	
<i>Yersinia enterocolitica</i>	CS080	10	R. Ernst	
<i>Yersinia pestis</i>	KIM6-pCDI-pgm	10	R. Ernst	
	KIM6+ (Bliska)	2	R. Ernst	
<i>Yersinia pseudotuberculosis</i>	01:b	6	R. Ernst	
Gram-positive bacteria	<i>Clostridium difficile</i>	630	1	R. Ernst
		uk1	1	R. Ernst
	<i>Enterococcus faecalis</i>	FN1	3	J.K. Johnson
		FN2	7	J.K. Johnson
		FN14	5	J.K. Johnson
		FN39	8	J.K. Johnson
		FN45	5	J.K. Johnson
		FN46	4	J.K. Johnson
		FN59	8	J.K. Johnson
		FN69	6	J.K. Johnson
		FN71	6	J.K. Johnson
		FN77	7	J.K. Johnson
		YD258	3	Y. Doi
		YD259	3	Y. Doi
		YD260	3	Y. Doi
		YD261	2	Y. Doi
	<i>Staphylococcus epidermidis</i>	POS 10235	6	BD Biosciences
	<i>Staphylococcus haemolyticus</i>	POS 10866	6	BD Biosciences
		POS 8764	3	BD Biosciences
	<i>Staphylococcus lugdunensis</i>	POS 8659	3	BD Biosciences
		POS 10768	1	BD Biosciences
	<i>Streptococcus mitis</i>	POS 4489	6	BD Biosciences
	<i>Streptococcus mitis</i>	POS 5586	6	BD Biosciences
	<i>Streptococcus mutans</i>	POS 1260	6	BD Biosciences
		POS 5593	5	BD Biosciences
	<i>Streptococcus pneumoniae</i>	POS 6289	4	BD Biosciences
		POS 6892	3	BD Biosciences
		POS 10164	2	BD Biosciences
	<i>Streptococcus sanguinis</i>	POS 4696	6	BD Biosciences
POS 5589		6	BD Biosciences	
Fungi	<i>Candida albicans</i>	YST 1032	3	BD Biosciences
		YST 1369	4	BD Biosciences

**Table 2.2 Continued**

Class	Organism	Strain	# replicates	Origin
Fungi	<i>Candida albicans</i>	YST 1862	4	BD Biosciences
		YD262	3	Y. Doi
		YD263	3	Y. Doi
	<i>Candida glabrata</i>	YD264	4	Y. Doi
		YD265	3	Y. Doi
	<i>Candida krusei</i>	YD266	3	Y. Doi
	<i>Candida parapsilosis</i>	YD267	3	Y. Doi
<b>TOTAL</b>	<b>44</b>	<b>117</b>	<b>655</b>	

**Lipid extraction and MALDI-TOF-MS reproducibility.** To evaluate the reproducibility of mass spectra produced by analysis of extracts between different glycolipid extractions and cultures, five independent biological cultures of *P. aeruginosa* were grown daily (intra-day) over five consecutive days (inter-day) producing a total of 25 mass spectra. In addition, 30 technical extraction replicates were generated from a single culture and processed on the same day. A single mass spectrum from each sample was recorded per day. Under consistent culture, extraction, and analysis conditions, similar profiles were produced with the expected *P. aeruginosa* signature ions at  $m/z$  1430, 1446, and 1616 (**Figure 2.2**). As shown in **Figure 2.3**, signature ions are defined as those ions that are unique to a given species. The mass spectra were combined to generate an MSP (Main SPectra), which is a projection of multiple mass spectra used by the MALDI Biotyper, and added to the library containing MSPs from 50 unique microorganisms including the ESKAPE pathogens within the Biotyper software package. Using the Biotyper's software platform, each individual mass spectrum was then compared against the library of summed mass spectra. Confidence scores, which reflect the strength of the identification, were subsequently determined with a mean log confidence score of  $2.87 \pm 0.014$  (mean  $\pm$  variance) for intra-/inter-day variability and  $2.86 \pm 0.004$  (mean  $\pm$  variance) for 30-replicate variability (**Figure 2.2**). These values are comparable to Bruker's protein-based scores that advise any score between 2.0 and 3.0 as a high positive species identification probability.

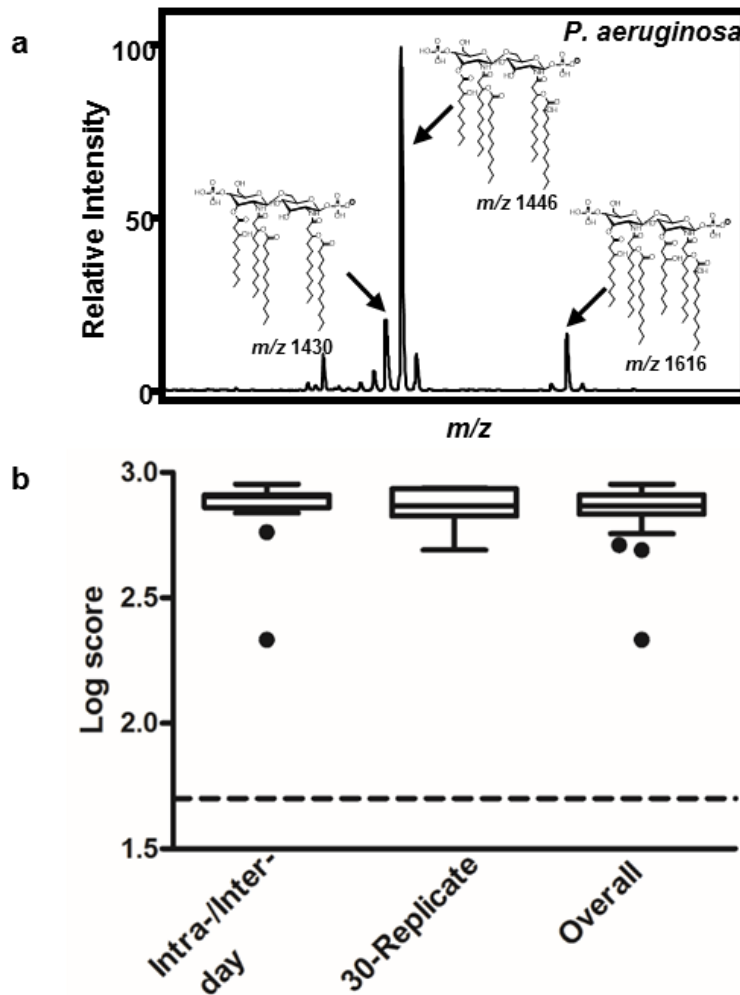


**Figure 2.2. Variability determination for *P. aeruginosa*.** Bacterial cultures of *P. aeruginosa* PAK laboratory strain were grown, lipids were extracted, and extracts were analyzed by MALDI-TOF to ensure reproducibility of biological and technical replicates during mass spectral library generation. (a) One mass spectrum is shown here with chemical structures of lipid A molecules for the annotated ions listed and (b) Median log confidence scores of the MALDI Biotyper when *P. aeruginosa* mass spectral replicates were compared against the glycolipid library for the Intra-/Inter-day and 30-replicate variability assays. Dashed line indicates the threshold cutoff of a probable positive identification (=1.7).

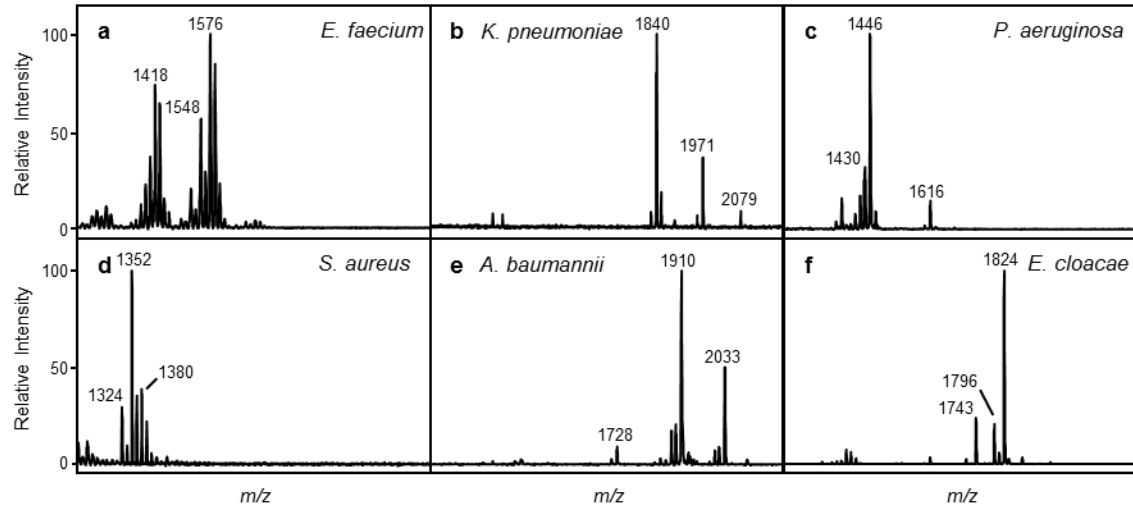


**Figure 2.3. Representative mass spectra from ESKAPE pathogens: (a)** Enterococcus faecium; **(b)** Klebsiella pneumoniae; **(c)** Pseudomonas aeruginosa; **(d)** Staphylococcus aureus; **(e)** Acinetobacter baumannii; and, **(f)** Enterobacter cloacae. m/z values of select ions are given.

**Species-specific signature ions differentiate all ESKAPE pathogens.** To objectively determine whether the observed differences between mass spectra for all ESKAPE pathogens (**Figure 2.3**) would permit differentiation, we carried out pair-wise dot product analyses of all ESKAPE mass spectra (133). A minimum signal-to-noise of 8.0 (optimized to ensure only *bona fide*  $m/z$  values for glycolipid ions were considered) was used to cull low-quality mass spectra with the remainder being assembled into lists of ions containing  $m/z$  and normalized ion intensity for each mass spectrum. The dot product between pairs of ion lists was calculated as a measure of similarity between mass spectra. This resulted in a mass spectral similarity score between 0 (least similar) and 1 (identical), shown as a heat map of representative strains in **Figure 2.4** with similarity scores listed in **Table 2.3**. In addition to the ability to distinguish all ESKAPE species from one another, glycolipid mass spectra were able to distinguish *K. pneumoniae*, *P. aeruginosa*, and *E. cloacae* grown at 25 and 37°C, temperatures that mimic insect and mammalian growth conditions, respectively. As an example, we observed a shift in the base peak from  $m/z$  1796 to 1840 for *K. pneumoniae* strains grown at 37°C versus those grown at 25°C (**Figure 2.5**), which is known to result from an exchange of a laurate (C12:0) for a myristate (C14:0) at the C-2' position of the glucosamine backbone and a hydroxylation of the 2' acyl-oxo-acyl group (134). **Figure 2.6** provides a more comprehensive dot product comparison with ten strains per ESKAPE pathogen. Hierarchical clustering further demonstrates the ability to differentiate between the individual ESKAPE pathogens by their glycolipid mass spectra. In addition, *K. pneumoniae* and *A. baumannii* strains with resistance to colistin clustered together, illustrating the potential to distinguish resistant isolates.

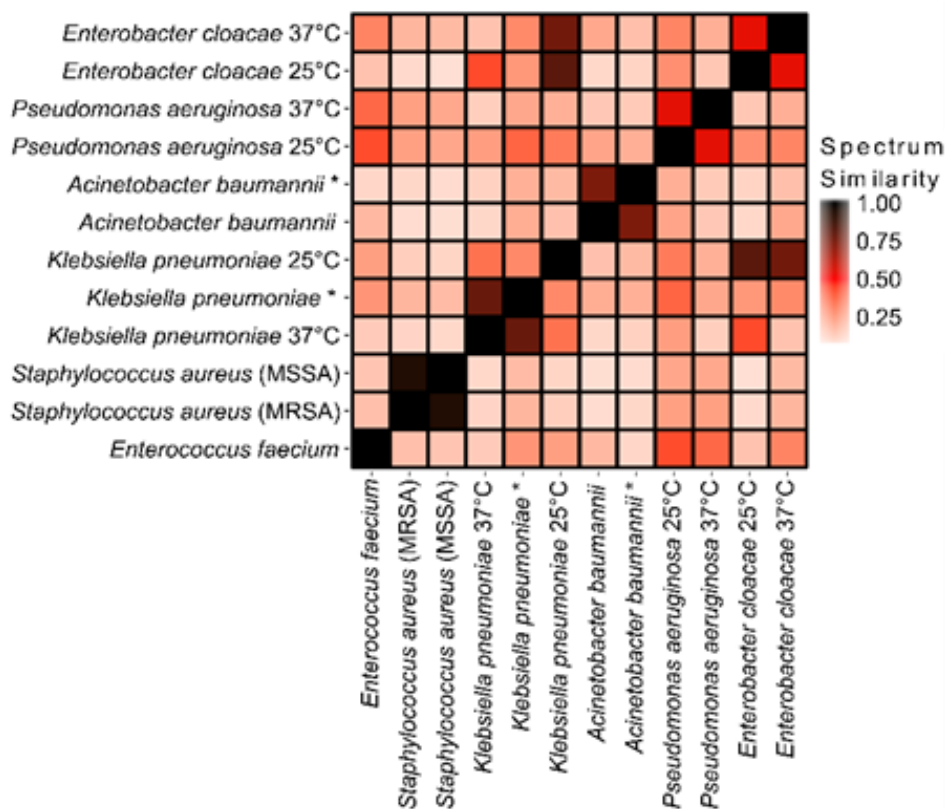


**Figure 2.4. Dot product analysis of mass spectra for differentiation of ESKAPE pathogens.** Mass spectra were acquired from lipid extracts of each ESKAPE pathogen. Species were compared by calculating a pairwise dot product between mass lists of ions from each mass spectrum, a measure of spectrum similarity. A similarity score of 1.0 is an identical match (black squares). White squares represent a score of 0.0 where there is no match. (\*) indicate colistin-resistant strains.

Table 2.3. Similarity scores for small heat map dot product comparison.

	<i>Enterococcus faecium</i>	<i>Staphylococcus aureus</i> (MRSA)	<i>Staphylococcus aureus</i>	<i>Klebsiella pneumoniae</i> 37°C	<i>Klebsiella pneumoniae</i> *	<i>Klebsiella pneumoniae</i> 25°C	<i>Acinetobacter baumannii</i>	<i>Acinetobacter baumannii</i> *	<i>Pseudomonas aeruginosa</i> 25°C	<i>Pseudomonas aeruginosa</i> 37°C	<i>Enterobacter cloacae</i> 25°C	<i>Enterobacter cloacae</i> 37°C
<i>Enterobacter cloacae</i> 37°C	0.31	0.19	0.18	0.16	0.30	0.77	0.23	0.17	0.31	0.21	0.54	1.00
<i>Enterobacter cloacae</i> 25°C	0.16	0.10	0.09	0.43	0.27	0.82	0.10	0.11	0.29	0.15	1.00	0.54
<i>Pseudomonas aeruginosa</i> 37°C	0.38	0.25	0.23	0.13	0.23	0.21	0.15	0.14	0.55	1.00	0.15	0.21
<i>Pseudomonas aeruginosa</i> 25°C	0.43	0.25	0.23	0.25	0.38	0.33	0.24	0.21	1.00	0.55	0.29	0.31
<i>Acinetobacter baumannii</i> *	0.11	0.11	0.09	0.12	0.21	0.18	0.75	1.00	0.21	0.14	0.11	0.17
<i>Acinetobacter baumannii</i>	0.18	0.09	0.09	0.11	0.21	0.16	1.00	0.75	0.24	0.15	0.10	0.23
<i>Klebsiella pneumoniae</i> 25°C	0.25	0.13	0.11	0.35	0.30	1.00	0.16	0.18	0.33	0.21	0.82	0.77
<i>Klebsiella pneumoniae</i> *	0.27	0.19	0.18	0.79	1.00	0.30	0.21	0.21	0.38	0.23	0.27	0.30
<i>Klebsiella pneumoniae</i> 37°C	0.14	0.11	0.10	1.00	0.79	0.35	0.11	0.12	0.25	0.13	0.43	0.16
<i>Staphylococcus aureus</i>	0.15	0.95	1.00	0.10	0.18	0.11	0.09	0.09	0.23	0.23	0.09	0.18
<i>Staphylococcus aureus</i> (MRSA)	0.17	1.00	0.95	0.11	0.19	0.13	0.09	0.11	0.25	0.25	0.10	0.19
<i>Enterococcus faecium</i>	1.00	0.17	0.15	0.14	0.27	0.25	0.18	0.11	0.43	0.38	0.16	0.31

\* (\*) indicates colistin resistance

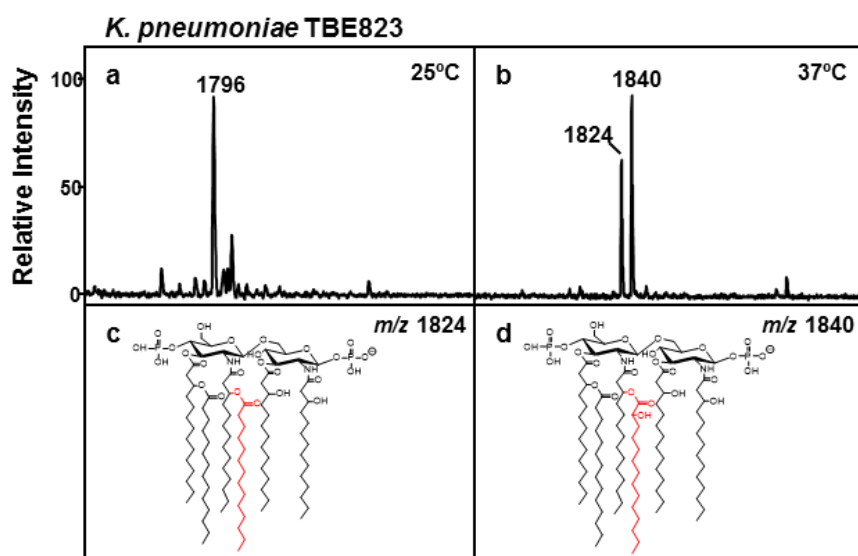


**Figure 2.5. MALDI-TOF MS of *K. pneumoniae* grown at different temperatures.** *K. pneumoniae* TBE823 strain grown overnight in liquid culture at 25°C (**a**) and 37°C (**b**) shows a base peak at  $m/z$  1796 at 25°C that shifts to  $m/z$  1824 (**c**) and 1840 (**d**) as the predominate ions at 37°C corresponding to transacylation and hydroxylation events, respectively, of the original hexa-acylated lipid A structure at  $m/z$  1796.

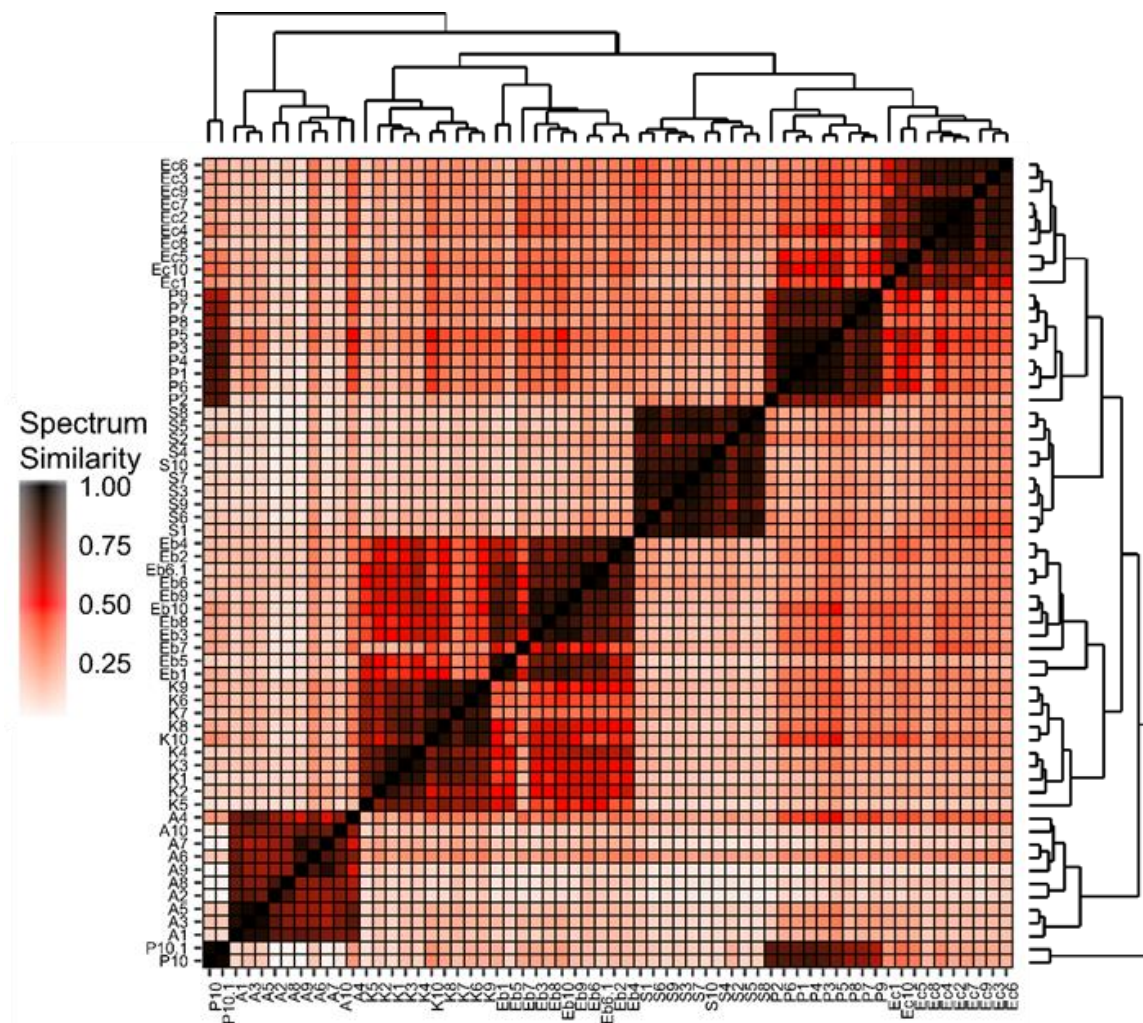
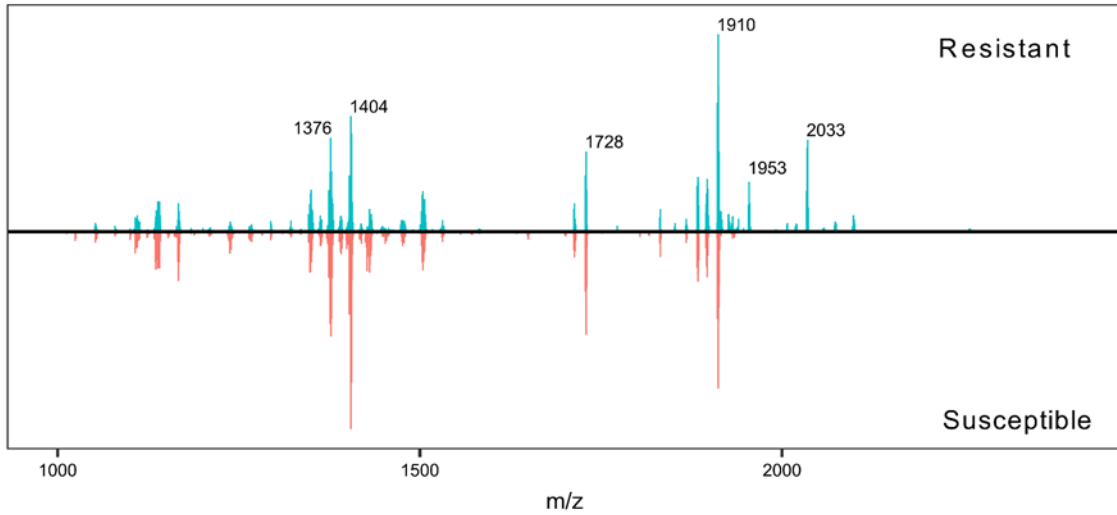


**Figure 2.6. Dot product analysis with hierarchical clustering for multiple replicates per ESKAPE pathogen.** Mass spectra from ten strains per ESKAPE species were compared by dot product and hierarchical clustering (Ec = *Enterococcus faecium*, S = *Staphylococcus aureus*, K = *Klebsiella pneumoniae*, A = *Acinetobacter baumannii*, P = *Pseudomonas aeruginosa*, Eb = *Enterobacter cloacae*). For *Acinetobacter* and *Klebsiella*, strains 1-5 are colistin-susceptible and 6-10 are colistin-resistant. Only  $m/z$  values for ions above an 8.0 signal-to-noise ratio were selected for comparison. The spectrum similarity score is the calculated dot product between mass lists from two mass spectra. A similarity score of 1.0 is an identical match (black squares). White squares represent a score of 0.0 where there is no match. Arrangement of strains in heat map reflect clustering shown in dendrogram (above).

**Detection of antimicrobial resistance.** To further assess the ability of our approach to identify resistance patterns to CAMPs, we examined clinical isolates of *K. pneumoniae* (60 clinical isolates) and *A. baumannii* (213 clinical isolates) obtained from patients admitted to the University of Pittsburgh Medical Center. For this analysis, colistin-susceptible isolates were determined to have a minimum inhibitory concentration (MIC)  $\leq 2$   $\mu\text{g/mL}$  colistin; resistant strains were determined by an MIC  $\geq 4$   $\mu\text{g/mL}$  according to recommendations of the Clinical and Laboratory Standards Institute (135). The colistin-resistant *A. baumannii* strain shows an additional ion at  $m/z$  2033 (summation of detected ions in **Figure 2.7a** and representative mass spectra in **Figure 2.8b**), reflecting an ethanolamine addition onto the terminal phosphate of  $m/z$  1910 (**Figure 2.8d**). In **Figure 2.7b** and **Figure 2.8f**, colistin-resistant *K. pneumoniae* strains clearly show unique ions at  $m/z$  1955 and 1971 that are not present in susceptible strains, a mass shift caused by an aminoarabinose addition to the hexa-acylated LA structures at  $m/z$  1824 and 1840 (**Figure 2.8g,h**). Ions at  $m/z$  1953 and 1891 result from a difference of one phosphate moiety ( $\Delta 80$  Da) from the modified lipid A structures at  $m/z$  2033 and 1971, respectively, and occur either from monophosphorylated lipid A residing in the membrane or degradation during extraction; these ions are also considered markers of resistance (129, 136). Consequently, there is a high positive correlation between these ions and resistance: when all library mass spectra were examined, we found that the presence of resistance ions (above a signal-to-noise ratio of 8) was detected by MS in 97.3% of *K. pneumoniae* and 88.9% of *A. baumannii* resistant isolates (as determined by MIC). Furthermore, we used dot product as a means to distinguish colistin susceptibility. Detected ions from 50% of all mass spectral replicates were summed to generate a consensus spectrum for each phenotype (A.

*baumannii* v. *K. pneumoniae*, susceptible v. resistant), and dot products were calculated between the remaining test set of mass spectra and the consensus spectrum in that phenotype (**Figure 2.9**). In general, mass spectra tended to achieve a higher similarity score when compared to the consensus spectrum with concurrent susceptibility; this is particularly evident for the *K. pneumoniae* strains. Finally, this platform was adapted to an existing clinical diagnostic, the MALDI Biotyper informatics package. All mass spectra from similar groups (susceptible and resistant) for these two species were assembled into MSPs. A randomized 30% of mass spectra were designated, and identifications were scored against the remaining 70% in addition to 50 organisms in the library (**Table 2.4**). Colistin-resistant strains of *K. pneumoniae* and *A. baumannii* were identified with accuracy rates of 69% and 92, respectively, for correctly predicting colistin susceptibility in tested strains and 88% and 92% positive species identification overall.

**a** *Acinetobacter baumannii*



**b** *Klebsiella pneumoniae*

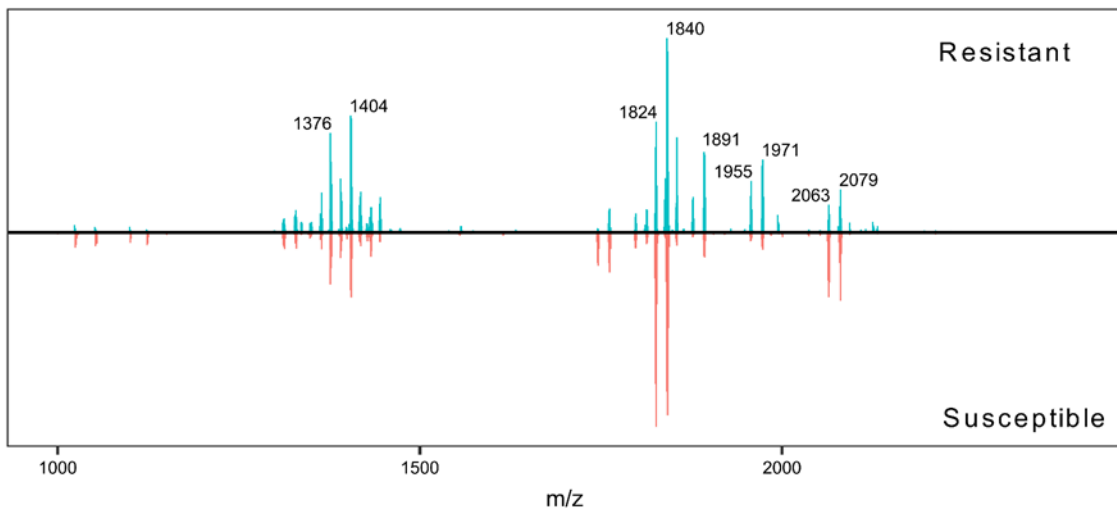


**Figure 2.7.** Consensus mass spectra were created by summation of detected ions from all replicates of colistin-resistant (top panels) and colistin-susceptible (bottom panels) *A. baumannii* (a) and *K. pneumoniae* (b). The mirrored consensus mass spectra highlight ions of core lipid A structures for *A. baumannii* ( $m/z$  1376, 1404, 1728, 1910) and *K. pneumoniae* ( $m/z$  1376, 1404, 1824, 1840, 2063, 2079). Importantly, these consensus spectra reveal consistent diagnostic ions for detecting colistin resistance in *A. baumannii* ( $m/z$  1953, 2033) and *K. pneumoniae* ( $m/z$  1891, 1955, 1971).

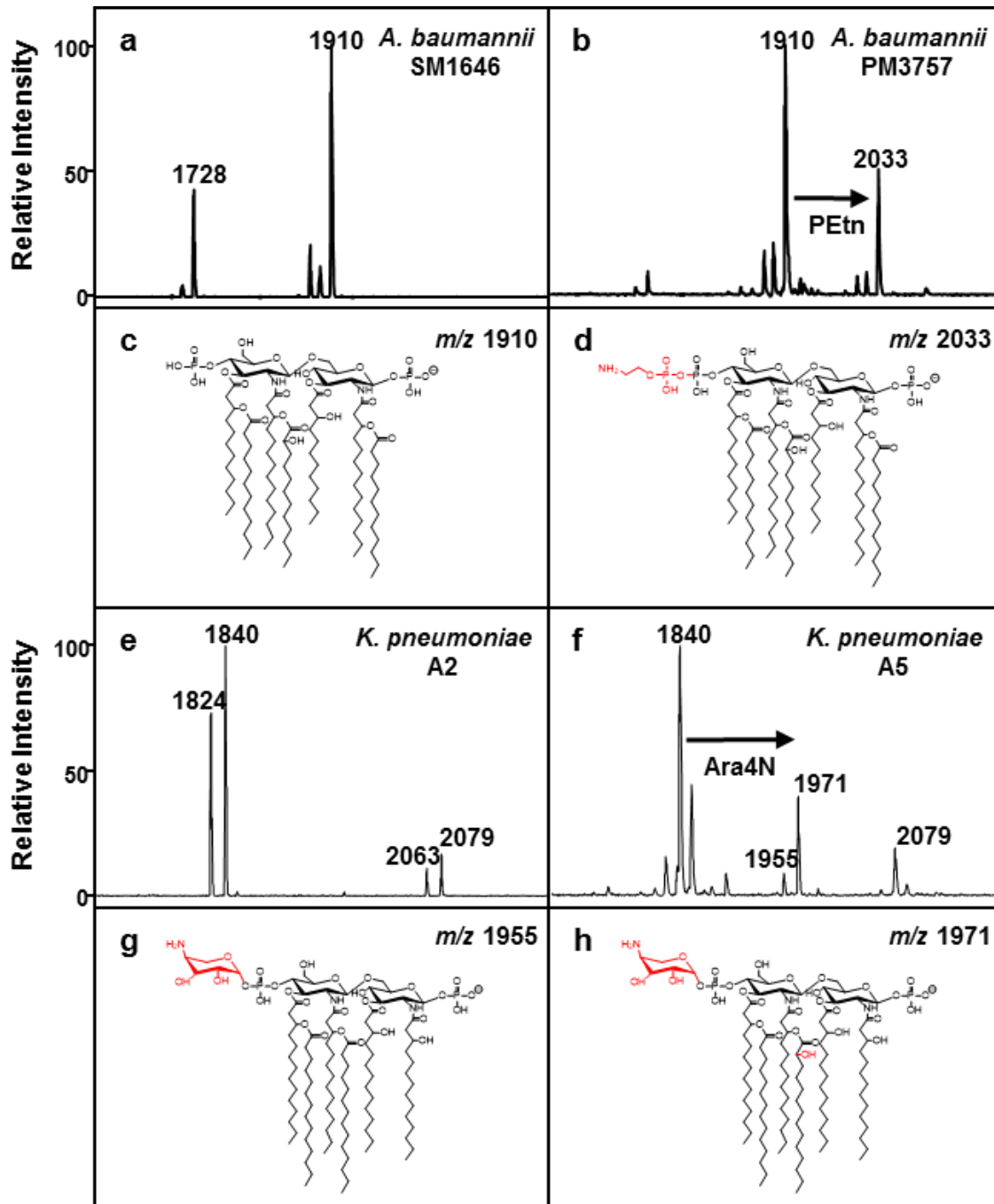


**Figure 2.8. MALDI-TOF-MS of *A. baumannii* and *K. pneumoniae* with differential colistin resistance.** Mass spectrum from *A. baumannii* colistin-susceptible strain SM1646 (a) and colistin-resistant strain PM3757 (b) with signature ions of hepta-acylated LA structure at  $m/z$  1910 (c) and  $m/z$  2033 (d) corresponding to a phosphoethanolamine (PEtn) addition to  $m/z$  1910. Mass spectrum from *K. pneumoniae* colistin-susceptible strain A2 (e) and colistin-resistant strain A5 (f) showing additional ions at  $m/z$  1955 (g) and 1971 (h) corresponding to an aminoarabinose (Ara4N) addition to the base structures at  $m/z$  1824 and 1840.

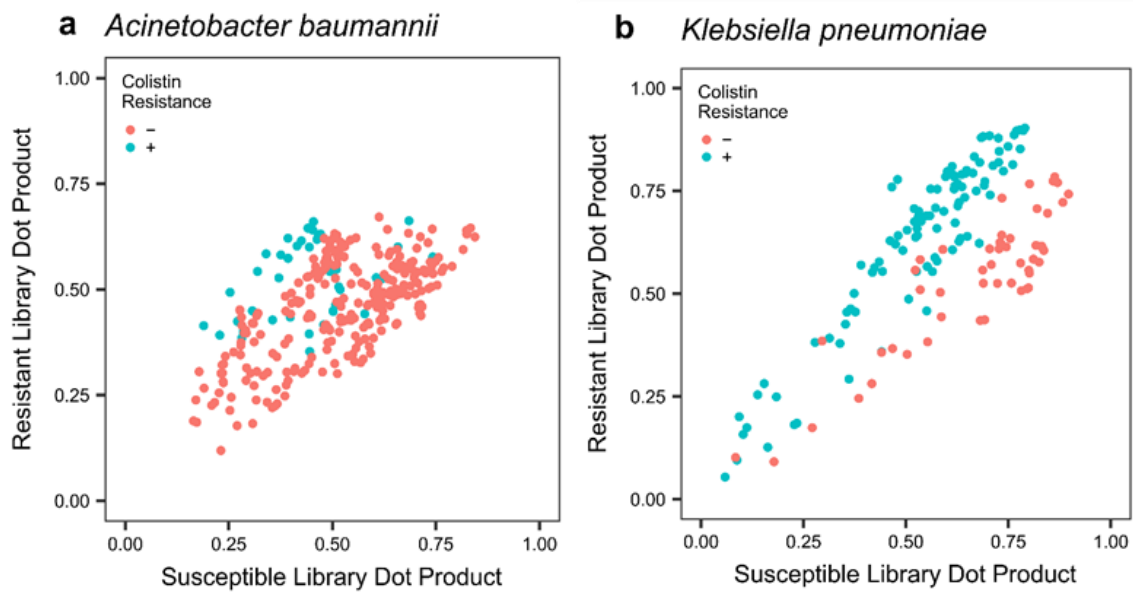


**Figure 2.9. Dot product scores between library consensus spectra and test spectra partitioned by colistin resistance.** Library consensus mass spectra were created from the summation of detected ions in 50% of colistin-resistant and susceptible *A. baumannii* (a) and *K. pneumoniae* (b) replicates. Dot products were calculated between each of the remaining replicates and the colistin-resistant and susceptible consensus mass spectra for each species.

**Table 2.4. MALDI Biotyper results for identifying *K. pneumoniae* and *A. baumannii*.**

<b>Organism</b>		<b># strains</b>	<b># replicates</b>	<b>Mean confidence log score</b>	<b>% positive sub-species identification</b>	<b>% positive species identification</b>
<b><i>Klebsiella pneumoniae</i></b>	Colistin-susceptible	26	96	2.528	<b>100.0</b>	<b>100.0</b>
	Colistin-resistant	34	220	2.536	<b>69.2</b>	<b>87.7</b>
<b><i>Acinetobacter baumannii</i></b>	Colistin-susceptible	188	555	2.270	<b>55.9</b>	<b>77.2</b>
	Colistin-resistant	25	93	2.615	<b>92.3</b>	<b>92.3</b>

\* 30% of strains were used as testing sets to determine ID rates of accuracy

† Positive identifications were determined to be the top-scoring organism and a log score > 1.7

**Identification from polymicrobial mixtures.** In order to highlight the potential of our method to analyze polymicrobial mixtures, mass spectra from samples containing three ESKAPE pathogens, *S. aureus*, *K. pneumoniae*, and *P. aeruginosa*, often found together in polymicrobial infections (137) were generated. Mass spectra, including those from either co-cultured organisms or those produced by mixing extracts post-culture of individual organisms, allowed each of the three species to be visually identified based on detection of each species' signature ions (**Figure 2.10**).

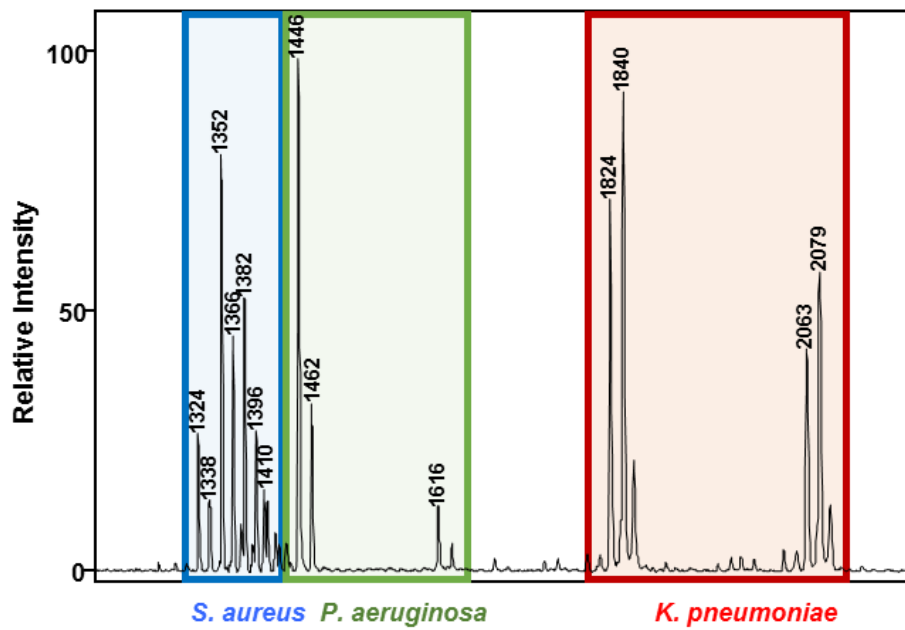


**Figure 2.10. Mass spectrum from a mixed sample.** *S. aureus* NRS384, *K. pneumoniae* TBE818, and *P. aeruginosa* BE399 were co-cultured, cultured separately and co-extracted, or extracted separately and mixed (shown above). Mass spectral profiles were determined.  $m/z$  values of ions are given and assigned to their respective organisms.

**Direct identification from blood culture.** In order to demonstrate applicability of our platform to relevant clinical samples, *K. pneumoniae* and *S. aureus* were cultivated in blood culture (BC) bottles (to which sterile blood had been added) at an initial inoculum of  $10^3$  CFU/mL. We achieved detection from this initial inoculum after six hours for *K. pneumoniae* and after 24 hours for *S. aureus* (**Figure 2.11**). **Figure 2.11a** shows a mass spectrum of a sterile BC control demonstrating that there are minimal background contaminants within the  $m/z$  range of these glycolipids of interest. Samples were compared against the Biotyper glycolipid library, and positive identifications were determined to be the top-scoring organism with a confidence log score  $> 1.7$  as throughout the study. The mass spectrum from *K. pneumoniae* in blood culture was correctly identified as *K. pneumoniae* with a score of 2.155. The *S. aureus* mass spectrum was positively identified at the genus level, but at the species level as *Staphylococcus haemolyticus*. This was attributable to a change in the signature ions after growth in blood bottles (**Figure 2.12**) that was consistent when multiple *S. aureus* strains were tested, thereby representing a unique phenotype for this bacterium in the context of a blood infection that will be included in future libraries. When a novel MSP was generated for *S. aureus* in blood culture, test mass spectra were positively identified as *S. aureus* with a score of 2.467. Currently, the limit of detection (LOD) of these bacteria in blood bottles is  $10^8$  CFU/mL whereas the LOD from cells grown in pure laboratory culture is  $10^5$  CFU/mL.

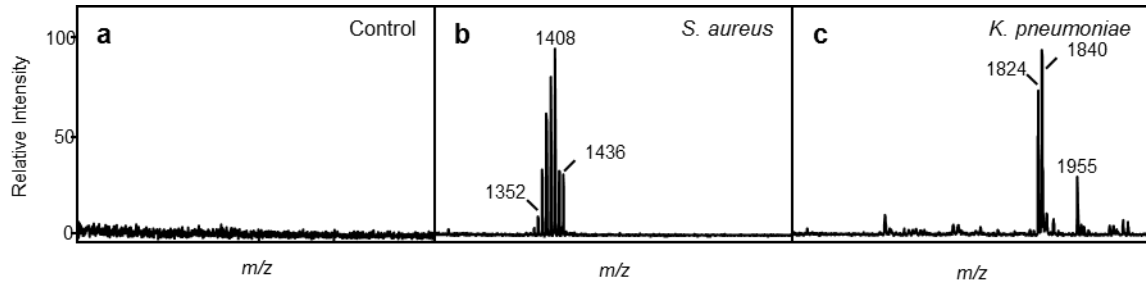


**Figure 2.11. Detection of *S. aureus* and *K. pneumoniae* from blood culture.** (a) Blood culture control containing sterile blood (b) Blood culture containing MRSA M2 after overnight growth (24 hours), and (c) Blood culture containing *K. pneumoniae* B6 after six hours growth. A  $10^4$  CFU inoculate was seeded into 10 mL blood, transferred to standard aerobic culture bottles and sampled at 0, 2, 4, 6, and 24 hours. Differential centrifugation allowed separation of human cells. Extraction and mass analysis was performed.

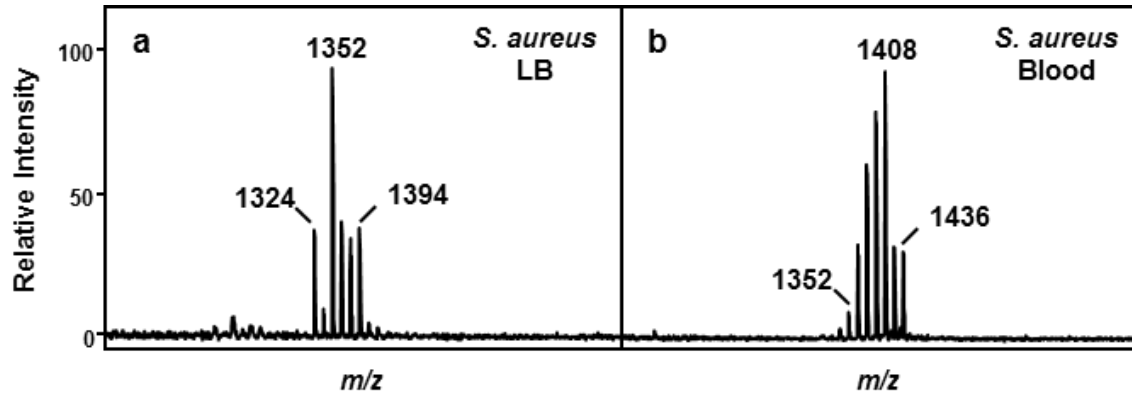


**Figure 2.12. Mass spectra from *S. aureus* confirming mass shift in blood culture.** *S. aureus* strain M2 grown in laboratory medium (a) and overnight blood culture. (b) A mass shift was observed from  $m/z$  1352 to  $m/z$  1408 as the base peak when bacteria are cultured in blood bottles. Changes in signal intensities were present at  $t_0$  indicating immediate modifications which suggests an altered growth condition. Neighboring  $m/z$  values are separated from one another by 14 mass units which suggest differences of a single methylene group ( $-CH_2$ ) and likely results from variations in fatty acid chain lengths of the DAG unit.

## **Discussion**

Infectious diseases have a significant global health impact. Conventional diagnostics involving microbiological, biochemical, and molecular assays typically require days or even weeks to undertake for fastidious organisms, often yielding inaccurate or incomplete diagnoses (11, 138–140). This can have devastating consequences during an infection; therefore, innovative technologies are urgently needed to improve patient outcomes. In this study, we investigated a novel approach to bacterial identification, namely, analysis of microbial membrane glycolipids by MALDI-TOF-MS. Prior research has shown that complex glycolipids found in high abundance in bacterial membranes exhibit species-specific structural characteristics that present “signature ions” unique to a given species. We hypothesized that mass spectrometric analysis of these glycolipid fingerprints could differentiate and identify bacterial species as well as provide practical sub-species information. To demonstrate the validity of this approach, a library of glycolipid mass spectra was built representing 35 Gram-negative bacteria, 11 Gram-positive bacteria, and 4 fungal species. Glycolipid mass spectra were shown to be highly reproducible between mass spectral replicates. Furthermore, all ESKAPE species produced unique profiles visually but also objectively by dot product analysis.

Mass spectrometric phenotyping of bacterial proteins for identification exists on two commercial systems, the Bruker MALDI Biotyper (Bruker Daltonics Inc., Billerica MA) and bioMérieux VITEK MS (bioMérieux S.A., France). Both identify organisms via pattern-matching of a sample mass spectrum to a reference database of known organisms, and both achieve accuracy of ~90% for organisms in their clinical platforms. In the most recent study comparing them (66), study authors determined accuracy rates of 86.4% for

the Biotyper and 92.3% for the VITEK MS for correctly identifying a diverse range of microorganisms. This is comparable to our results using Biotyper (**Table 2.4**) although accuracy rates improve for routinely isolated strains (138) or strains for which specialized databases exist on these platforms (76, 77). Limitations to the capabilities of these platforms include identification of antibiotic resistance, identification from complex samples like blood, and identification from polymicrobial samples (62). We successfully used our approach to solve these three unmet needs from the protein-based phenotyping approach. Importantly, we were able to adapt the existing Biotyper software to recognize glycolipid mass spectra and make species identifications as well as distinguish colistin-susceptible from resistant *K. pneumoniae* and *A. baumannii*, suggesting an immediate use for our approach that could augment protein-based identifications that fail to distinguish antibiotic resistance strains.

Most Gram-negative bacteria are susceptible to polymyxins (including colistin), but emergence of resistant isolates is increasing. Transfer of neutral or positively-charged functional groups onto LA are believed to decrease its electronegativity and protect it from attack by polymyxins, as well as host antimicrobial peptides (127). As observed with *K. pneumoniae* and *A. baumannii*, this well-characterized adaptation produces large shifts in  $m/z$  values that are readily identified by MALDI-TOF-MS, and we have shown a high positive correlation between these mass spectral profiles and incidence of resistance. While we achieved compelling accuracy rates on the Biotyper platform and demonstrated adaptability of our platform to a commercially available diagnostic, they do not fully reflect how different the glycolipid mass spectra are due to the manner in which the Biotyper makes an identification, necessitated by the complexity of a bacterial protein spectrum.

Continuing development of algorithms specific to our glycolipid approach promise to improve the performance of the platform both for identification and susceptibility prediction, as demonstrated by manual selection of colistin resistance associated ions and calculation dot products against consensus mass spectra.

Our glycolipid-based approach to bacterial identification was also able to identify bacteria after culture in blood culture bottles, a clinically relevant source where identification of organisms is crucial in guiding appropriate therapy. During a suspected bloodstream infection, patient blood samples are introduced directly into a blood culture identification system. A sensor in the bottle indicates when the culture is positive and can be processed by downstream diagnostics, a process that can take 72 hours or longer (71). Our study shows that *S. aureus* and *K. pneumoniae* cultured in blood bottles produced mass spectra that uniquely identifies them with the Biotyper software package, albeit with a shift in the signature ions observed for *S. aureus*. Importantly, the clean mass spectrum baseline from the control blood culture bottle illustrates an important point for analysis of human clinical samples, namely, that the lipid extraction process produces mass spectra devoid of host lipids in the  $m/z$  range examined. This fact allows identification directly from blood culture, hours earlier than other methods. The estimated LOD for detecting bacterial glycolipids directly from blood bottle culture was  $10^8$  cells, which is presently higher than the bacterial concentration of  $10^1$  to  $10^3$  CFU/mL that typically occurs in septic patients. This means our current method requires some degree of amplification (6 to 24 hours in this present study) for clinical use. However, we believe that optimization through refinement of extraction and sample preparation will further reduce amplification and processing time

with the ultimate goal of detection of infectious agents directly from biological fluids with no amplification by our method.

Mass spectrometry of microbial lipids has been previously explored as a diagnostic through hydrolysis and analysis of total membrane fatty acids. Recent renewed interest has focused on analysis of the complex glycolipids used here, which are exclusive to microbial membranes and found in a higher  $m/z$  range than most host phospholipids and fatty acids produced by hydrolysis of LA and LTA. For example, others have reported detection of LA via MALDI-TOF by direct analysis of bacterial colonies (113) and by use of rapid evaporative ionization mass spectrometry (REIMS) of select colonies (115), the latter being an ambient ionization method involving electrical current applied directly to the surface of an analyte (in this case a colony) at the inlet of the mass analyzer. While these two reports offer direct analysis from pure colonies, our strategy uses an extraction step to isolate glycolipids of interest that can be done directly from biological fluids such as blood, urine, and wound effluent. While our less direct method could be seen as a disadvantage, our results produce higher quality mass spectra devoid of host lipids, which in turn produces higher confidence scores. Furthermore, we are working to develop an extraction protocol that will appreciably reduce the time for sample preparation to less than one hour from start to finish, improve LOD, and ultimately bypass the need for culture.

In conclusion, our work presents a novel diagnostic approach for identifying harmful pathogens as well as common organisms that can offer a complementary approach with added value to existing clinical protein-based platforms to strengthen the overall diagnostic power of the clinical lab.

## Materials and Methods

**Selection of strains.** Strains were chosen in consultation with and individual clinical isolates were obtained through established collaborations with our infectious disease collaborators, Drs. Yohei Doi (University of Pittsburgh) and J. Kristie Johnson (University of Maryland). *S. aureus* strains were obtained from Dr. Mark Shirliff (University of Maryland). All protocols were approved by the institutional review boards of the University of Pittsburgh (IRB #: PRO12060302) and the University of Maryland – Baltimore (IRB #: HP-00041044). Informed consent was not obtained since study involves de-identified, leftover biological specimens from standard patient care. Strains were identified by standard clinical laboratory methods including microbiological culture and confirmed by MS protein typing. A full list of strains can be found in **Table 2.1** to include 12 strains of *E. faecium*, 19 strains of *S. aureus*, 60 strains of *K. pneumoniae*, 213 strains of *A. baumannii*, 15 strains of *P. aeruginosa*, and 13 strains of *E. cloacae*. Within species, strains with different antimicrobial susceptibility were evaluated where there is a high prevalence of resistance. MICs for colistin were determined by broth dilution, agar dilution, and/or Etest (bioMérieux S.A., France) using recommendations stipulated by the Clinical and Laboratory Standards Institute breakpoints for *E. coli* ATCC 25922 and *P. aeruginosa* ATCC 27853 (135).

**Analysis from blood culture bottles.** Sterile blood was obtained from the University of Maryland Medical Center (UMMC) blood bank and stored at 4°C upon receipt. Blood (5-10 mL) was inoculated into BACTECT™ blood culture bottles (Becton Dickinson, Sparks MD) according to manufacturer's recommendations. Strains were seeded into blood bottles at 10<sup>1</sup> to 10<sup>8</sup> CFU. These were sampled immediately and incubated at 37°C with shaking

then sampled every two hours up to six hours and after 24 hours growth. Bacterial numbers (CFU/mL) were made at these time points by serial dilution, plating, and direct colony counts. For MS analysis, 2 mL of each sample were harvested and spun at  $500 \times g$  for one minute to pellet blood cells. The supernatant was transferred to a clean tube and spun at  $4000 \times g$  to generate a bacterial pellet. Extraction of pelleted cells and MS analysis were carried out by our standardized protocol described below.

**Analysis of mixed samples.** Mixture samples were acquired from pure cultures that were mixed or from bacteria co-cultured together. Additionally, bacterial cultures were grown and extracted separately, and pure extracts mixed together to better control for the amount of lipids in these samples. Bacterial enumeration for all samples and MS analysis were performed. Cells were harvested to generate a pellet and extracted by the standardized protocol described below.

**Small-scale ammonium isobutyrate lipid extraction.** To obtain samples of the highest purity that generated high-quality mass spectra for inclusion in and validation of the library, strains were streaked onto lysogeny broth agar plates to obtain pure colonies. Overnight liquid cultures (1 single colony in 1-5 mL lysogeny broth at  $37^{\circ}\text{C}$ ) were harvested, processed and converted to lipid A/LTA by an optimized hot ammonium isobutyrate-based protocol originally described by El Hamidi et al. (131) Briefly, bacterial pellets were treated with a 5:3 mixture of 70% (v/v) isobutyric acid/1 M ammonium hydroxide (250  $\mu\text{L}$ /150  $\mu\text{L}$ ) (Sigma-Aldrich, St. Louis MO) and incubated at  $100^{\circ}\text{C}$  for 30 to 45 minutes. Reactions were spun down at  $2000 \times g$  for 15 minutes to remove cell debris, and supernatants were transferred to clean tubes, combined in a 1:1 ratio of distilled water, and

lyophilized overnight. The resulting dry pellets contain whole cell extracts of membrane lipids.

**MALDI-TOF.** Extracts were washed twice with methanol and then resuspended in 50-200  $\mu\text{L}$  of a 2:1:0.25 chloroform/methanol/water (Fisher Scientific, Waltham MA; Quality Biological, Gaithersburg MD) solvent mixture. Aliquots of 1  $\mu\text{L}$  each were spotted directly onto stainless steel target plates. Mass spectra were recorded in negative ion mode by direct analysis of extracts within the lipid matrix norharmane (10 mg/mL in 2:1 v/v chloroform/methanol) (Sigma-Aldrich, St. Louis MO) using a Bruker Microflex LRF MALDI-TOF MS (Bruker Daltonics Inc., Billerica MA) operated in reflectron mode. The instrument is equipped with a 337 nm nitrogen laser, and analyses were performed at 39.5% global intensity. Typically, 900-1000 laser shots were summed to acquire each mass spectrum.

**Statistical analyses.** Mass spectra were imported and analyzed using R (v3.3.1) with the MALDIquant (v1.16.2) and MALDIquantForeign (v0.10) R packages (141). Intensities of each mass spectrum were square root transformed and smoothed with a 21 point Savitzky-Golay filter (142). Mass spectra were base line corrected using the SNIP method over 60 iterations, then aligned (143). *Bona fide* glycolipid ions were detected by selecting ions with an 8.0 signal-to-noise ratio, with noise calculated by 21 point median absolute deviation and binning matching ions between spectra using a 0.5  $m/z$  tolerance. Hierarchical clustering was performed using the pvclust (v2.0-0) R package (144). A pairwise dot product was calculated from unit vectors created from a mass list of ions from each mass spectrum, containing the normalized ion intensity of each ion.

For generation of consensus spectra for discrimination between colistin-susceptible and resistant *A. baumannii* and *K. pneumoniae*, 50% of replicate mass spectra were chosen at random to build a consensus spectra and the remaining 50% were held out as a test set. Detected ions for the chosen mass spectra were normalized relative to the base peak and summed together to yield a consensus spectrum. Dot products between each of the test set mass spectra and the consensus mass spectra for specific species were calculated as described above.

**Software analyses.** The MALDI Biotyper (Bruker Daltonics Inc., Billerica MA) is a data acquisition and analysis software workflow, which incorporates Bruker FLEX series mass spectrometers including the Bruker Microflex LRF. The Biotyper was trained to recognize glycolipid mass spectra by adjusting parameters within the framework of the software to ID bacteria as follows: 1) Adjusting mass range to 1000 through 2400  $m/z$  and 2) Altering peak picking thresholds to at least 10 ions to account for simpler spectra and adjusting signal-to-noise ratio to 8. Mass spectra were filtered prior to analysis in Biotyper using the filterSpectra.R script, which is available in the GitHub repository (provided below in **Code availability**). Parameters were optimized to reject the maximum amount of low-quality spectra: passing mass spectra were required to contain 10 ions with signal-to-noise ratios greater than or equal to 8.0. Mass spectra were loaded into the Biotyper OC software. A Main SPectra (MSP) was created for each species or phenotype (susceptible *v.* resistant, growth temperature), which is a representation of the mass spectra within each group. The number of mass spectral replicates per MSP can be found in **Tables 2.1, 2.2, and 2.4**. For identification of *A. baumannii* and *K. pneumoniae*, 70% of randomly selected mass spectra from a single organism were used to create an MSP and the remaining 30% are tested

against the generated library. The MALDI Biotyper picks peaks by Spectra Differentiation filter and generates mass lists for a test sample that are then compared by pattern matching algorithm to mass lists of all MSPs in the reference database. The software then outputs a list of the top ten identifications based on the highest log scores calculated from these comparisons. We opted to use the preprogrammed confidence log score value criteria of the software (2.0 to 3.0=positive identification; 1.7 to 1.999=probable identification; 0 to 1.699=unreliable identification).

**Data availability.** All data generated or analyzed during this study are included in this published article (and its Supplementary Information files).

**Code availability.** All scripts used for this analysis are freely available and can be found in the following GitHub repository:  
[https://github.com/wfondrie/ESKAPE\\_Glycolipid\\_MS](https://github.com/wfondrie/ESKAPE_Glycolipid_MS).

## CHAPTER THREE: Structural modification of lipopolysaccharide in colistin-resistant, KPC-producing *Klebsiella pneumoniae*

### Synopsis

**Background:** Colistin resistance in *Klebsiella pneumoniae* typically involves inactivation or mutations of chromosomal genes *mgrB*, *pmrAB* or *phoPQ*, but data regarding consequent modifications of lipopolysaccharide (LPS) are limited.

**Objectives:** To examine the sequences of chromosomal loci implicated in colistin resistance and the respective LPS-derived lipid A profiles using 11 pairs of colistin-susceptible and resistant KPC-producing *K. pneumoniae* clinical strains.

**Methods:** The strains were subjected to high-throughput sequencing with Illumina HiSeq. *mgrB* was amplified by PCR and sequenced. Lipid A profiles were determined using matrix-assisted laser desorption/ionization time-of-flight (MALDI-TOF) mass spectrometry.

**Results:** All patients were treated with colistimethate prior to the isolation of colistin-resistant strains (MIC of >2 mg/L). Seven of 11 colistin-resistant strains had deletion or insertional inactivation of *mgrB*. Three strains, including one with *mgrB* deletion, had non-synonymous *pmrB* mutations associated with colistin resistance. When analyzed by MALDI-TOF mass spectrometry, all colistin-resistant strains generated mass spectra containing ions at  $m/z$  1955 and 1971 consistent with addition of 4-amino-4-deoxy-L-arabinose (Ara4N) to lipid A, whereas only one of the susceptible strains displayed this lipid A phenotype.

**Conclusion:** The pathway to colistin resistance in *K. pneumoniae* primarily involves lipid A modification with Ara4N in clinical settings.

## Background

*Klebsiella pneumoniae* producing (KPC)-type carbapenemase is the most common and clinically problematic carbapenem-resistant Enterobacteriaceae (CRE) in healthcare institutions in the U.S. (145, 146). Infections due to KPC-producing *K. pneumoniae* are difficult to manage and often require the use of colistin, which is a decades-old cyclic polypeptide that is active against most *K. pneumoniae* strains (147). Colistin exerts its activity by binding the bacterial membrane through electrostatic interactions with the lipid A moiety of lipopolysaccharide (LPS), causing disruption of the outer membrane and cell death (148), and bacteria can develop resistance to colistin by modifying the structures of the lipid A moiety hindering colistin binding (149). In *K. pneumoniae*, the LPS structure has been characterized for spontaneous colistin-resistant strain OM-5 (128). In strain OM-5, lipid A was mostly modified with 4-amino-4-deoxy-L-arabinopyranose (Ara4N), whereas little or no modification was observed in its colistin-susceptible parental strain, suggesting this as a primary mechanism of resistance in this organism. Other studies have also implicated palmitoylation (150) and/or hydroxylation (151) as conferring resistance in *K. pneumoniae* to antimicrobial peptides including colistin.

The increasing clinical use of colistin has led to development of colistin resistance in *K. pneumoniae*, and outbreaks due to colistin-resistant KPC-producing *K. pneumoniae* have been reported (152, 153). Clinically, the most commonly reported genetic pathway for colistin resistance has involved loss of function mutations of *mgrB*, encoding a negative regulator of PhoPQ, which in turn modulates PmrAB leading to activation of the *pmrHFIJKLM* operon (153–155). Using a pair of colistin-susceptible and resistant clinical strains identified from the same patient, a non-synonymous mutation in the gene encoding

PmrB, the sensor kinase component of the PmrAB two-component regulatory system, has been associated with upregulation of *pmrA* and *pmrHFIJKLM*, the latter encoding a LPS modification system that is presumed to facilitate biosynthesis and lipid A transfer of Ara4N (156, 157). The potential role of another two-component regulatory system CrrAB has also been suggested (156). However, little information is available regarding the lipid A modifications that occur in response to mutations or modulation of these genes in KPC-producing *K. pneumoniae*. The aim of the present study was to investigate mutations of *mgrB*, *pmrAB*, *phoPQ*, *crrAB* and *pmrFIJKLM* with Ara4N diesterization of the lipid A phosphate as determined by mass spectrometric analysis that characterize colistin resistance using multiple pairs of colistin-susceptible and resistant KPC-producing *K. pneumoniae* strains identified within patient prior to and following treatment with colistimethate.

## Methods

**Bacterial strains.** Twenty-two carbapenem-resistant *K. pneumoniae* clinical strains were collected at the University of Pittsburgh Medical Center between 2008 and 2012 under waiver of informed consent (University of Pittsburgh IRB # 0510165 and PRO12060302) and tested for colistin susceptibility using the standard agar dilution method. Strains with minimum inhibitory concentrations (MICs)  $\geq 4$   $\mu\text{g/ml}$  were considered resistant to colistin using the clinical breakpoint for *Pseudomonas aeruginosa* and *Acinetobacter baumannii* (158). Strains from the same patients which demonstrated discordant colistin susceptibility (susceptible and resistant) were included in the study.

**PCR and sequencing of the *mgrB* gene.** The *mgrB* gene was amplified and sequenced by the Sanger method for all study strains using the primer set reported previously (159) to

identify clinical strains with full or partial deletion of the gene, the inactivation of which reportedly accounts for the majority of colistin-resistant *K. pneumoniae* strains worldwide (155, 159).

**High-throughput sequencing.** The genomes of all study strains were sequenced on a HiSeq 2500 (Illumina, San Diego, CA). In addition, strain C2 was sequenced by RS II (Pacific Biosciences, Menlo Park, CA) to provide the internal reference genome for the analysis, which yielded a total of 150,292 reads with an average read length of 9,408 bp. *De novo* assembly of the C2 PacBio reads using hierarchical genome assembly process (HGAP) available in the SMRT Analysis v2.1 software generated 6 contigs with 84x coverage. The assembly was annotated using Prokka. The reads were aligned to reference genome C2 using BWA-MEM (<http://bio-bwa.sourceforge.net/>). Duplicate reads were marked using Picard MarkDuplicates. SNPs were identified using GATK HaplotypeCaller with ploidy of 1 (160). SNPs with low mapping quality (MQ <20), evidence of strand bias (FS > 60.0), low variant confidence (QD <2), only seen near the ends of the reads (ReadPosRankSum < -8.0), or low depth (DP <5) were filtered and removed using GATK VariantFiltration. Sequence type (ST) was determined by uploading contigs assembled *de novo* by CLC Genomics Workbench version 7.5.1 using the default settings to the *K. pneumoniae* multilocus sequence typing (MLST) website (<http://bigsdw.web.pasteur.fr/klebsiella/klebsiella.html>). The raw sequence reads were deposited to the short read archive under BioProject PRJNA375812.

**Lipid A isolation from whole cells.** Membrane lipids were extracted and LPS was converted to lipid A by an optimized small-scale hot ammonium isobutyrate-based protocol (131). Bacteria were streaked onto lysogeny broth (LB) agar plates to obtain pure colonies.

Overnight cultures (1-5 ml at 37°C) in lysogeny broth with or without 2 µg/ml of colistin sulfate (Sigma-Aldrich, St. Louis, MO) were harvested at 4000 × g for 10 minutes. Bacterial pellets were treated with a 5:3 mixture of 70% (v/v) isobutyric acid/1 M ammonium hydroxide (250 µl/150 µl) and incubated at 100°C for 30 to 45 minutes. Reactions were spun down at 2000 × g for 15 minutes to remove cell debris, and supernatants were transferred to clean tubes, combined in a 1:1 ratio of distilled water (400 µl), frozen on dry ice, and lyophilized overnight. The resulting dry pellets contain whole cell extracts of membrane lipids.

**Lipid A characterization by mass spectrometry.** Dry lipid extracts were washed twice with 1 ml methanol and then resuspended in 200 µl of a 2:1:0.25 chloroform/methanol/water solvent mixture. Aliquots of 1 µl each norharmane matrix (10 mg/ml in 2:1 v/v chloroform/methanol) (Sigma-Aldrich, St. Louis, MO) then analyte were spotted directly onto stainless steel target plates. Mass spectra were recorded in negative ion mode using a Bruker Microflex LRF MALDI-TOF mass spectrometer (Bruker Daltonics Inc., Billerica, MA) operated in reflectron mode. The instrument is equipped with a 337 nm nitrogen laser, and analyses were performed at 39.5% global intensity. Typically, 900 laser shots were summed to acquire each spectrum. Data were acquired and processed using flexControl and flexAnalysis version 3.4 (Bruker Daltonics Inc., Billerica, MA).

Structural analysis was carried out on a Waters Synapt G2 Q-TOF mass spectrometer (Waters Corporation, Milford, MA) operated in sensitivity mode. Lipid extract resuspensions were diluted 2:1 in a solvent mixture of CHCl<sub>3</sub>/CH<sub>3</sub>OH (v/v). The solution was infused at 3 µl/min flow rate. The source block temperature was set to 150°C. Tandem

MS was carried out using trap collision induced dissociation (CID). For mass selection in the quadrupole, we used the instrument standard values (LM resolution 4.7 and HM resolution 15.0). To mitigate the effect of instantaneous signal fluctuations, the data were averaged for 3 minutes.

## **Results**

**Characteristics of clinical cases associated with colistin-resistant *K. pneumoniae*.** Both colistin-susceptible and resistant *K. pneumoniae* strains spanning treatment with colistin were identified in 11 patients between 2008 and 2012. All except one of them were solid organ transplant recipients, and nine of them were in an intensive care unit at the time of the culture (**Table 3.1**). While the time between isolation of the susceptible and resistant strains varied (range, 6 to 101 days), all had received treatment with intravenous colistin methanesulfonate (CMS; the prodrug of colistin) and three had received prolonged inhaled CMS prior to the isolation of colistin-resistant *K. pneumoniae*.

**Table 3.1. Characteristics and outcomes of patients with carbapenem and colistin-resistant *K. pneumoniae*.**

Pt	Colistin-resistant strain	Date	Days from the susceptible strain	Age	Sex	Underlying diseases	Culture site	Type of infection	ICU	Prior intravenous CMS (days)	Prior inhaled CMS (days)	Treatment of colistin-resistant infection	30-day mortality
1	A5	02/25/08	31	49	M	Multivisceral transplant	BAL	VAP, BSI	Yes	23	34	AMK, TGC	No
2	B6	03/10/10	47	63	M	Liver transplant	Urine	Asymptomatic bacteriuria	No	2	-	None	No
3	B9	04/13/10	24	25	F	Multivisceral transplant	Abdominal clot	Intra-abdominal abscess	Yes	18	-	CMS, TZP, TIG	No
4	C3	04/17/10	14	43	M	Liver transplant	Blood	Intra-abdominal abscess	Yes	12	-	CMS, DOR, TIG, MTZ	No
5	C5	06/01/10	49	67	F	Lung transplant	Bronchial washing	Acute cellular rejection	No	5	24	CMS DOR, then DOX, MEM (inh)	No
6	D7	06/24/11	49	47	M	Heart/lung transplant	Bronchial washing	VAP	Yes	2	43	CMS, DOR, ERT, TOB (inh)	No
7	E6	01/12/12	21	60	M	Liver transplant	BAL	Tracheal colonization	Yes	19	-	None	No
8	F3	03/13/12	11	60	M	Necrotizing pancreatitis	Blood	Intra-abdominal abscess	Yes	8	-	CMS, DOR, GEN	Yes
9	F9	03/30/12	6	63	F	Liver transplant	Blood	Intra-abdominal abscess, BSI	Yes	8	-	CMS, DOR, ERT	No
10	H5	07/12/12	101	37	F	Liver transplant	Liver tissue	Intra-abdominal abscess	Yes	5	-	CMS, DOR, FEP	No
11	I2	11/19/12	40	58	F	Liver transplant	BAL	Intra-abdominal abscess	Yes	38	-	CMS, DOR, TIG	No

<sup>a</sup>BAL, bronchoalveolar lavage; VAP, ventilator-associated pneumonia; BSI, bloodstream infection; ICU, intensive care unit; CMS, colistin methanesulfonate; AMK, amikacin; TGC, tigecycline, TZP, piperacillin-tazobactam; DOR, doripenem; DOX, doxycycline; MEM, meropenem; ERT, ertapenem; TOB, tobramycin; GEN, gentamicin; FEP, cefepime.

<sup>b</sup>30-day mortality is defined as death within 30 days from the day the culture growing the colistin-resistant strain was collected.

**Overview of the colistin-susceptible and resistant *K. pneumoniae* strains.** For 9 of the 11 patients, both the colistin-susceptible and resistant strains belonged to the epidemic sequence type (ST) 258 (**Table 3.2**) (161). A phylogenetic tree based on 2718 SNPs identified by the GATK method was generated using RAxML v8.2.9 by running 100 bootstrap replicates under the generalized time-reversible model (GTRCAT) and Lewis correction for ascertainment bias, which supported within-patient development of colistin resistance upon exposure to CMS for all patients except one (**Figure 3.1**). Both the susceptible and resistant strains from the first patient identified belonged to ST17 and were also closely related on the expanded phylogenetic tree (data not shown). A *bla*<sub>KPC-2</sub>-carrying *K. pneumoniae* ST17 strain has been reported from Greece previously (162). The likely exception to within-patient evolution of colistin resistance was Patient 7, who initially had a colistin-susceptible ST258 strain but then a colistin-resistant ST37 strain 21 days later, which suggests either re-infection with the latter strain or initial co-infection with ST258 and ST37 strains that was undetected at the time.

**Table 3.2. Colistin MICs, lipid A modification and *mgrB*, *pmrAB*, *phoPQ* loci.**

Pt	Strain	Sequence type	KPC type	Colistin MIC (µg/ml)	Extra <i>m/z</i> consistent with L-Ara4N	<i>mgrB</i>	<i>crbB</i>	<i>pmrA</i>	<i>pmrB</i>	<i>pmrF</i>	<i>pmrI</i>	<i>pmrJ</i>	<i>pmrK</i>	<i>phoP</i>	<i>phoQ</i>
1	A2	ST17	KPC-3	0.5	1955/1971*	WT									
	A5	ST17	KPC-3	>256	1955/1971*	Ah89Gln Gln30Arg	Leu94Met		His340Arg						
2	B5	ST258	KPC-2	0.25		WT									
	B6	ST258	KPC-2	>256	1955/1971	Trp6stop	Pro151Gln			Phe236Leu					
3	B8	ST258	KPC-2	0.25		WT									
	B9	ST258	KPC-2	>256	1955/1971	Gly19frameshift †									
4	C2	ST258	KPC-2	0.25	1955/1971	WT									
	C3	ST258	KPC-2	128	1955/1971	WT			Ser85Arg						
5	C4	ST258	KPC-2	0.5		WT									
	C5	ST258	KPC-2	128	1955/1971	Gln308stop									
6	D4	ST258	KPC-2	0.5		WT									
	D7	ST258	KPC-2	256	1955/1971	WT									
7	E5	ST258	KPC-2	0.25		WT									
	E6	ST37	KPC-2	128	1955/1971*	nr70insIsI903B- Ile	Leu296Gln			Ala253Val Thr257Met † Cys258Phe Ala261fs Ile276Val Ter277Ser	Ser470Trp	Glu25Ala Arg29Cln Ile53Val Leu94Ile	Ile117Val His156Gln Asp441Gln		
8	F2	ST258	KPC-2	0.25		WT									
	F3	ST258	KPC-2	128	1955/1971	Not detected by PCR or WGS			Thr157Pro						
9	F8	ST258	KPC-2	0.5		WT									
	F9	ST258	KPC-2	128	1955/1971*	nr75insIsKpn26 -Ile									
10	H4	ST258	KPC-2	0.5		WT									
	H5	ST258	KPC-2	64	1955/1971	WT									
11	I1	ST258	KPC-2	0.25		WT									
	I2	ST258	KPC-2	>256	1955/1971	Not detected by PCR or WGS	Leu133Arg								

<sup>a†</sup>The sequences of the colistin-resistant strains were compared with those of the colistin-susceptible strains from the same patients.  
<sup>b\*</sup> indicates mass spectral profiles detected in antibiotic media.

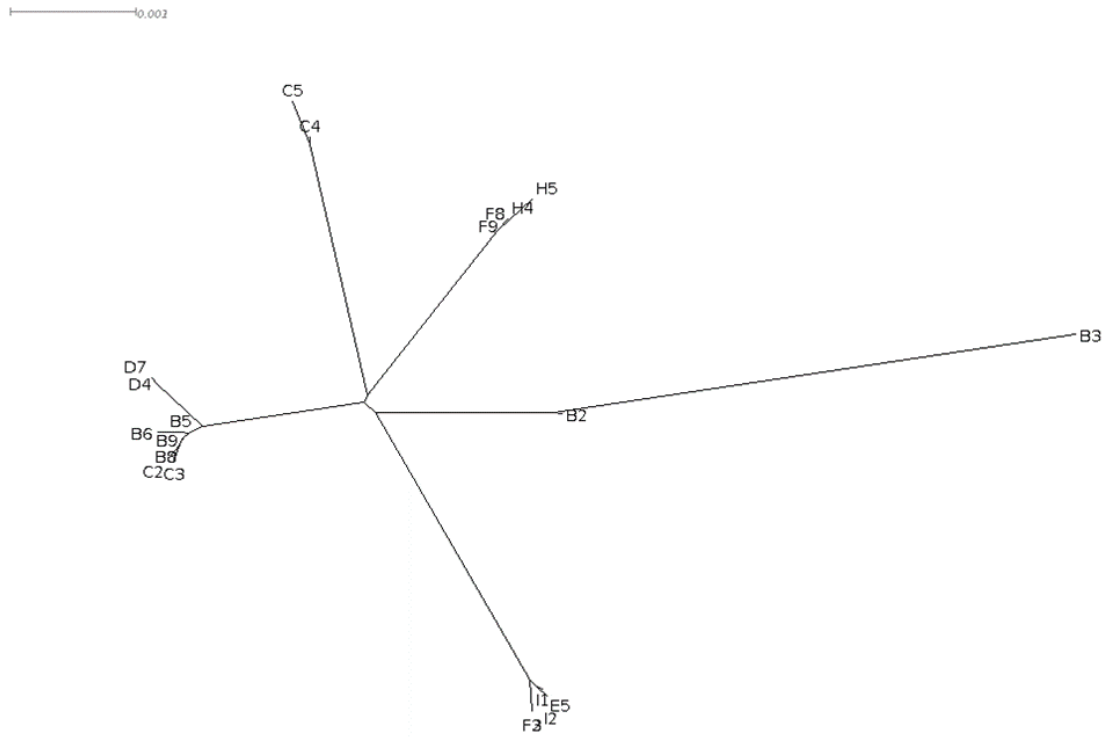
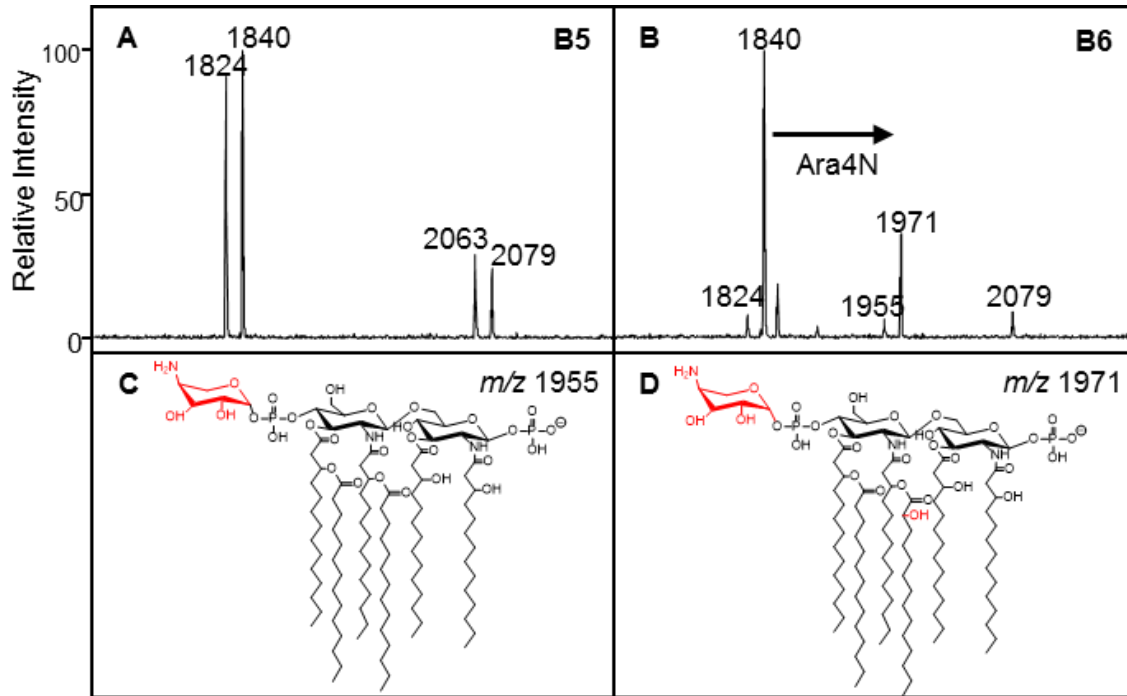


**Figure 3.1. Genome-based phylogeny of the *K. pneumoniae* strains.** Strains A2, A5 (ST17) and E6 (ST37) were excluded because they do not belong to this cluster composed of ST258 strains.

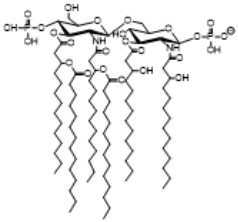
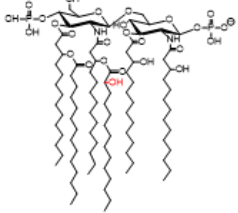
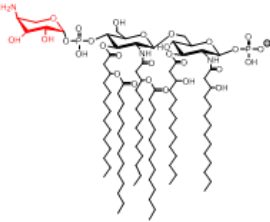
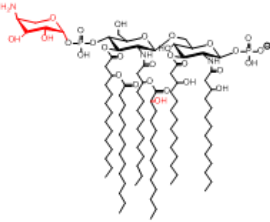
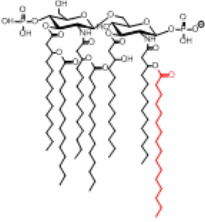
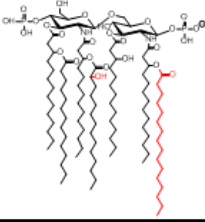
**Genetic changes consistent with colistin resistance.** The *mgrB* gene encodes a regulatory transmembrane protein that negatively regulates the PhoPQ signaling system, which in turn activates the PmrAB signaling system leading to LPS modification and colistin resistance (155, 159). Major loss-of-function mutations in *mgrB* (premature stop codon, insertional inactivation, or deletion) were detected in 7 of the 11 colistin-resistant strains (**Table 3.2**). In one of these strains (F3), a non-synonymous mutation in *pmrB* that has been associated with colistin resistance (T157P) was also detected (163). Of the 4 colistin-resistant strains with intact *mgrB*, 2 strains (A5 and C3) contained non-synonymous mutations in *pmrB* (S85R and H340R). S85R has been previously associated with colistin resistance in *K. pneumoniae* (154), whereas H340R has been previously associated with resistance in *Pseudomonas aeruginosa* (164). Two colistin-resistant strains (D7 from Patient 6 and H5 from Patient 10) did not contain any non-synonymous mutations in any of the genetic loci that have been implicated in colistin resistance in *K. pneumoniae* (*mgrB*, *crrAB*, *pmrAB*, *phoPQ*, *pmrHFIJKLM*). The pairwise comparison results are shown in **Table 3.1**.

**Identification of Ara4N addition to lipid A isolated from *K. pneumoniae* LPS.** All strains were subjected to mass spectrometric analysis of extracted membrane lipids to characterize lipid A modifications associated with the observed genetic changes. The strains showed ions at  $m/z$  1824 and 1840 (**Figure 3.2**) that represent a bisphosphorylated, hexa-acylated lipid A molecule either with or without a hydroxylation, respectively, on the C'-2 fatty acyl chain. Most strains excluding B9, D4, D7, and E6 also showed ions at  $m/z$  2063 and 2079, which result from a palmitoylation at the C-1 acyl-oxo-acyl position of the structures at  $m/z$  1824 and 1840. These findings are consistent with previous studies (149), and lipid A structures and the corresponding  $m/z$  values of these signature ions can be found

in **Figure 3.3**. Mass spectra of colistin-resistant *K. pneumoniae* strains are characterized by the presence of ions at  $m/z$  1955 and 1971, a mass shift of  $m/z$  131 caused by addition of Ara4N to the hexa-acylated LA structures at  $m/z$  1824 and 1840 (**Figure 3.2**). The addition of Ara4N was confirmed using tandem MS. Collision induced dissociation of  $m/z$  1955 and 1971 resulted in loss of a neutral mass equivalent to that of Ara4N producing ions at  $m/z$  1824 and 1840 as the main product ions, respectively (**Figures 3.4, 3.5 and 3.6**). In general, these mass spectra correlated well with observed disruptions to *mgrB*, except for colistin-susceptible strain C2 and resistant strains C3, D7 and H5 that possess the wild-type form of the gene. With the exception of strain C2, these also correlated with resistance to colistin (**Table 3.2**).



**Figure 3.2. MALDI-TOF MS of *K. pneumoniae* with differential colistin susceptibility.** Within-patient strains B5 and B6 were grown overnight in liquid culture at 37°C, and lipids were extracted and analyzed by MALDI-TOF MS. (A) Colistin-susceptible B5 shows a mass ion at  $m/z$  1824 corresponding to a base lipid A structure that also exists either with an additional hydroxylation ( $m/z$  1840), palmitoylation ( $m/z$  2063), or hydroxylation and palmitoylation ( $m/z$  2079). (B) Colistin-resistant B6 shows  $m/z$  1840 as the base peak with additional ions at  $m/z$  1955 and 1971 indicating an Ara4N addition to the base structures at  $m/z$  1824 and 1840. (C) and (D) Molecular structures of the lipid A molecules found in mass spectra from resistant isolates.

<i>m/z</i>	Structure	Modification
1824		
1840		<ul style="list-style-type: none"> <li>Hydroxylation (–OH) of the C'-2 acyl-oxo-acyl chain</li> </ul>
1955 *		<ul style="list-style-type: none"> <li>Glycosylation (–Ara4N) of the C'-1 phosphate group</li> </ul>
1971 *		<ul style="list-style-type: none"> <li>Hydroxylation (–OH) of the C'-2 acyl-oxo-acyl chain</li> <li>Glycosylation (–Ara4N) of the C'-1 phosphate group</li> </ul>
2063		<ul style="list-style-type: none"> <li>Palmitoylation (–C-16) of the C-1 acyl-oxo-acyl chain</li> </ul>
2079		<ul style="list-style-type: none"> <li>Hydroxylation (–OH) of the C'-2 acyl-oxo-acyl chain</li> <li>Palmitoylation (–C-16) of the C-1 acyl-oxo-acyl chain</li> </ul>

**Figure 3.3. Lipid A structures with corresponding *m/z* values found in clinical isolates.** Lipid A *m/z* values and molecular structures found in mass spectra of the *K. pneumoniae* clinical isolates with descriptions of the modifications responsible for the observed mass shifts. Structures in red indicate modifications to base structure at *m/z* 1824. \* denotes ions associated with colistin resistance.

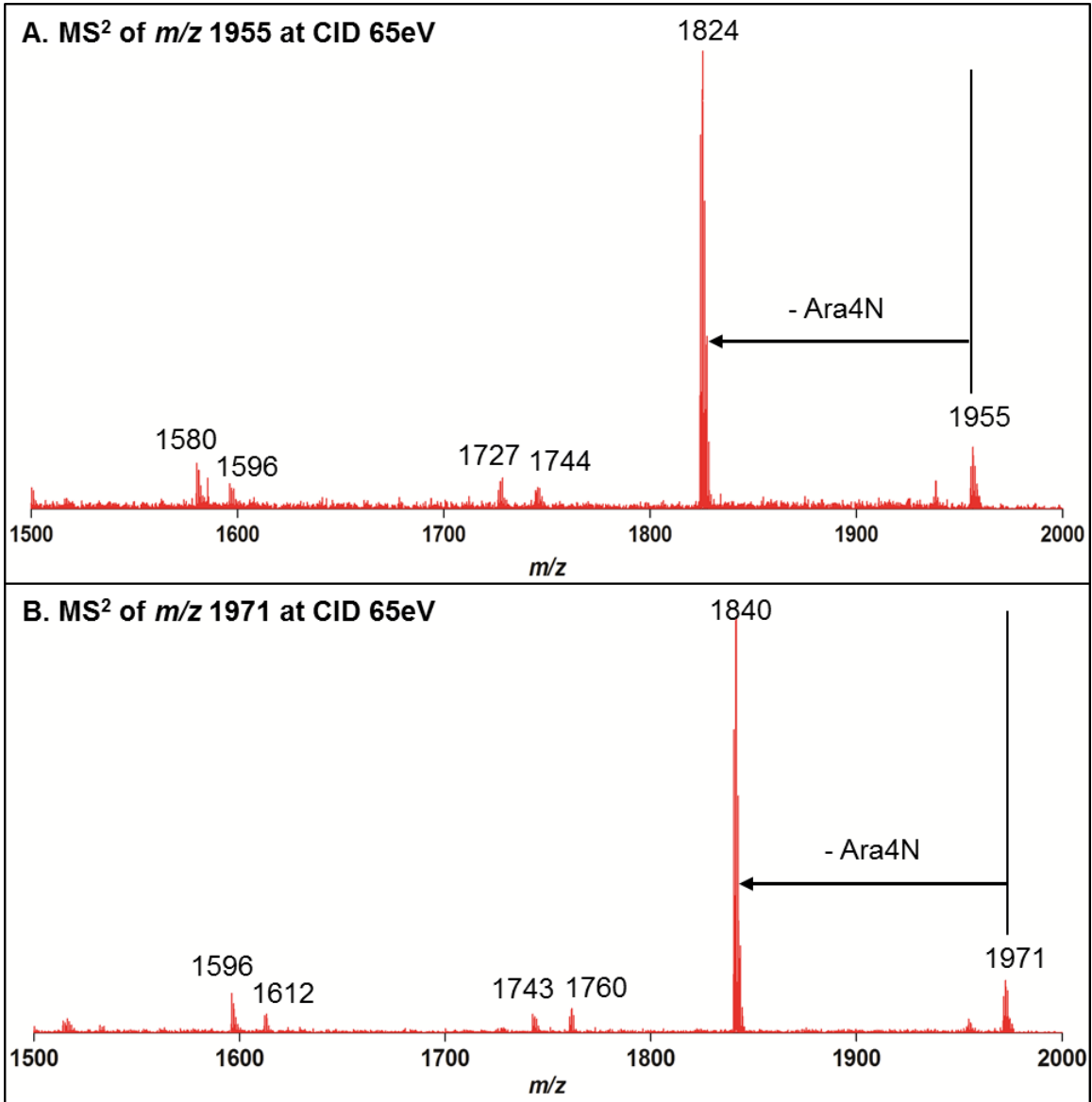


**Figure 3.4. Tandem mass spectrometry (MS<sup>2</sup>) of *K. pneumoniae* A3 showing fragment ions of (A) *m/z* 1955 and (B) *m/z* 1971.**

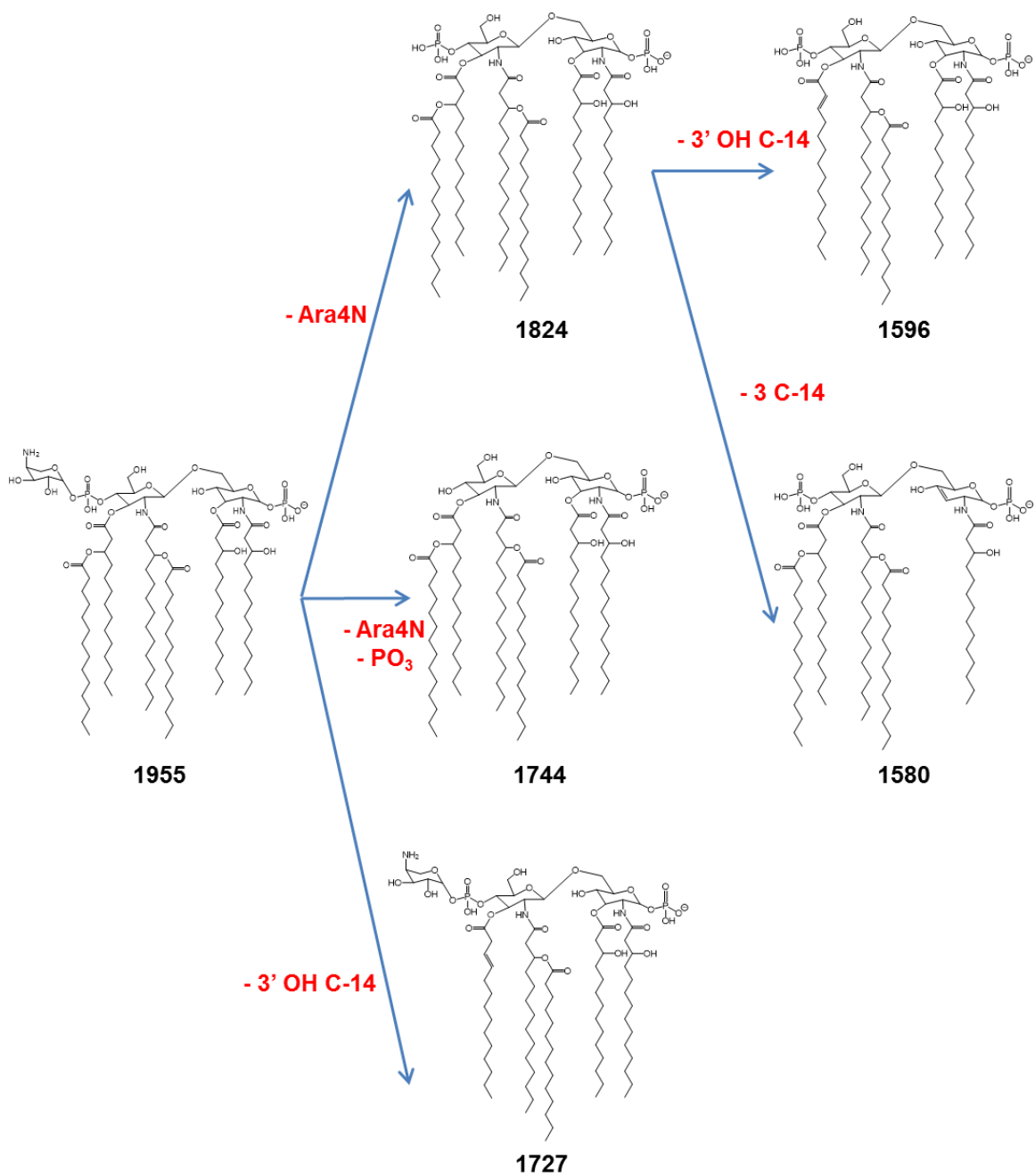


**Figure 3.5. Structures of  $m/z$  1955 lipid A and fragment ions at  $m/z$  1824 (loss of Ara4N), 1744 (loss of Ara4N + phosphite), 1727 (loss of 3'-oxo-acyl group), 1596 (loss of Ara4N + 3'-oxo-acyl group), and 1580 (loss of Ara4N + 3'-acyl group).**

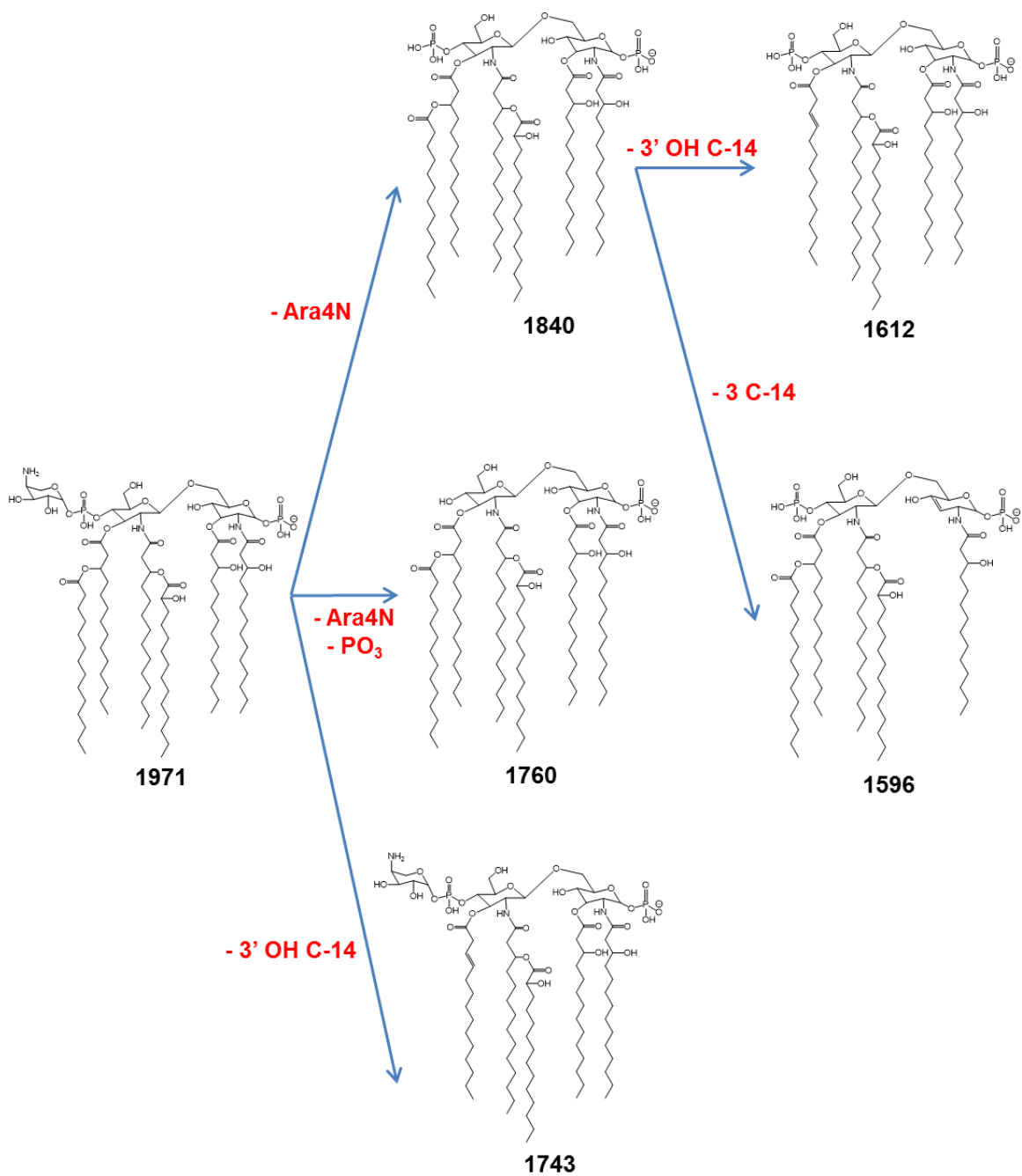


**Figure 3.6. Structures of  $m/z$  1971 lipid A and fragment ions at  $m/z$  1840 (loss of Ara4N), 1760 (loss of Ara4N + phosphite), 1743 (loss of 3'-oxo-acyl group), 1612 (loss of Ara4N + 3'-oxo-acyl group), and 1596 (loss of Ara4N + 3'-acyl group).**

## Discussion

The rapid dissemination of carbapenem-resistant Enterobacteriaceae has resulted in hard-to-treat infections and high mortality rates. Facing a shortage of effective antimicrobials, clinicians have turned to colistin, a last-line antibiotic that has now become a valuable clinical treatment option (147). Increased colistin consumption has led to the emergence of colistin-resistant Gram-negative Enterobacteriaceae and *A. baumannii*. In *K. pneumoniae*, lipid A is modified with Ara4N by the *pmrHFIJKLM* operon and under the control of *phoPQ* and *pmrAB* (156). Colistin resistance is associated with mutations to *phoPQ* and *pmrAB* or the negative regulator *mgrB* resulting in the upregulation of this LPS modification system (157, 159).

Here we presented a study of colistin-susceptible and resistant pairs of *K. pneumoniae* clinical strains collected from 11 patients. We examined only strains obtained from patients with independently acquired infections in which evolution of resistance occurred as a response to CMS treatment. We found that 7 of 11 resistant strains possessed loss-of-function *mgrB* mutations consistent with previous findings (153–155, 159, 165). While there is strong association between mutations in specific genetic loci regulating lipid A synthesis and modifications to lipid A in susceptible versus resistant strains, different locations or types of loss-of-function mutations did not produce significantly different MICs or mass spectrometric profiles of lipid A (**Table 3.2**). Interestingly, resistant strains A5, D7, E6, and F9 only displayed the Ara4N-specific ions following culture in sub-lethal colistin concentration indicating that there is regulation of LPS modification. The findings in this study are congruent with previous work demonstrating high variability in resistance

profiles and in which strains incur some fitness cost of resistance yet resistance persists in the absence of selection (150, 166).

This work demonstrated that genetic alterations previously implicated in colistin resistance of *K. pneumoniae* displayed a corresponding LPS modification as shown by an altered mass spectral profile (**Figures 3.2 and 3.3**). Notably, strains C2, D7, and H5 shared this same mass spectral profile, but contained no non-synonymous mutations of the aforementioned genes. Park et al. similarly identified a colistin-resistant *A. baumannii* with WT *pmrAB* (167). Furthermore, strain C2 was found to be susceptible to colistin upon repeated susceptibility testing. Clearly there may be additional genes involved in regulation or modification of LPS, and this was previously posited (149, 154). Other factors may contribute to this phenomenon including: heterogeneity or hetero-resistance between cells within a strain (MIC measurements and mass spectrometry phenotyping were conducted on the same cultures from single colonies), which was observed in *A. baumannii* (168) and *P. aeruginosa* (169); or emergence of cross-resistance due to contact with host antimicrobial peptides.

Finally, the discovery of a colistin resistance mechanism mediated by a plasmid-encoded MCR phosphoethanolamine transferase should be addressed: effective colistin resistance monitoring must include this novel mechanism (170). The current study links alterations in the bacterial genome with a physiological response in these resistant organisms and lends further understanding to the role these mutations play in resistance acquisition, and this could certainly be applied to the study of the impact of MCR-conferred, colistin-resistant organisms. We have also recently shown that *mcr-1*-containing plasmids expressed in colistin-resistant *K. pneumoniae* strains gave an altered resistance

ion profile in which phosphoethanolamine is added to lipid A overriding Ara4N modification (171). Furthermore, our determination of structural differences between resistant and susceptible strains elucidated by mass spectrometry in both studies suggests the potential of this platform as a diagnostic to improve antibiotic stewardship of colistin-resistant organisms.

**Nucleotide accession number.** The raw sequence reads were deposited to the short read archive under BioProject PRJNA375812.

# **CHAPTER FOUR: Characterization of *Acinetobacter* spp. Isolates from a Large Cohort of Patients and Colistin Resistance Monitoring Following Colistimethate Treatment**

## **Abstract**

Infections by *Acinetobacter baumannii* and *Acinetobacter baumannii* complex organisms are prevalent nosocomial infections acquired in hospitals with a high incidence of antimicrobial resistance (AR). Treatment of these drug-resistant organisms with colistin, a last resort antibiotic of the polymyxin class has resulted in emergence of strains for which limited therapeutic options are effective; therefore, it has become increasingly important to rapidly detect and monitor the spread and prevalence of these pathogens in a clinical setting. Colistin resistance occurs via sugar modifications to the terminal phosphate moieties of lipopolysaccharide (LPS)-derived lipid A reducing membrane electronegativity and is readily identified by mass spectrometry. Here we present a study of a large cohort of *Acinetobacter* spp. clinical isolates in which species identification and prevalence of resistance to colistin is monitored by classical phenotypic testing as well as mass spectrometric (MS) analyses. MALDI-TOF-based MS protein phenotyping allowed speciation of *A. baumannii* complex species indicating a higher clinical prevalence of non-*A. baumannii* *Acinetobacter* spp. than previously reported. Overall, high correlation was observed between determinations of resistance by MIC and MS of lipid A modification although high intra- and inter-variability between MIC testing methods suggest MS analysis may be a more reliable means of identifying colistin-resistant *A. baumannii* isolates.

## Introduction

The Gram-negative coccobacillus pathogen *Acinetobacter baumannii* has established itself as a serious threat in health care institutions. According to the Centers for Disease Control and Prevention (CDC), it is implicated in 7,300 drug-resistant infections and 500 deaths per year, and it is a prominent pathogen in hospital-acquired pneumonia, wound infections, and sepsis (9). The World Health Organization (WHO), in releasing its global priority list of antibiotic-resistant bacteria this year, gave *A. baumannii* its highest priority level: critical (172). It is joined by the other ESKAPE pathogens to occupy the top five spots on the WHO's list; the ESKAPE pathogens, *Enterococcus faecium*, *Staphylococcus aureus*, *Klebsiella pneumoniae*, *Acinetobacter baumannii*, *Pseudomonas aeruginosa*, and *Enterobacter* spp., are so called due to their ability to “escape” antibiotic therapies by rapid acquisition of resistance (126). Therefore, the WHO and the CDC have prioritized development of novel diagnostics and therapeutics to address the global threat of these AR bacteria (9, 172).

*A. baumannii* has demonstrated resistance to a wide array of antimicrobials, most notably to those in the carbapenem class. It exerts its resistance through expression of  $\beta$ -lactamases that degrade the antibiotic and includes class D oxacillinases and class B metallo- $\beta$ -lactamases (173). Colistin (polymyxin E), a polycationic polypeptide, is used to treat infections caused by these carbapenem-resistant organisms leading to a corresponding increase in resistance to colistin, which would have devastating consequences as one of the last remaining antimicrobials would become ineffective against these organisms (174). In *A. baumannii*, resistance is conferred through lipopolysaccharide (LPS) modifications:

addition of phosphoethanolamine onto the terminal phosphate of the lipid A (LA) moiety of LPS decreases the molecule's electronegativity reducing the binding affinity of colistin. This occurs through genetic mutations to *pmrAB* or indirectly through *pmrD* via mutations to *phoPQ*, both are two-component regulatory systems required for the expression of LPS-modifying enzymes including PmrC, which is upstream of PmrAB and a phosphoethanolamine transferase. Expression of PmrC results in the conversion of a subset of the newly synthesized LPS, which when transported to the outer membrane disrupts membrane attack and cell lysis by colistin (149). The growing incidence of colistin-resistant *A. baumannii* has profound clinical implications since early initiation of targeted antimicrobial therapy has been exhaustively determined to significantly improve patient morbidity and mortality (6, 7), necessitating the development of novel platforms to more rapidly detect these antibiotic-resistant bacteria.

In a health care setting, determination of antimicrobial susceptibility is key to directing appropriate chemotherapies. The classical method of antibiotic susceptibility testing (AST) is a culture-based method: a minimum inhibitory concentration (MIC) is determined by the lowest concentration of antibiotic at which microbial growth inhibition is observed when an isolate is grown in a panel of different antibiotic media at a range of concentrations. AST is accomplished through disk diffusion testing, agar/broth dilution assays, and/or Etest (14). However, significant concerns have been raised over susceptibility testing of colistin, including discrepant results based on the methods used, and lack of reproducibility (175, 176). Microbial phenotyping by matrix-assisted laser desorption/ionization time-of-flight mass spectrometry (MALDI-TOF MS) has emerged as

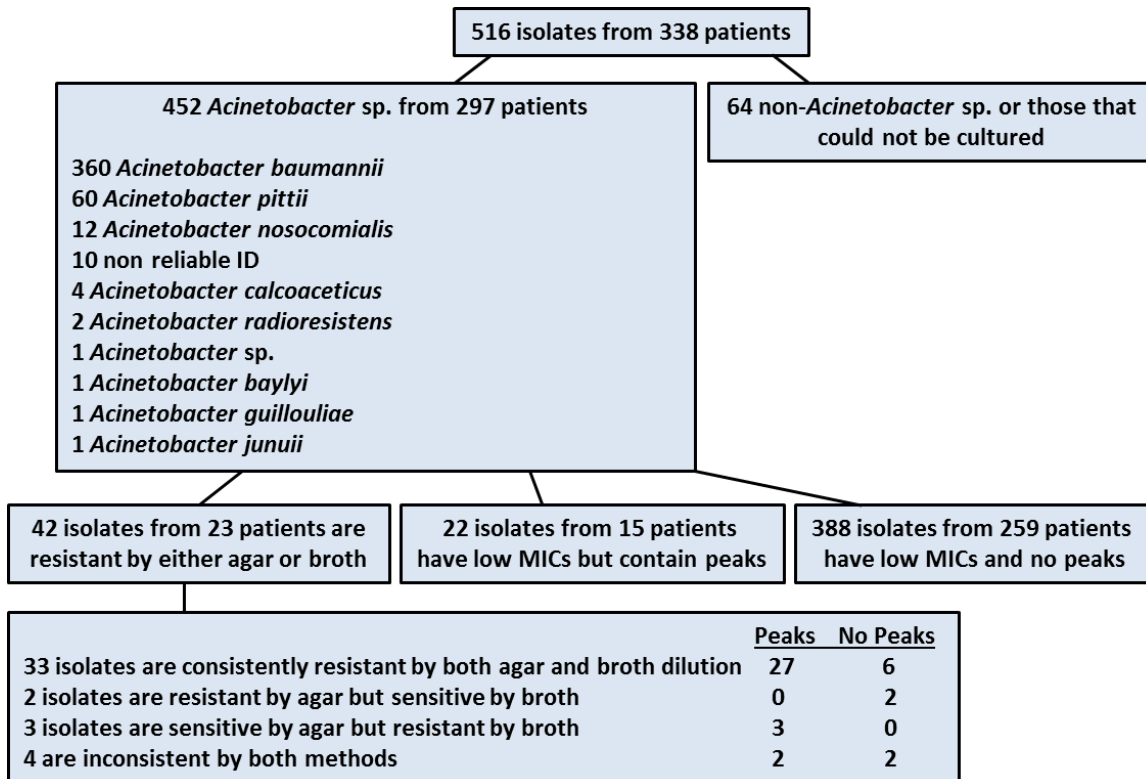
a dominant technology for the identification of infectious agents; the clinical platform utilizes a mass spectrum of microbial proteins to make an identification by comparison against a reference database of mass spectra from known sources. MS-based protein typing has also been used to detect resistance, most notably identifying  $\beta$ -lactam hydrolysis products in microbial protein mass spectra that would indicate resistance to the  $\beta$ -lactam class of antibiotics (18). Recently, we have shown that the complex glycolipids that reside in microbial membranes (such as LA of LPS in Gram-negative bacteria) offer a novel chemical signature that could be exploited for microbial identification (116). Furthermore, we and others have shown that colistin-resistant *K. pneumoniae*, *P. aeruginosa*, and *A. baumannii* are characterized by modifications to LPS that are readily visualized on a mass spectrum of microbial glycolipids (117, 128, 129, 177).

To test the hypothesis that MS-based glycolipid profiling can accurately predict colistin resistance of *A. baumannii*, we prospectively collected all *A. baumannii* clinical isolates at a major healthcare system for three years and correlated their susceptibility to colistin, as defined by MIC testing (broth microdilution and agar dilution methods) and MS-based glycolipid profiling.

## **Results**

**Overview of *Acinetobacter* clinical isolates in this study.** A total of 516 isolates were taken from 338 patients collected between 2014 and 2016 at the University of Pittsburgh Medical Center. Sixty-four isolates either could not be cultured or were identified as non-*Acinetobacter* species by MALDI-TOF protein phenotyping, which likely resulted from specimen contamination or initial misidentification, and were excluded from further

consideration. The remaining 452 isolates were culturable and identified as *Acinetobacter* spp. using the protein-based MS Bruker Biotyper diagnostic platform. Among these, 79.7% (360 isolates) were determined to be *A. baumannii*, 13.3% (60 isolates) *Acinetobacter pittii*, 2.7% (12 isolates) *Acinetobacter nosocomialis*, and <1% came from the following: *Acinetobacter calcoaceticus* (4 isolates), *Acinetobacter radioresistens* (2 isolates), *Acinetobacter baylyi* (1 isolate), *Acinetobacter guillouliae* (1 isolate), *Acinetobacter juniii* (1 isolate), and unassigned (*Acinetobacter* sp., 1 isolate). Ten isolates (2.2 %) could not be reliably identified by MS protein typing and were excluded from further consideration. **Figure 4.1** shows a schematic characterization of the clinical isolates collected for this study.

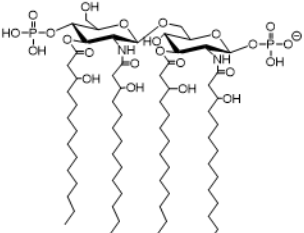
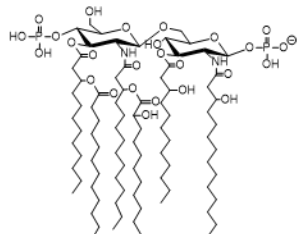
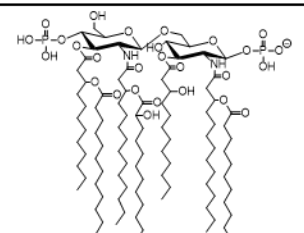
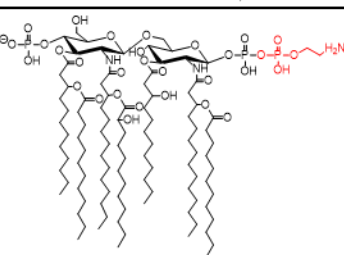


**Figure 4.1. Classification scheme according to identifications and MIC/MS determinations of clinical isolates collected during the course of this study.**

**MIC determination of study isolates.** For the 452 clinical isolates identified as *Acinetobacter* isolates during standard patient care and confirmed by MS protein typing, MICs were determined by standard agar dilution or broth microdilution assay. A total of 42 isolates (9.3%) were identified as resistant by broth and agar dilution assay. Among these, 33 isolates were found to be resistant by both assays, 2 were found susceptible by broth dilution but resistant by agar dilution assay, 3 were found susceptible by agar but resistant by broth, and 4 gave inconsistent results for both methods by repeated testing. **(Figure 4.1)**

**Colistin susceptibility determination by MALDI-TOF.** Strains positively identified as *Acinetobacter* spp. were subjected to mass spectrometric analysis of extracted membrane lipids to characterize LA modifications associated with the observed MIC measurements. Ions were most often observed at  $m/z$  1404, 1728, and 1910 and their predicted structures are shown in **Figure 4.2**. These have been previously characterized (129) with  $m/z$  1910 representing the full bis-phosphorylated, hepta-acylated lipid A structure,  $m/z$  1728 occurring from loss of a laurate (C12) fatty acyl group (or  $m/z$  1712 resulting from loss of C12(3-OH)), and  $m/z$  1404 (also known as lipid IVa), which is likely a biosynthetic precursor as this analysis involves whole cell extracts or a degradative product that occurs during extraction or ionization. There are additional minor ions at  $m/z$  1882 and 1376, representing the replacement of a laurate (C12) instead of myristate (C14) at the C-2 position of the glucosamine backbone (loss of 28 mass units) corresponding to the lipid A structures at  $m/z$  1910 and 1404, respectively. In resistant isolates, an additional ion is observed at  $m/z$  2033 corresponding to a mass increase of  $m/z$  123 representing a

phosphoethanolamine addition onto one of the phosphate moieties of the  $m/z$  1910 structure  
**(Figure 4.3).**

<i>m/z</i>	Predicted Structure	Modification
1404		The lipid IVa biosynthetic precursor
1728		Demyristoylation at the C-1 acyl-oxo-acyl position
1910		Full lipid A structure found in the outer membrane
2033*		Phosphoethanolamination (-PEtN) of the C-1 phosphate moiety

**Figure 4.2. Lipid A structures of “signature” ions with corresponding *m/z* values.** Lipid A *m/z* values and molecular structures found in mass spectra of the *A. baumannii* clinical isolates with descriptions of the modifications responsible for the observed mass shifts. Structures in red indicate modifications to base structure at *m/z* 1910. (\*) denotes ions associated with colistin resistance.

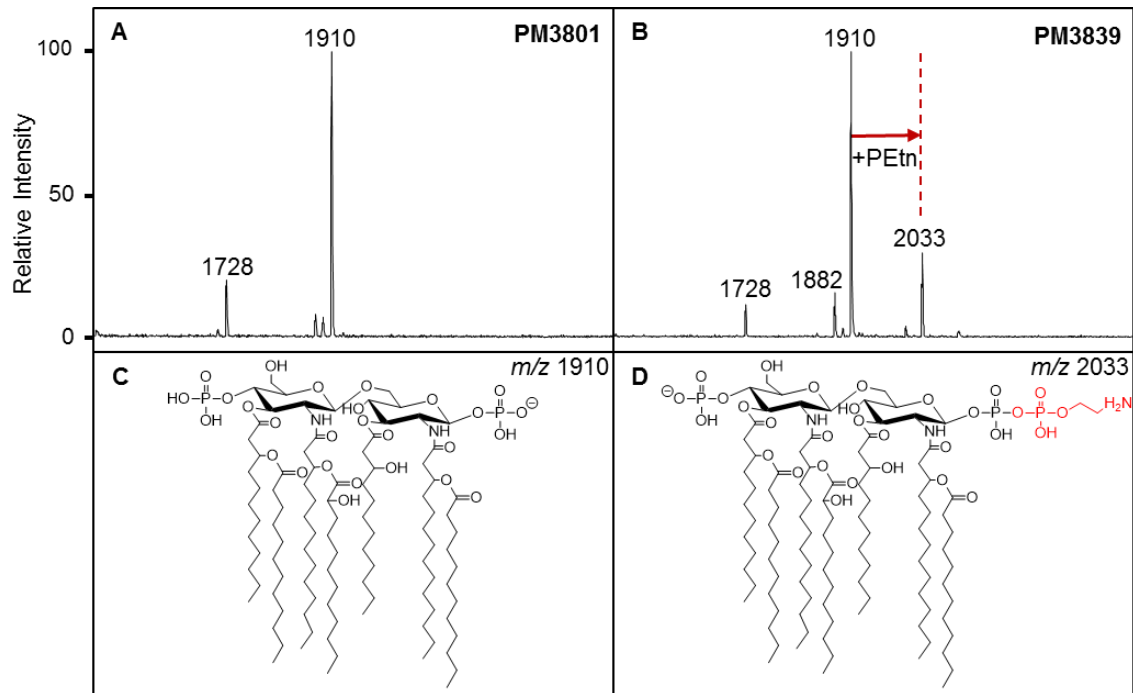


**Figure 4.3. MALDI-TOF MS of *A. baumannii* with differential colistin susceptibility collected within-patient.** **A)** Colistin-susceptible strain PM 3801 shows an ion at  $m/z$  1910 corresponding to the full structure that exists in the outer membrane, a bis-phosphorylated, hepta-acylated lipid A. **B)** Colistin-resistant strain PM 3839 shows an additional ion at  $m/z$  2033 indicating an phosphoethanolamine addition to the base structure at  $m/z$  1910. **C)** and **D)** Molecular structures of the lipid A molecules found in the mass spectra.

**Susceptibility correlation between MIC methods and LA modification of *A. baumannii* LPS.** Of the 42 isolates determined to be resistant by either agar dilution or broth microdilution, 32 displayed the  $m/z$  2033 ion, representing a positive correlation of 76.2% between MIC and MS findings. Of the 33 isolates determined to be resistant by both MIC assays, 27 displayed the resistant ion, a positive correlation of 81.8%. Of the five isolates with discrepant results between the two MIC assays, MS findings highly correlated with the results of broth microdilution: the resistant ion was present in the three isolates determined resistant by broth and absent in the two isolates determined resistant by agar. Therefore, of the 36 isolates determined to be resistant by broth, 30 displayed the resistant ion at  $m/z$  2033 by MS analysis with a positive correlation rate of 83.3%. (**Figure 4.1**) Furthermore, MS data support the most recent European Committee on Antimicrobial Susceptibility Testing (EUCAST) release recommending broth microdilution assay for determination of colistin susceptibility in *A. baumannii* (158).

**Comparison of *Acinetobacter* isolates by MALDI-TOF.** In the MS analysis, differences were observed between spectra collected from the *A. baumannii* complex isolates, *A. baumannii*, *A. pittii*, and *A. nosocomialis* (**Figure 4.4**). In general, the ion at  $m/z$  1882 displayed higher signal intensity in *A. pittii* and *A. nosocomialis* isolates, which may indicate differences in relative abundances of the LPS molecules in the membrane. In addition, they showed the presence of novel ions at  $m/z$  1866 and 1894, which may indicate differences in hydroxylation events (loss of 16 amu) from ions at  $m/z$  1882 and 1910, respectively, although further analyses would need to be conducted for positive structural determinations. Interestingly, among the six resistant isolates that lacked modified lipid A,

three of these were identified as *A. pittii* and one as *A. haemolyticus*, suggesting a potential novel mechanism of resistance among non-*A. baumannii* *Acinetobacter* species. And in fact, among the 27 isolates displaying resistance ions, 26 are *A. baumannii* and only one is *A. nosocomialis*. (**Figure 4.1**)

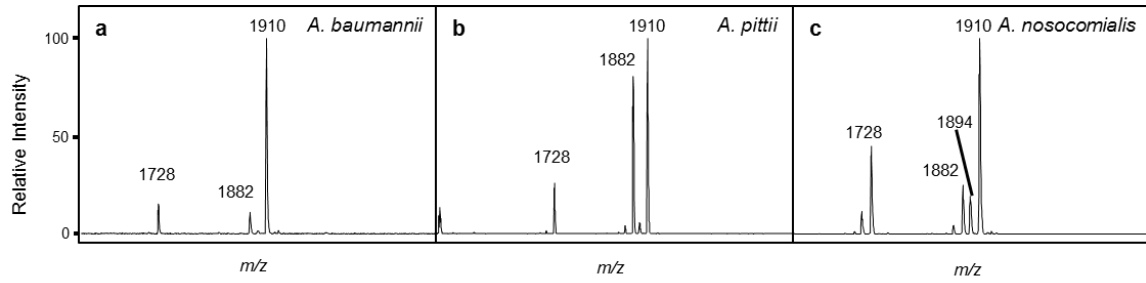


**Figure 4.4. MALDI-TOF MS comparison of representative *A. baumannii* complex isolates A) *A. baumannii* strain MWH019, B) *A. pittii* strain PM3950, and C) *A. nosocomialis* strain MWH017.**

## Discussion

The genus *Acinetobacter* consists of over 50 genospecies ([www.bacterio.net/acinetobacter.html](http://www.bacterio.net/acinetobacter.html)). The three most common genospecies that are considered to be clinically significant are *A. baumannii*, *A. nosocomialis* and *A. pittii*. These species are not differentiated by biochemical methods and often grouped together as the *A. baumannii* complex. Speciation based on genetic methods (*e.g.* *rpoB* sequencing, rRNA intergenic spacer sequencing) has enabled differentiation of the *A. baumannii* complex species for research purposes. It has been demonstrated that MALDI-TOF MS can be utilized as an alternative method to reliably identify *A. baumannii* complex species (178–181). Using these methods, the prevalence of *A. baumannii*, *A. nosocomialis* and *A. pittii* within *A. baumannii* complex has been shown to be highly variable among clinical isolates depending on epidemiological settings (182–186). In our prospective study, we observed that *A. baumannii* isolates were the predominant species yet represented a smaller proportion than what has previously been observed in above studies.

For this study, we evaluated both the agar and broth dilution assays for our clinical cohort; however, as of March 2016, the CLSI-EUCAST joint Polymyxin Breakpoints Working Group recommended the ISO-standard broth microdilution method for determination of colistin MIC. As in previous studies (117, 128, 129, 177), we found a strong association between resistant MIC determinations and the observation of higher *m/z* ions consistent with modification to LA previously demonstrated to confer resistance. Therefore, glycolipidomic profiles by MALDI-TOF analyses were generated for all *Acinetobacter* isolates collected during our study. In general, MALDI-TOF data correlated

more highly with the CLSI-EUCAST-recommended broth microdilution assay. Discrepancies between MIC and MS data, while occurring infrequently, need to be explored in more detail. In examining discordant results within MIC determinations, these isolates had wildly variable resistance profiles from multiple testing while, in general, MS data tended to be more consistent. For example, the MIC of strain PM3826 was found to be 0.5 and >256  $\mu\text{g}/\text{mL}$  by broth microdilution, and six separate tests by agar and broth found an MIC range of 1 to >128  $\mu\text{g}/\text{mL}$  for strain MWH024. In both instances, there were no resistance-associated ions in any of the mass spectra. Similarly, strain PM3808 was determined to be susceptible by multiple agar and broth tests but resistant by a single agar dilution test (32  $\mu\text{g}/\text{mL}$ ), and resistance-associated ions were consistently observed by two different technicians conducting separate MS analyses. In contrast, there was only one incidence, strain PM3918, where mass spectral replicates were in disagreement. Another possibility is the loss of LPS modification in the absence of selection. Conferral of resistance results from genetic mutations leading to constitutive expression of LPS-modifying enzymes (149); however, we have previously demonstrated an increase in abundances of resistance-associated ions in mass spectra upon exposure of resistant *K. pneumoniae* strains to sub-lethal concentrations of colistin (117) indicating that expression is amplified by antimicrobial challenge (187, 188). Therefore, we plan to repeat MS analyses from cultures grown in selective media for these isolates for which resistance was determined by MIC yet lacked resistance-associated ions.

An alternative explanation is the existence of heteroresistance within an infection. Li et al. (168) used concentration-dependent killing assays to observe this in multidrug-

resistant *A. baumannii* isolates and Hermes et al. (169) performed similar assays in determining polymyxin B heteroresistance in *P. aeruginosa* clinical isolates. A heterogeneous population in which only a few organisms are strongly colistin-resistant would explain some of our discrepant results. For example, it could be the case that when cultured in the presence of colistin, the resistant cells would grow and the population deemed “resistant” by MIC despite the fact that susceptible cells are inhibited. Yet, if the susceptible subpopulation is otherwise found in disproportionately higher ratios in the absence of colistin, as was the case for our liquid cultures used for MS, the resulting signature of colistin resistance would be small as compared to the stronger signal from the sensitive subpopulation. Studies are currently underway to perform similar analyses on select multiple isolates (*i.e.* chose 50 individual bacterial colonies for MS analysis from a single isolate) from this study cohort. Finally, it is possible that alternate mechanisms other than PEtN modification of LPS may be influencing resistance. Park et al. (167) observed overexpression of lipid A-modifying proteins in resistant *A. baumannii* compared to susceptible yet no non-synonymous mutations were observed in *pmrAB* or *pmrC* genes. Furthermore, other resistance pathways have been suggested involving additional operons, defense mechanisms (*e.g.* capsule or efflux pumps) (149, 189), as well as alternate modifications either to LPS or lipid A (127, 129, 149, 190).

Here we present a study of a large cohort of 452 *Acinetobacter* spp. clinical isolates collected from patients for a three-year period and characterized according to speciation and colistin resistance. Strains were identified by conventional phenotypic methods and confirmed by MS protein typing, and antimicrobial susceptibility to colistin was evaluated

by agar and broth dilution assays as well as MS analysis of lipopolysaccharide-derived lipid A. Overall, we can conclude that glycolipid MS can effectively detect colistin resistance in *A. baumannii*, supports broth microdilution for accurate determination of MIC, and has the potential to direct antimicrobial stewardship in the clinic.

## **Materials and Methods**

**Bacterial strains.** All available clinical isolates that were identified as *A. baumannii* or *A. baumannii* complex by MicroScan WalkAway (Beckman Coulter, Brea CA) were prospectively collected, irrespective of antimicrobial susceptibility patterns, at a clinical microbiology laboratory serving four academic hospitals belonging to a major health system in Western Pennsylvania for a three-year period between 2014 and 2016. The isolates were then stored at -80°C until use.

**Strain identification by MALDI-TOF protein typing.** Speciation of the collected isolates was confirmed by the MALDI Biotyper v4.0 (Bruker Daltonics, Billerica MA) coupled to the Bruker Microflex LRF MALDI-TOF mass spectrometer (Bruker Daltonics, Billerica MA) in the research laboratory according to the manufacturer's "direct method" for spotting samples. Using a sterile toothpick, a single colony was picked and a thin layer smeared directly onto the stainless steel target plate. Colony smears were overlaid with 1 µL matrix (10 mg/mL  $\alpha$ -cyano-4-hydroxycinnamic acid (CHCA) in 50% acetonitrile and 2.5% trifluoroacetic acid [v/v]) and allowed to dry. The Biotyper Bacterial Test Standard was used for calibration. Mass spectra were acquired using the Biotyper Real Time Classification (RTC), the associated software for automated data acquisition and analysis. After the run is initiated, the RTC program acquires all raw data, compares the mass

profiles against an integrated database of reference spectra, and outputs the top ten most likely identifications with the highest confidence log scores. The highest scoring ID with a log score  $\geq 1.7$  was considered a positive identification.

**Susceptibility testing.** Colistin sulfate salt was purchased from Sigma-Aldrich (C4461; St. Louis MO). The MICs of colistin were determined by both the agar dilution method and the broth microdilution method. For the latter, testing was performed without the addition of polysorbate-80 ([http://www.eucast.org/fileadmin/src/media/PDFs/EUCAST\\_files/General\\_documents/Recommendations\\_for\\_MIC\\_determination\\_of\\_colistin\\_March\\_2016.pdf](http://www.eucast.org/fileadmin/src/media/PDFs/EUCAST_files/General_documents/Recommendations_for_MIC_determination_of_colistin_March_2016.pdf)). MICs of  $\leq 2$   $\mu\text{g}/\text{mL}$  or  $> 2$   $\mu\text{g}/\text{mL}$  were considered susceptible and resistant, respectively, according to the clinical breakpoint provided by the EUCAST. The MIC measurements were repeated when i) there was discrepancy between the agar dilution and broth microdilution methods, and ii) there was discrepancy between the MICs and the MS-based lipid profiles.

**Lipid A isolation from whole cells.** A single colony of each isolate was inoculated in 5 mL of lysogeny broth (LB) and incubated at 37°C overnight with agitation. Cultures were harvested at  $4000 \times g$  for 10 minutes. Membrane lipids were extracted and LPS was converted to LA by heat-assisted ammonium isobutyrate extraction that has been previously described (131). Briefly, bacterial pellets were treated with a 5:3 mixture of 70% [v/v] isobutyric acid/1 M ammonium hydroxide (250  $\mu\text{L}$ /150  $\mu\text{L}$ ) and incubated at 100°C for 30 minutes. Tubes were transferred to ice to halt the reaction and centrifuged at  $2000 \times g$  for 15 minutes to remove cell debris. Supernatants were transferred to clean tubes,

combined in a 1:1 ratio of distilled water (400  $\mu$ L), snap frozen on dry ice, and lyophilized overnight. The resultant dry pellets contain whole cell extracts of membrane lipids.

**Lipid A characterization by MALDI-TOF.** Isolates were blinded to the technician during mass analysis. Dry lipid extracts were washed twice with 1 mL of methanol then resuspended in 100  $\mu$ L of a 2:1:0.25 chloroform/methanol/water solvent mixture and centrifuged at  $2000 \times g$  to pellet insolubilized debris. Aliquots of 1  $\mu$ L each of norharmane matrix (10 mg/mL in 2:1  $\text{CHCl}_3/\text{CH}_3\text{OH}$  [v/v]) then analyte were spotted onto stainless steel target plates. Mass spectra were recorded in negative ion mode using a Bruker Microflex LRF MALDI-TOF mass spectrometer (Bruker Daltonics Inc., Billerica MA) operated in reflectron mode. The instrument is equipped with a 337 nm nitrogen laser, and analyses were performed at 39.5% global intensity. Typically, 900 laser shots were summed to acquire each spectrum, and at least three mass spectra were acquired per sample. Electrospray tuning mix (Agilent, Palo Alto, CA) was used for mass calibration. Data were acquired and processed using flexControl and flexAnalysis version 3.4 (Bruker Daltonics Inc., Billerica MA). Mass spectra were smoothed and baseline corrected using the default processing parameters of the software. The determination of a mass spectrum associated with resistance was made by the technician in a blinded manner by observing the “resistance-associated ions” in the majority of acquired spectra for that sample above a signal-to-noise ratio (SNR) of 3.

## CHAPTER FIVE: Structural Modification of Lipopolysaccharide Conferred by *mcr-1* in Gram-Negative ESKAPE Pathogens

### Abstract

*mcr-1* was initially reported as the first plasmid-mediated colistin resistance gene in clinical isolates of *Escherichia coli* and *Klebsiella pneumoniae* in China and has subsequently been identified worldwide in various species of the family Enterobacteriaceae. *mcr-1* encodes a phosphoethanolamine transferase and its expression has been shown to generate phosphoethanolamine-modified bis-phosphorylated hexa-acylated lipid A in *E. coli*. Here, we investigated the effect of *mcr-1* on colistin susceptibility and lipopolysaccharide structures in laboratory and clinical strains of the Gram-negative ESKAPE pathogens, which are often treated by colistin clinically. The effects of *mcr-1* on colistin resistance were determined using minimum inhibitory concentration (MIC) assays of laboratory and clinical strains of *E. coli*, *K. pneumoniae*, *Acinetobacter baumannii*, and *Pseudomonas aeruginosa*. Lipid A structural changes resulting from MCR-1 were analyzed by mass spectrometry. Introduction of *mcr-1* led to colistin resistance in *E. coli*, *K. pneumoniae* and *A. baumannii* but only moderately reduced susceptibility in *P. aeruginosa*. Phosphoethanolamine modification of lipid A was observed consistently for all four species. These findings highlight the risk of colistin resistance as a consequence of *mcr-1* expression among ESKAPE pathogens, especially in *K. pneumoniae* and *A. baumannii*. Furthermore, the observation that lipid A structures were modified despite only modest increases in colistin MICs in some instances suggests more

sophisticated surveillance methods may need to be developed to track the dissemination of *mcr-1* or plasmid-mediated phosphoethanolamine transferases in general.

## **Introduction**

Polymyxins, which include colistin (polymyxin E) and polymyxin B, are active against the majority of clinically relevant Gram-negative bacteria and are increasingly used as salvage therapy for infections caused by strains that have become resistant to all other commonly used antibacterial agents (191). Clinically, the key species against which colistin is most implemented due to extensive drug resistance (XDR) include *Klebsiella pneumoniae*, *Acinetobacter baumannii* and *Pseudomonas aeruginosa*. These three ESKAPE pathogens, along with *Enterobacter* spp. and the Gram-positive organisms *Enterococcus faecium* and *Staphylococcus aureus*, are notable for their rapid drug resistance acquisition and nosocomial prevalence. Colistin is a polycationic peptide that acts by targeting the negative charges in bacterial lipopolysaccharide (LPS), the complex lipoglycan that comprises the majority of the Gram-negative outer membrane (191). Specifically, colistin attacks the highly electronegative phosphate groups associated with lipid A, the membrane-anchoring molecule of LPS and its glycol core, resulting in lysis and death of Gram-negative bacteria.

The canonical lipid A structure found in Gram-negative bacteria consists of a  $\beta$ -1',6-linked disaccharide glucosamine backbone that is hexa-acylated and phosphorylated at positions 1 and 4' (**Figure 5.1**). Lipid A-modifying enzymes can introduce changes to the canonical lipid A structure by adding, removing, or altering different chemical moieties. These species can naturally develop resistance to colistin by modifying the structure of the

lipid A component of LPS, reducing the overall negative charge of the lipid A moiety and therefore binding of colistin (191). *K. pneumoniae* and *P. aeruginosa* accomplish this by the addition of 4-amino-4-deoxy-L-arabinose (L-Ara4N) to lipid A, a process that is governed by the *arnBCADTEF* operon (192). In contrast, *A. baumannii* uses phosphoethanolamine (PEtN) as the moiety to modify lipid A through a phosphoethanolamine transferase encoded by *pmrC* (193). In either of these pathways, the end result is clinically relevant levels of colistin resistance (i.e., minimum inhibitory concentrations [MICs] of 4 µg/mL or higher).

Colistin resistance in patients usually occurs with exposure to this agent and was considered to be a strictly chromosomally mediated process (129, 159, 177). This paradigm changed when we reported the first plasmid-mediated colistin resistance mechanism in 2015 (194). Based on the observation that colistin resistance was transferable from some *E. coli* strains of swine origin to *E. coli* laboratory strains, we identified *mcr-1*, a 1,626-bp gene with moderate sequence identity to known phosphoethanolamine transferase genes. Introduction of *mcr-1* to *E. coli* resulted in resistance to colistin by addition of PEtN to lipid A. In addition to swine and poultry *E. coli* strains, the report also identified *mcr-1* in several colistin-resistant *E. coli* and *K. pneumoniae* strains of human origin (194). Subsequently, *mcr-1* has been identified in colistin-resistant strains of animal and human origins worldwide, indicating that this gene is widely disseminated. In addition to *E. coli* and *K. pneumoniae*, *mcr-1*-mediated colistin resistance has been found in *Salmonella enterica*, *Enterobacter cloacae*, and *Enterobacter aerogenes*, all of which belong to the family Enterobacteriaceae (195). A major concern from the epidemiological perspective is

the potential for *mcr-1* to spread into healthcare-associated XDR pathogens including *Klebsiella pneumoniae*, *Acinetobacter baumannii* and *Pseudomonas aeruginosa*, which would lead to truly untreatable infections. The goal of this study was to investigate the impact of *mcr-1* on colistin resistance and lipopolysaccharide structure in these species.

## **Results**

***mcr-1* confers colistin resistance in *E. coli*, *K. pneumoniae* and *A. baumannii* and reduced susceptibility in *P. aeruginosa*.** *mcr-1*-carrying recombinant plasmids were successfully introduced and maintained in the laboratory and clinical strains tested. In all species tested, colistin MICs were elevated upon introduction of *mcr-1* (**Table 5.1**). Colistin MICs increased by 16- to 32-fold in *E. coli*, 32- to 256-fold in *K. pneumoniae*, 64- to >128-fold in *A. baumannii* and 2- to 4-fold in *P. aeruginosa*.

**Table 5.1. Minimum inhibitory concentrations of *mcr-1*-positive strains used in the study.**

<b>Strain</b>	<b>PCR for <i>mcr-1</i></b>	<b>MIC (µg/mL)</b>	<b>Fold change</b>
<i>E. coli</i> ATCC 25922	-	0.125	32
<i>E. coli</i> ATCC 25922 (pMQ124- <i>mcr-1</i> )	+	4	
<i>E. coli</i> YD626	-	0.125	16
<i>E. coli</i> YD626 (pMQ124- <i>mcr-1</i> )	+	2	
<i>K. pneumoniae</i> 2210291	-	0.125	32
<i>K. pneumoniae</i> 2210291 (pMQ124- <i>mcr-1</i> )	+	4	
<i>K. pneumoniae</i> ATCC 13883	-	0.125	256
<i>K. pneumoniae</i> ATCC 13883 (pBCSK- <i>mcr-1</i> )	+	32	
<i>A. baumannii</i> ATCC 17978	-	0.25	64
<i>A. baumannii</i> ATCC 17978 (pMQ124WH1266- <i>mcr-1</i> )	+	16	
<i>A. baumannii</i> SM1536	-	1	>128
<i>A. baumannii</i> SM1536 (pMQ124WH1266- <i>mcr-1</i> )	+	>128	
<i>A. baumannii</i> D773	-	0.25	>128
<i>A. baumannii</i> D773 (pMQ124WH1266- <i>mcr-1</i> )	+	>128	
<i>P. aeruginosa</i> TRPA179	-	2	4
<i>P. aeruginosa</i> TRPA179 (pMQ124- <i>mcr-1</i> )	+	8	
<i>P. aeruginosa</i> 8542455	-	0.5	2
<i>P. aeruginosa</i> 8542455 (pMQ124- <i>mcr-1</i> )	+	1	
<i>P. aeruginosa</i> ATCC 47085	-	0.5	4
<i>P. aeruginosa</i> ATCC 47085 (pMQ124- <i>mcr-1</i> )	+	2	

**Lipid A is modified by the addition of phosphoethanolamine in all species examined.**

To investigate structural changes conferred by the phosphoethanolamine transferase activity of MCR-1, we isolated lipid A from wild-type and *mcr-1*-expressing strains and performed matrix-assisted laser desorption/ionization (MALDI) mass spectrometry (MS). PEtN addition can be tracked by MS using the known mass for PEtN, which is determined by its structure (M.W. 141; upon addition to lipid A, correlates to  $\Delta m/z$  of 123 in the negative ion mode accounting for dehydration between PEtN and the lipid A phosphate moiety). All of the predicted lipid A structures were accessible to analysis in negative ion mode, and therefore only negative ion mode MS using the lipid matrix norharmane was performed. The resulting spectra were used to estimate the lipid A structures present in each strain, again based on their predicted structures and molecular weights.

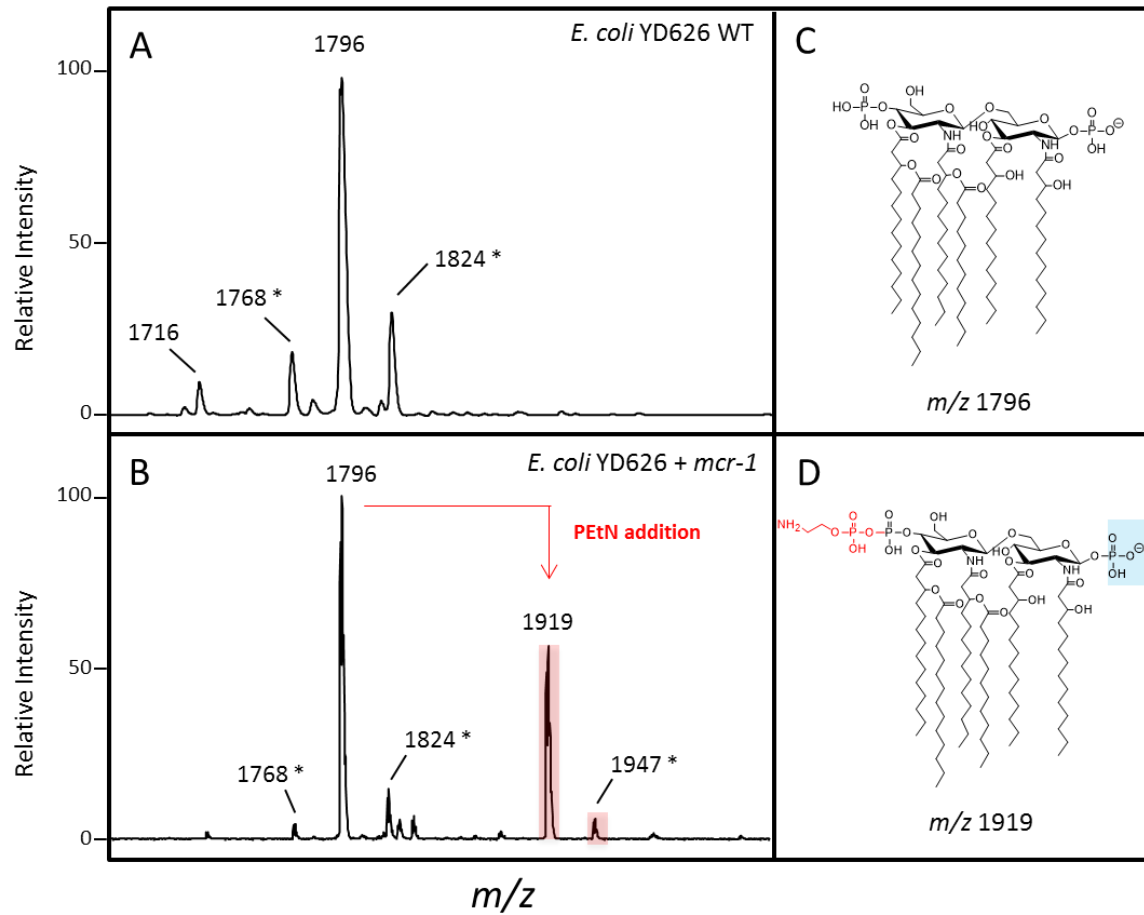


**Figure 5.1. MS analysis of strain *E. coli* YD626, WT and expressing *mcr-1* (A, B).** PEtN-modified species are represented in red ( $m/z$  1919, 1947). (C, D) Proposed structures of WT *E. coli* lipid A and PEtN-modified lipid A, respectively. Location of PEtN is suggestive; blue represents the lost phosphate moiety, position also suggestive. Asterisk (\*) represents lipid A structures that vary in acyl chain length or hydroxylation status.

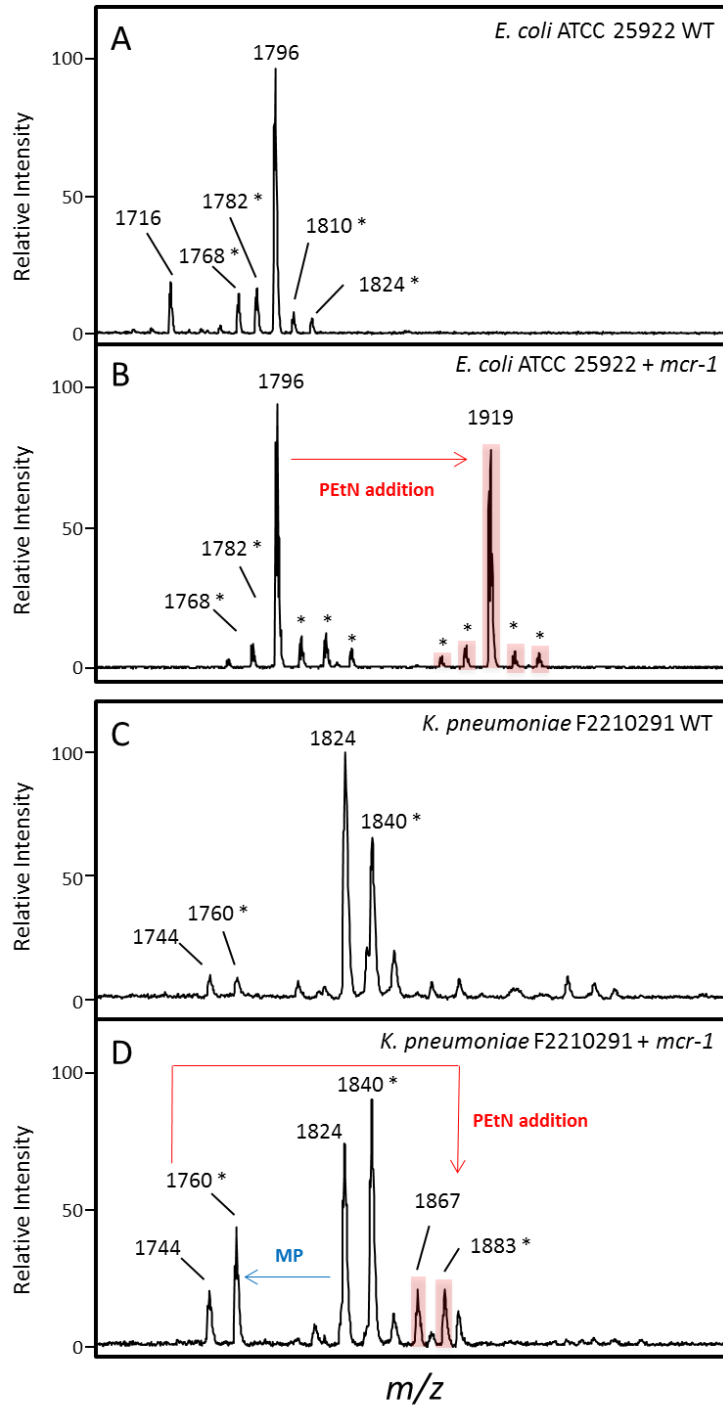


**Figure 5.2.** MS analysis of *E. coli* strains expressing *mcr-1* (A,B) and *K. pneumoniae* strains expressing *mcr-1* (C,D). PEtN-modified species are represented in red (*m/z* 1919 (B), and *m/z* 1883, 1867 (D)). Mono-phosphorylated (MP) species are represented by blue arrows. Asterisk (\*) represents lipid A structures that vary in acyl chain length or hydroxylation status.

*E. coli*. *E. coli* expressing *mcr-1* contain lipid A with a PEtN addition ( $m/z$  1919), which were in agreement with the lipid A structures previously described by Liu et al. (**Figure 5.1 and Figure 5.2**) (194). MS analysis also confirmed wild-type lipid A structures ( $m/z$  1796) in WT and plasmid-only strains *E. coli* YD626 and ATCC 25922 (**Figures 5.1, 5.2 and 5.3**). This canonical structure is bis-phosphorylated and hexa-acylated, with acyl chains varying from 12-14 carbons in length (**Figure 5.1C**). Mass differences of  $m/z$  28 ( $m/z$  1768, 1824) were assigned to acyl chain heterogeneity, namely in fatty acid chain length (a change of  $m/z$  28 in the negative ion mode correlates to a two-carbon change, for example an exchange from a 12-carbon to 14-carbon acyl chain). Ion “clusters” differing by 28  $m/z$  units were found across all samples and species, and were therefore attributed to acyl chain heterogeneity independent of *mcr-1* activity. These differences are noted with an asterisk (\*) in each figure. The ion at  $m/z$  1716 represents the canonical lipid A structure with a mono-phosphate group, annotated in blue (**Figure 5.1D**). Loss of the phosphate moiety is suggested to be due to the nature of the extraction method, in which the labile phosphate bonds are susceptible to cleavage. Alternatively it could represent a biosynthetic intermediate, as both the inner and outer membrane are captured during the extraction process and lipid A biosynthesis occurs across both membranes (92). A complete list of predicted lipid A structures for all strains can be found in **Table 5.2**.

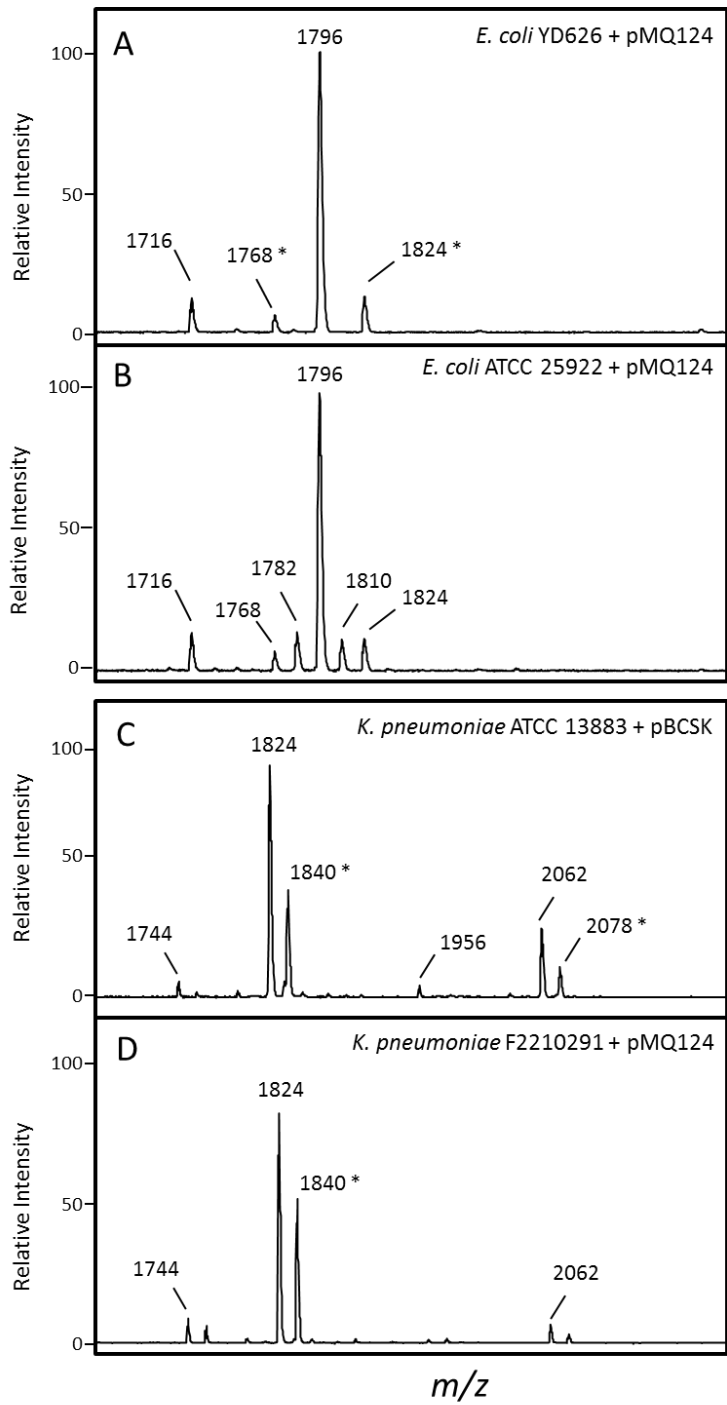


**Figure 5.3. MS analysis of *E. coli* strains (A, B) and *K. pneumoniae* strains (C, D) containing empty plasmid. Asterisk (\*) represents lipid A structures that vary in acyl chain length or hydroxylation status.**

**Table 5.2.  $m/z$  proposed structure assignments.**

Strain	Predicted $m/z$	Observed $m/z$	Proposed Structure
<i>E. coli</i> WT	1796.25, 1768.18, 1824.24	1796, 1768, 1824	Hexa-acylated, bis-phosphorylated
<i>E. coli</i> – <i>mcr-1</i>	1919.22 1947.25	1919, 1947	Hexa-acylated, bis-phosphorylated, PEtN addition
<i>K. pneumoniae</i> WT	1824.24, 1840.24	1824, 1840	Hexa-acylated, bis-phosphorylated
<i>K. pneumoniae</i> – <i>mcr-1</i> & WT	1744.28, 1760.27	1744, 1760	Hexa-acylated, mono-phosphorylated
<i>K. pneumoniae</i> – <i>mcr-1</i> & WT	2062.47	2062	Hexa-acylated, bis-phosphorylated, palmitate addition
<i>K. pneumoniae</i> – <i>mcr-1</i>	1947.25	1947	Hexa-acylated, bis-phosphorylated, PEtN addition
<i>K. pneumoniae</i> – <i>mcr-1</i>	1867.29, 1883.28	1867, 1883	Hexa-acylated, mono-phosphorylated, PEtN addition
<i>K. pneumoniae</i> – <i>mcr-1</i>	2105.47	2105	Hepta-acylated, mono-phosphorylated, palmitate addition, PEtN addition
<i>K. pneumoniae</i> – <i>mcr-1</i>	2185.48	2185	Hepta-acylated, bis-phosphorylated, palmitate addition, PEtN addition
<i>A. baumannii</i> WT	1910.28, 1882.25, 1894.29	1910, 1882, 1894	Hepta-acylated, bis-phosphorylated
<i>A. baumannii</i> – <i>mcr-1</i>	1830.31	1830	Hepta-acylated, mono-phosphorylated
<i>A. baumannii</i> – <i>mcr-1</i>	2033.29, 2005.26	2033, 2005	Hepta-acylated, bis-phosphorylated, PEtN addition
<i>A. baumannii</i> – <i>mcr-1</i>	1953.32	1953	Hepta-acylated, mono-phosphorylated, PEtN addition
<i>P. aeruginosa</i> WT	1445.86, 1461.85	1446, 1462	Penta-acylated, bis-phosphorylated
<i>P. aeruginosa</i> – <i>mcr-1</i> & WT	1616.99	1616	Hepta-acylated, bis-phosphorylated
<i>P. aeruginosa</i> – <i>mcr-1</i> & WT	1365.89	1366	Penta-acylated, mono-phosphorylated
<i>P. aeruginosa</i> – <i>mcr-1</i>	1568.87	1569	Penta-acylated, bis-phosphorylated, PEtN addition
<i>P. aeruginosa</i> – <i>mcr-1</i>	1488.90	1489	Penta-acylated, mono-phosphorylated, PEtN addition

Predicted  $m/z$  for the various candidate lipid A structures were determined by exact molecular weight using ChemDraw software. Observed  $m/z$  reflects what was seen on the spectra itself using FlexAnalysis software. The lipid A structure listed is proposed based on structural expectations.

*K. pneumoniae*. *K. pneumoniae*, also a member of the Enterobacteriaceae family, has likewise been reported to have *mcr-1*-mediated colistin resistance (194, 196, 197). MIC analysis of *K. pneumoniae* strains ATCC 13883 and 2210291 containing the *mcr-1* plasmid showed increases in colistin resistance by 256- and 32-fold respectively, suggesting the presence of PEtN-modified lipid A species in these isolates. Wild-type *K. pneumoniae* lipid A contains a 14-carbon acyl chain at the 3 position of the 3' chain, compared to the 12-carbon acyl chain in the canonical *E. coli* lipid A structure (**Figure 5.3**). As expected, MS analysis revealed lipid A structures with PEtN modification in *mcr-1*-expressing strains ATCC 13883 and 2210291 (**Figure 5.2 and Figure 5.3**). *mcr-1*-expressing ATCC 13883 showed PEtN modifications on mono- and bis-phosphorylated species ( $m/z$  1867 and 1947, 1963 respectively). Interestingly, only the mono-phosphorylated lipid A structures were observed to have PEtN additions ( $m/z$  1867, 1883) in the 2210291 strain when *mcr-1* was present. Loss of the phosphate moiety could be due to the nature of the extraction method, as previously discussed. The observed  $m/z$  variation of 28 units is attributed to acyl chain length heterogeneity, as described previously and annotated with asterisk (\*). Also of note is  $m/z$  2062, which represents lipid A modified with palmitate (M.W. 238), a 16-carbon acyl chain. The outer membrane lipid A biosynthetic enzyme PagP is responsible for the transfer of palmitate from outer membrane phospholipids to lipid A (198). This palmitate-containing hepta-acylated lipid A species was also observed to be modified with PEtN in strain ATCC 13883 expressing *mcr-1* ( $m/z$  2185, 2105; **Figure 5.4B**). Palmitate-modified lipid A was observed in both WT and plasmid-only strains of *K. pneumoniae*, and is therefore not thought to be influenced by the presence or activity of *mcr-1*.

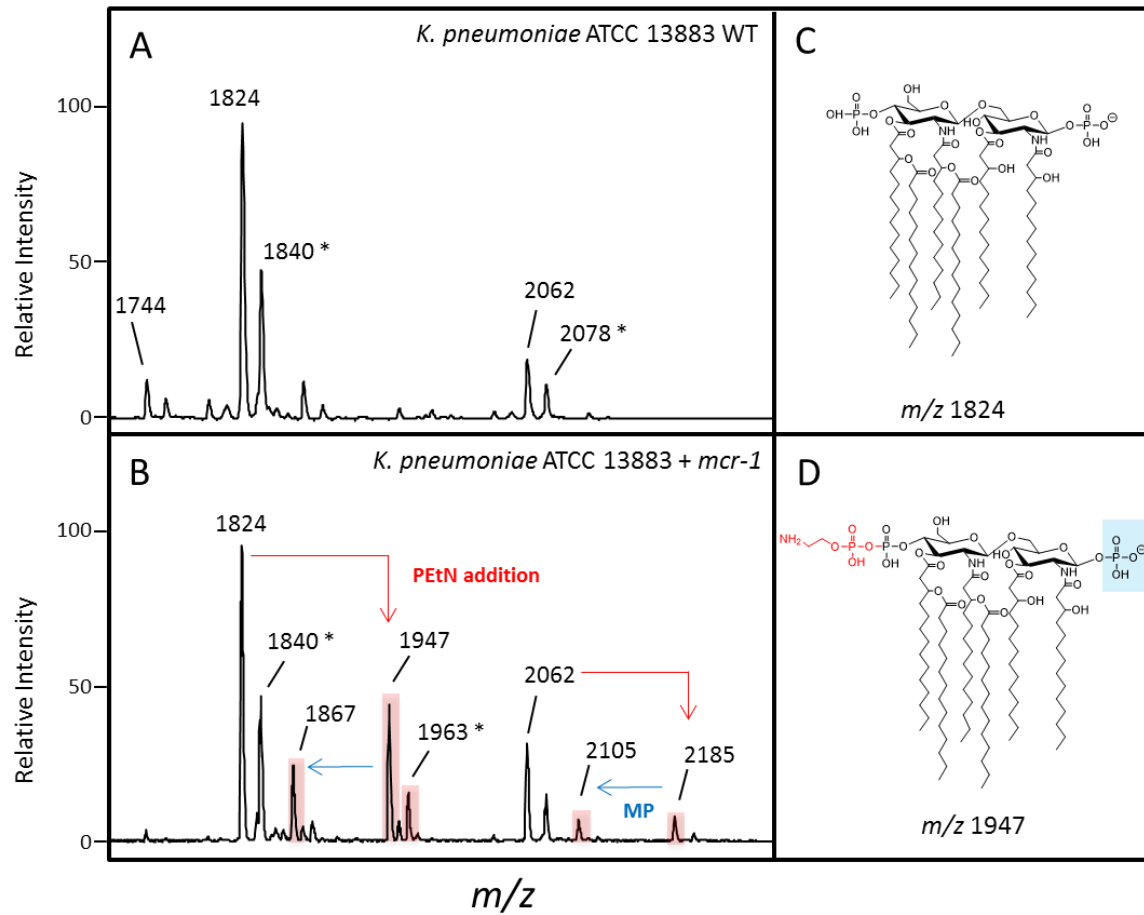


**Figure 5.4. MS analysis of *K. pneumoniae* strain ATCC 13883, WT and expressing *mcr* (A, B). PEtN-modified species are represented in red ( $m/z$  1867, 1947, 1963, 2105, 2185). (C, D) Proposed structure of WT and PEtN-modified *K. pneumoniae* lipid A, respectively. Location of PEtN is suggestive; blue represents the lost phosphate moiety, and mono-phosphate (MP) lipid A structures are designated with blue arrows. Asterisk (\*) represents lipid A structures that vary in acyl chain length or hydroxylation status.**

*A. baumannii*. *A. baumannii* strains ATCC 17978, SM1536, and D773 transformed with *mcr-1* had increased colistin resistance. ATCC 17978 had a 64-fold increase, while strains SM1536 and D773 had a fold-increase of greater than 128 (**Table 5.1**). We predicted PEtN additions on lipid A would be observed in these strains due to their colistin resistance. The wild-type lipid A structure was confirmed in both untransformed and plasmid-only *A. baumannii* strains (**Figure 5.5A**, **Figure 5.6A**, **Figure 5.7A,B**). This structure is hepta-acylated, with acyl chains ranging from 12 to 14 carbons in length ( $m/z$  1910; **Figure 5.5C**). In strains SM1536 and ATCC 17978, PEtN-modified bis-phosphorylated hepta-acylated lipid A species were observed ( $m/z$  2033; **Figure 5.5** and **Figure 5.6**). Mono-phosphorylated PEtN-modified lipid A species ( $m/z$  1953) were observed in strain ATCC 17978 (**Figure 5.6**). Furthermore, the mono-phosphorylated, non-PEtN-modified lipid A species ( $m/z$  1830) was seen in the *mcr-1*-expressing strain of ATCC 17978 but not in the wild-type strain. Mass differences of  $m/z$  28 and  $m/z$  16 were observed in both WT and *mcr-1*-expressing *A. baumannii* strains, including plasmid-only control strains. As previously described, differences of  $m/z$  28 can be attributed to heterogeneity in acyl chain length. Differences of  $m/z$  16 correlate to changes in hydroxylation status of the acyl chains, a common alteration in Gram-negative bacteria (199). As these acyl chain variations were observed in WT and plasmid-only control strains, they were not attributed to the presence of *mcr-1*. PEtN-modified lipid A was also observed in strain D773 (data not shown).

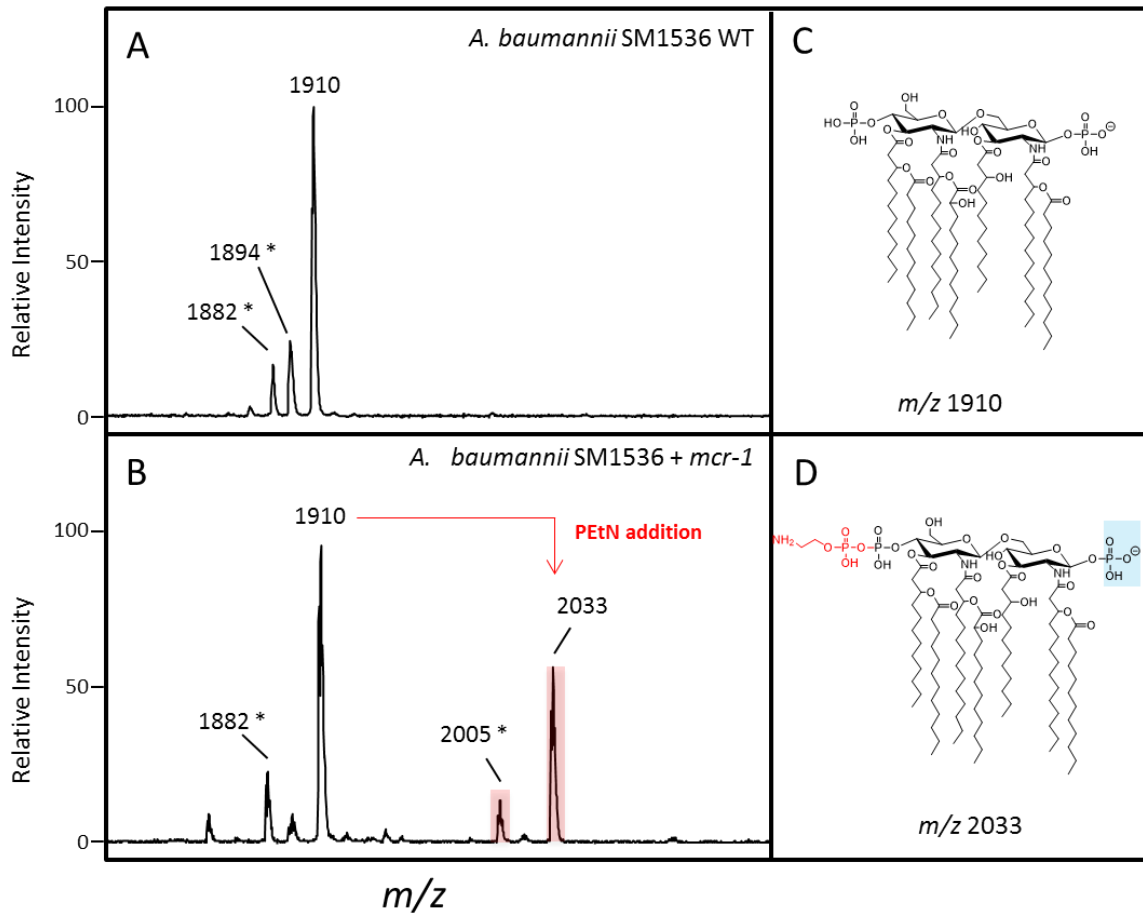


**Figure 5.5.** MS analysis of *A. baumannii* strain SM1536, WT and expressing *mcr-1* (A, B). PEtN-modified species are represented in red ( $m/z$  2005, 2033). (C, D) Proposed structure of WT and PEtN-modified *A. baumannii* lipid A, respectively. Location of PEtN is suggestive; blue represents loss of phosphate moiety. Asterisk (\*) represents lipid A structures that vary in acyl chain length or hydroxylation status.

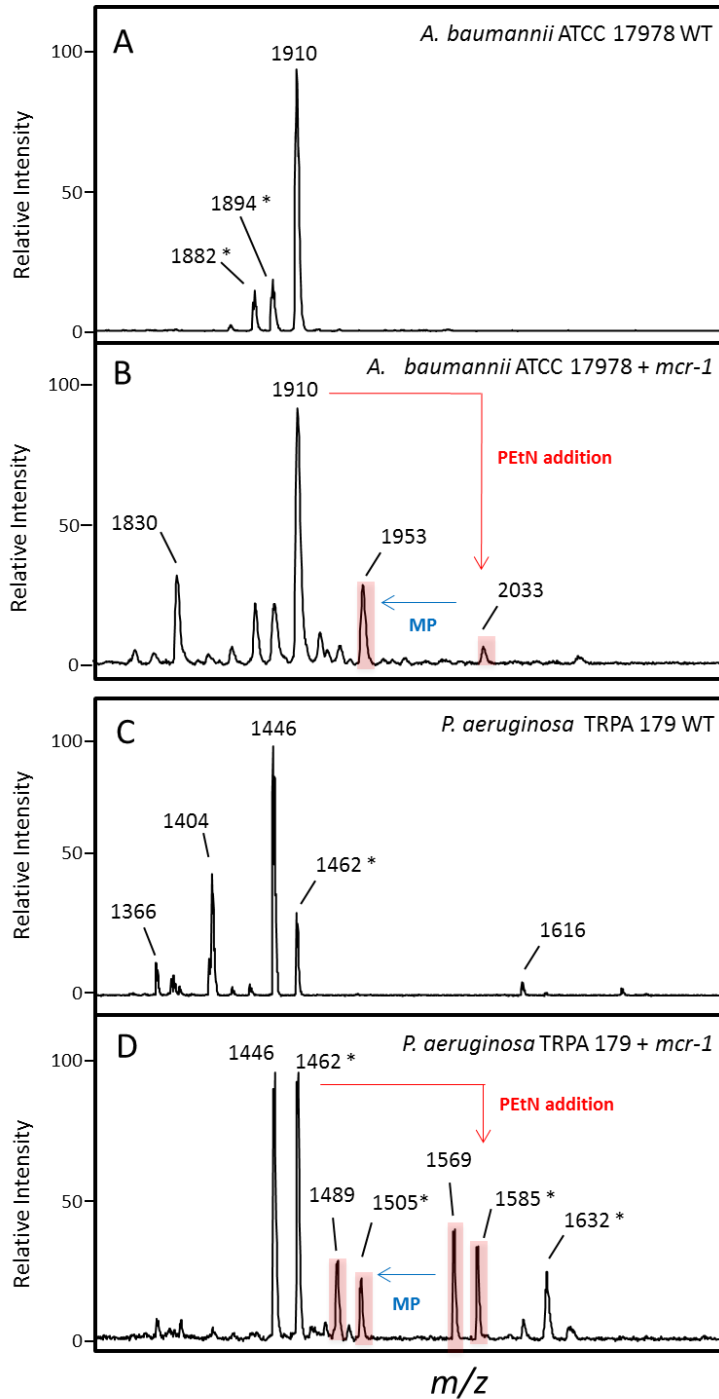


**Figure 5.6. MS analysis of *A. baumannii* strains expressing *mcr-1* (A,B) and *P. aeruginosa* strains expressing *mcr-1* (C,D).** PETN-modified species are represented in red ( $m/z$  2033, 1953 (B), and  $m/z$  1569, 1489 (D)). Mono-phosphorylated (MP) species are represented by blue arrows. Asterisk (\*) represents lipid A structures that vary in acyl chain length or hydroxylation status.

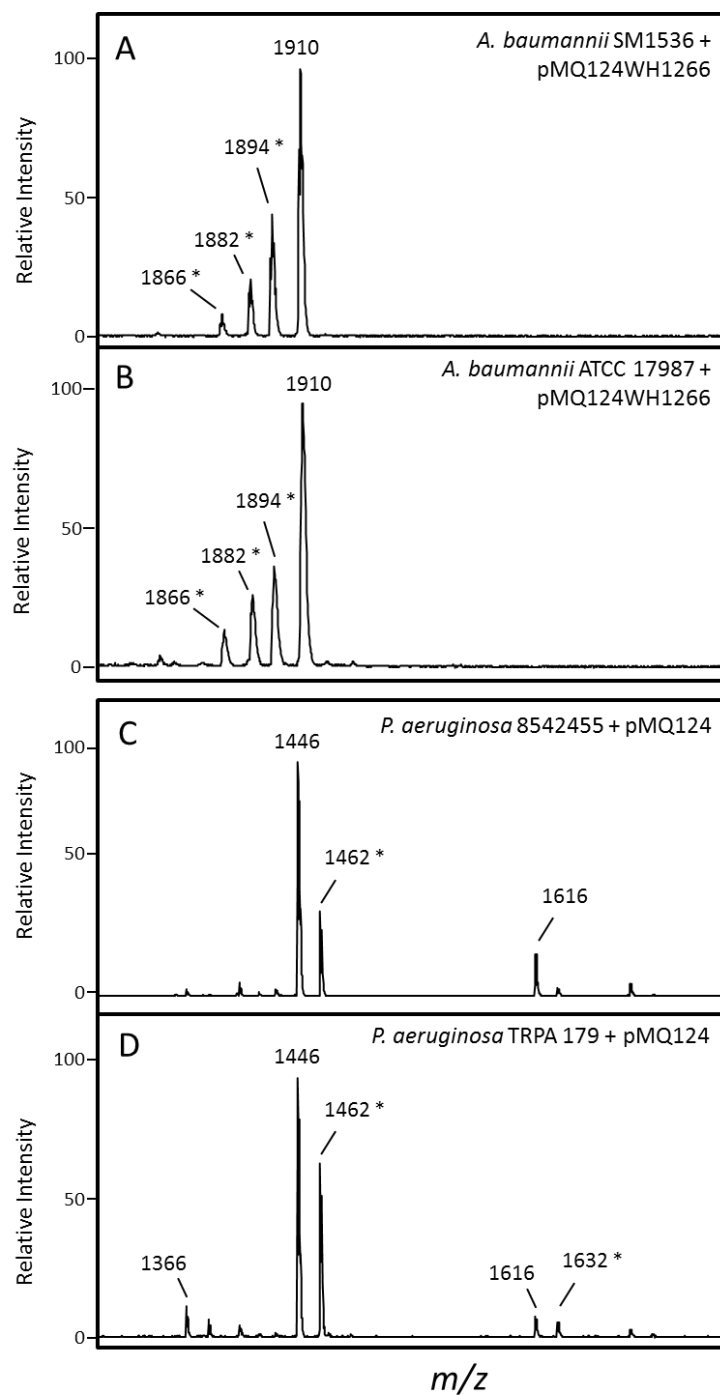


**Figure 5.7.** MS analysis of *A. baumannii* strains (A, B) and *P. aeruginosa* strains (C, D) containing empty plasmid pMQ124. Asterisk (\*) represents lipid A structures that vary in acyl chain length or hydroxylation status.

*P. aeruginosa*. Only moderate changes in colistin susceptibility were observed in *mcr-1*-expressing *P. aeruginosa* strains 8542455, TRPA179, and ATCC 47085 (2- or 4-fold increase) yet PEtN-modified lipid A was still readily detected. Notably, all *P. aeruginosa* strains with *mcr-1* showed PEtN-modified bis- and mono-phosphorylated lipid A species ( $m/z$  1569 and 1489, respectively; **Figure 5.8** and **Figure 5.6**; data not shown for ATCC 47085). The wild-type lipid A structure is penta-acylated (**Figure 5.8C**), but is synthesized in a mechanism that involves hexa- and hepta-acylated lipid A intermediates (200). This hexa-acylated intermediate ( $m/z$  1616) is observed in all strains of *P. aeruginosa* (including WT and plasmid-only control strains as seen in **Figure 5.8A** and **Figure 5.6C, 5.7C,D**) and is not attributed to the presence of *mcr-1*. Drug-resistant strains of *P. aeruginosa* have been reported to have 4-amino-4-deoxy-L-arabinose (L-Ara4N)-modified lipid A structures, which mediate resistance to cationic antibiotics such as polymyxins in a way similar to PEtN (192). This type of lipid A modification was not observed in any of the *P. aeruginosa* strains tested, reinforcing the idea that *mcr-1* specifically encodes PEtN lipid A modification and not general resistance modifications.

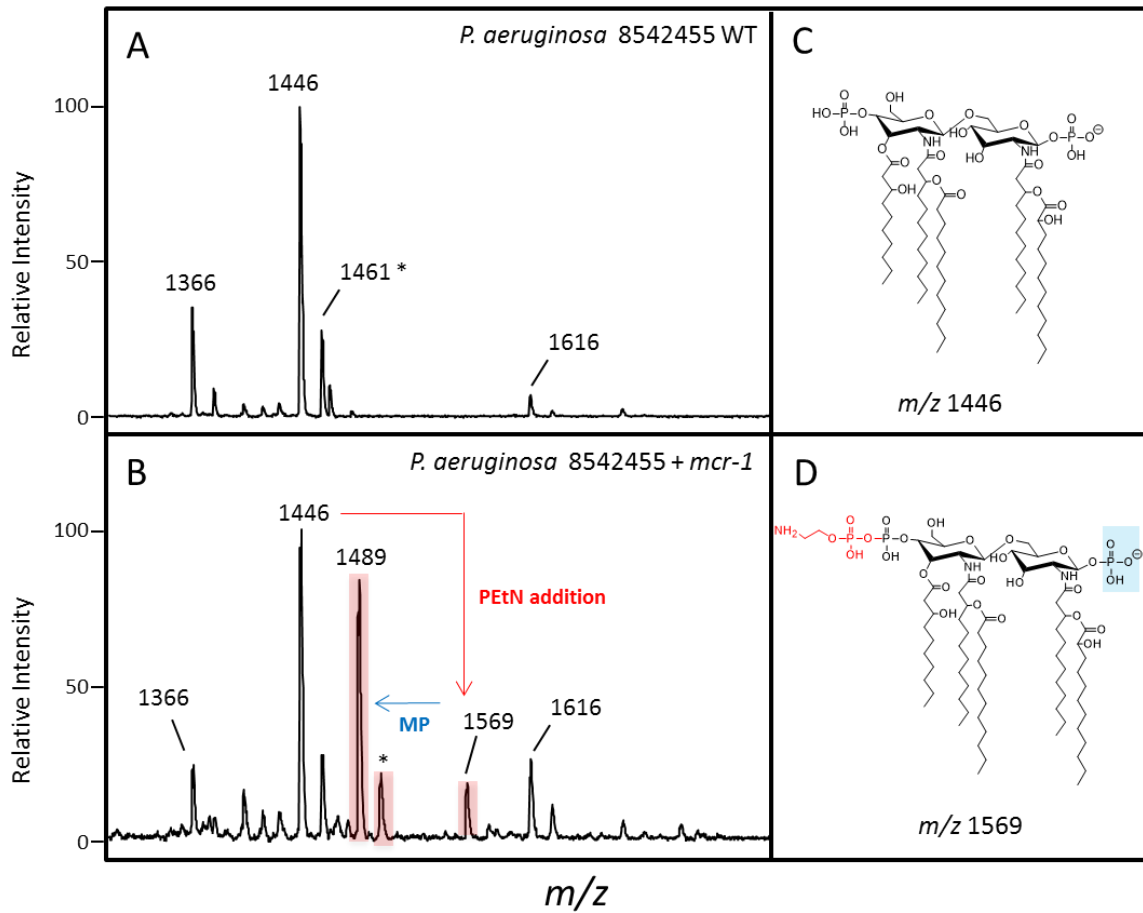


**Figure 5.8.** MS analysis of *P. aeruginosa* strain 8542455, WT and expressing *mcr-1* (A, B). PEtN-modified species are represented in red ( $m/z$  1568, 1488). (C, D) Proposed structure of WT and PEtN-modified *P. aeruginosa* lipid A, respectively. Location of PEtN is suggestive; blue represents the lost phosphate moiety, and mono-phosphate (MP) lipid A structures are designated with blue arrows. Asterisk (\*) represents lipid A structures that vary in acyl chain length or hydroxylation status.

## Discussion

Colistin is currently one of the last lines of defense against XDR Gram-negative bacteria, and resistance to colistin (or polymyxin B, which differs from colistin by a single amino acid and demonstrates comparable activity) in these organisms can result in pandrug resistance (PDR) (201). Colistin resistance in XDR bacteria mostly develops upon treatment of infection with this agent and is an imminent threat in intensive care settings. For example, over 40% of *K. pneumoniae* strains producing KPC-type carbapenemase in Italian hospitals are reportedly resistant to colistin (202). However, resistance to colistin outside this context had largely been overlooked, until the first plasmid-mediated colistin resistance gene *mcr-1* was reported from animals and humans in China in the fall of 2015 (194). *mcr-1* encodes a phosphoethanolamine transferase and its expression leads to addition of the phosphoethanolamine moiety to lipid A. Since this first report, over 150 articles and letters have been published on *mcr-1*. It is now clear that it has existed undetected for decades, has a worldwide distribution, is found more commonly in food animals than humans (especially in *E. coli*), and its prevalence is on the rise where data are available. Furthermore, a second plasmid-mediated colistin resistance gene *mcr-2*, which shares 76.7% nucleotide identity with *mcr-1*, was recently reported from Belgium (203). Fortunately, the majority, if not all, of *mcr-1*-carrying strains are still susceptible to other commonly used antimicrobial agents, and mortality due to colistin treatment failure of infections caused by *mcr-1*-expressing strains has not been reported.

Our objectives for this study were to determine the impact of *mcr-1* expression on the level of colistin resistance and the lipid A structure in three ESKAPE species against

which colistin is utilized the most clinically: *K. pneumoniae*, *A. baumannii* and *P. aeruginosa*. Of those tested, both laboratory and clinical strains from all four species were observed to have *mcr-1*-mediated increases in colistin resistance, as determined by MIC, and PEtN-modified lipid A. This supports the previous findings in *E. coli* that *mcr-1* mediates its effects through lipid A modification, namely by masking the negatively charged phosphates thereby reducing the affinity of cationic substances such as colistin for the bacterial membrane. It also indicates that the native promoter of *mcr-1* found in *E. coli* (204) is functional across the four species tested. *K. pneumoniae* and *A. baumannii* likewise showed correlative changes to colistin susceptibility into a clinically relevant resistant range (16 to 32 µg/mL) and lipid A structural modification. This suggests *K. pneumoniae* and *A. baumannii* would be amenable to *mcr-1* plasmid-mediated colistin resistance. Interestingly, we observed only modest changes in *P. aeruginosa* susceptibility to colistin despite the presence of PEtN-modified lipid A. This finding suggests that acquisition of *mcr-1* alone may not confer clinically relevant colistin resistance in *P. aeruginosa*, at least from the native promoter of *mcr-1*. However, it is still possible that the modest rise in MIC may negatively impact the activity of colistin against *mcr-1*-expressing *P. aeruginosa* considering the suboptimal pharmacokinetics of this agent (205). Another caveat of this modest resistance observed in *P. aeruginosa* is that traditional susceptibility-based surveillance assays intended to detect the presence of *mcr-1* may not prove effective for all bacterial species. Furthermore, the recently reported emergence of *mcr-2*, which only has moderate sequence identity to *mcr-1*, indicates that PCR-based surveillance methods may likewise have limitations (203). Given the prevalence of these pathogens as threats to

human health and the risk *mcr-1*-expressing strains pose to effectively treating bacterial infection, development of effective surveillance techniques is crucial.

In conclusion, our data demonstrate that *mcr-1* is capable of conferring variable levels of resistance to colistin in ESKAPE Gram-negative pathogens, and consistently results in phosphoethanolamine-modified lipid A in medically pervasive bacterial strains. This highlights the threat that *mcr-1* may disseminate into already difficult-to-manage XDR organisms, in particular *A. baumannii*.

## **Methods**

**Strains and plasmids.** *E. coli* TOP10 was used as the recipient strain for cloning of *mcr-1* into various vectors. *E. coli* ATCC 25922, *K. pneumoniae* ATCC 13883, *A. baumannii* ATCC 17978, and *P. aeruginosa* ATCC 47085 were the laboratory strains used as recipients of the recombinant plasmids. In addition, the following carbapenem-resistant clinical strains were used as the recipients: *E. coli* YD626, *K. pneumoniae* 2210291, *A. baumannii* SM1536, *A. baumannii* D773, *P. aeruginosa* TRPA 179, and *P. aeruginosa* 8542455. All the clinical strains except *A. baumannii* D773 were clinical strains previously identified at the University of Pittsburgh Medical Center. *A. baumannii* D733 was a kind gift from Dr. Carl Urban at the New York Hospital Presbyterian/Queens.

Cloning vector pBCSK was used for initial cloning of *mcr-1*. Shuttle vectors pMQ124 (20) and pMQ124XLAB1 (a derivative of pMQ124 possessing the replicon of *Acinetobacter* plasmid pWH1266) were used to introduce *mcr-1* to *P. aeruginosa* and *A. baumannii*, respectively.

**Cloning of *mcr-1* and MIC measurements.** Primers *mcr-1*-EcoRI (5'-CGAATTCCGAAGCACCAAGACATCAA-3') and *mcr-1*-XbaI (5'-GCTCTAGAATACGGCATAACAAACCCC-3') were used to amplify an approximately 2-kb fragment containing *mcr-1* and its native promoter from pHNSHP45 and ligated to pBCSK-. Electrocompetent *E. coli* TOP10 was transformed with either this construct, pBCSK-*mcr-1*, or pBCSK vector control, and selected on a lysogeny broth (LB) agar plate containing chloramphenicol at 30 µg/mL. The sequence of this 2-kb fragment was confirmed by Sanger sequencing and further ligated to pMQ124 and pMQ124XLAB1. The pMQ124-*mcr-1* construct was used to transform *E. coli*, *K. pneumoniae* and *P. aeruginosa* strains, whereas the pMQ124XLAB1-*mcr-1* construct was used to transform *A. baumannii* strains, all by electroporation. All strains were transformed with empty vector as controls. Cells were plated on LB agar plates containing gentamicin at 50 µg/mL. Introduction of *mcr-1* was confirmed by PCR using primers *mcr-1*-F (5'-TCCAAAATGCCCTACAGACC-3') and *mcr-1*-R (5'-GCCACCACAGGCAGTAAAAT-3') in all instances.

Colistin sulfate was purchased from Sigma (Sigma-Aldrich, St. Louis, MO). MICs of colistin were determined by the recommended ISO-standard broth microdilution method stipulated by the joint Clinical and Laboratory Standards Institute-EUCAST Polymyxin Breakpoints Working Group. *E. coli* ATCC 25922 was used as the control strain.

**Lipid A structural analysis.** Lipid A was extracted from cell pellets using an ammonium hydroxide-isobutyric acid-based procedure (131). Briefly, approximately 5 mL of cell culture was pelleted and resuspended in 400 µL of 70% isobutyric acid and 1M ammonium

hydroxide (5:3, vol/vol). Samples were incubated for 1 hour at 100°C and centrifuged at 2000 x g for 15 minutes. Supernatants were collected, added to endotoxin-free water (1:1 vol/vol), snap-frozen on dry ice, and lyophilized overnight. The resultant material was washed twice with 1mL methanol, and lipid A was extracted using 100 µL of a mixture of chloroform, methanol, and water (3:1:0.25, vol/vol/vol). Once extracted, 1 µL of the concentrate was spotted on a matrix-assisted laser desorption-time of flight (MALDI-TOF) plate followed by 1 µL of 10 mg/mL norharmane matrix in chloroform:methanol (2:1, vol:vol) (Sigma-Aldrich, St. Louis, MO) and then air dried. All samples were analyzed on a Bruker Microflex mass spectrometer (Bruker Daltonics, Billerica, MA) in the negative-ion mode with reflectron mode. Electrospray tuning mix (Agilent, Palo Alto, CA) was used for mass calibration. Spectral data were analyzed with Bruker Daltonics flexAnalysis software. The resulting spectra were used to estimate the lipid A structures present in each strain based on their predicted structures and molecular weights. Structural diversity of lipid A within a single bacterial membrane is well-described (206, 207).

## **CHAPTER SIX: Concluding Remarks**

### **The MS Glycolipidomic Library: A novel diagnostic platform**

#### **Introduction**

Ongoing development of novel diagnostics remains a vital and dynamic field of study, fueled by the ever-present health impacts of infectious diseases, enabling ever more rapid and accurate diagnoses and responding to new challenges, like the emergent threat of antibiotic-resistant bacteria, to improve patient treatment and care. Decades of research have introduced multiple platforms, each with its own advantages and limitations, with some notable advances that have gained prominence in the clinical laboratory. Use of mass spectrometry (MS) technologies has contributed significantly on this front in the last 20 years, harnessing the unique chemical fingerprint of microbial proteins to offer a faster, simpler, lower cost-per-sample alternative. There has been comprehensive investigation towards the utilization of MS with an array of biomarkers including exploitation of essential microbial membrane glycolipids, which has been the focus of the work presented here. In this closing chapter, noteworthy findings of this research are summarized and ongoing work, as well as future directions, are introduced for the further progression of this diagnostic platform towards clinical implementation.

#### **The MS glycolipid library identified the ESKAPE pathogens**

Utility of this novel platform was evidenced by development of a glycolipid library for the identification of the clinically important ESKAPE (*Enterococcus faecium*, *Staphylococcus aureus*, *Klebsiella pneumoniae*, *Acinetobacter baumannii*, *Pseudomonas aeruginosa*, and *Enterobacter* spp.) pathogens. The library, consisting of 50 species, 449

strains, and 2,014 biological or spectral replicates, demonstrated that each ESKAPE pathogen produced a unique mass/charge signature when compared to all other library entries, and this could be reliably used for speciation. The whole of this work validated individual aspects that are of note, specifically that: 1) a protocol for spectral generation including specimen handling, lipid extraction, sample preparation, and data acquisition and analyses is robust and highly reproducible; 2) direct specimen detection from complex biological fluids, including blood, urine, and wound effluent is achievable; 3) variations in growth temperature or specimen source often offer unique profiles providing additional diagnostic insight; 4) comparison against a database of reference spectra similar to protein typing, as well as nascent computational methods for making identifications, are feasible for this biomarker; and furthermore, 5) the establishment of a platform that is easily adapted to the protein typing platform suggesting a dual approach that could strengthen and validate the individual platforms. Importantly, this approach achieved sub-speciation on the basis of antimicrobial susceptibility, which is the most important determination after species identification due to its capacity to inform antimicrobial therapy and improve patient outcomes; therefore, this aspect was selected for further exploration.

### **Colistin resistance is detected by glycolipid mass spectra**

Colistin is a last resort antimicrobial used prolifically in livestock feed and has recently become a valuable clinical option for the treatment of carbapenem-resistant Enterobacteriaceae (CRE). Moreover, the discovery of plasmid-mediated colistin resistance, conferred by *mcr-1/mcr-2*-expressing plasmids isolated in *Escherichia coli* and *K. pneumoniae*, threatens rapid dissemination of resistance to this last line antibiotic (170,

203). Therefore, colistin, which acts by electrophilic attack of anionic LPS leading to cell lysis, and colistin resistance mechanisms, which occur mainly via LPS modifications to mask membrane electronegativity, have become the object of intense study (149). We have elucidated colistin-resistant organisms by glycolipid MS of 4-amino-4-deoxy-L-arabinopyranose (Ara4N)-modified lipid A in *K. pneumoniae* clinical isolates and phosphoethanolamine (PEtN)-modified lipid A in *A. baumannii* clinical isolates and conferred by MCR-1 in the Gram-negative ESKAPE pathogens *K. pneumoniae*, *A. baumannii*, and *P. aeruginosa* (Leung et al. 2017, *manuscript in preparation*; (117, 171)). High correlation rates were demonstrated between resistance ions present in mass spectra and determination of resistance by MIC. In the studies involving *K. pneumoniae* clinical strains or *mcr-1* plasmid-transformed Gram-negative ESKAPEs, resistant mass profiles also correlated with genetic changes in these organisms previously implicated in resistance. Additionally, an association between treatment with colistin and acquisition of resistance within patient was established in the *A. baumannii* and *K. pneumoniae* prospective studies. Finally, a preference for PEtN modification was observed when MCR-1, a putative phosphoethanolamine transferase, is expressed, even in *K. pneumoniae* where the typical mechanism of Ara4N addition is overridden. These findings contribute substantially to establishing the benefit for the glycolipid-based platform.

### **Feasibility studies for the potential development of the glycolipid library**

Continuation of this work beyond what has been presented here involves a multi-targeted approach that addresses the major limitations both of this specific platform as well

as current clinical tools in general. The following section describes work currently underway to expand the scope and depth of our glycolipid platform.

### **Library module: Culture-free**

One of the greatest impediments to a rapid time-to-diagnosis (<1 hour) is the need to cultivate organisms prior to identification; therefore, it is of great importance that our platform circumvents this time-consuming step. Previous work in our group has generated high-quality mass spectra from bacteria spiked into a variety of biological fluids such as serum, wound effluent, and bronchoalveolar lavage (BAL) (data not shown). We have also begun examining, in greater detail, the potential for this platform to achieve culture-free analysis with a focus on detecting pathogens directly from blood and urine.

*Blood.* Septicemia continues to be a leading cause of hospitalization and death in the United States (208, 209), of which risk factors for mortality are linked to inappropriate initial antimicrobial therapy (7, 210). In fact, Kumar et al. (211) found an hour-by-hour inverse correlation between patient survival rates and time to initiation of antimicrobial therapy. Direct analysis from blood represents an ongoing challenge due to data analyses complicated by an excess of host cells and the fact that blood infections involve low bacterial densities ( $10^1$  to  $10^3$  CFU/mL). An effective diagnostic with a shortened time-to-diagnosis that could be run in parallel with existing culture methods is a desirable goal. (89) To this end, we successfully detected the representative ESKAPE pathogens *S. aureus* and *K. pneumoniae* inoculated in blood at physiological concentrations after six hours in blood culture in the case of *K. pneumoniae*. Normally, blood culture bottles are incubated for 12-18 hours before activation of a sensor informs the laboratory technician to

commence culture-based techniques to determine bacterial identification. In total, we have analyzed five different species of bacteria directly from blood culture including *E. coli*, *A. baumannii*, and *P. aeruginosa*. Using *E. coli* K-12 strain W3110 as a test organism, we also undertook different control studies and demonstrated reproducibility of mass spectra produced from blood culture when different blood types or blood culture (BC) bottles are used (**Figure 6.1**). Of significant interest, the characteristic mass spectrum is unaffected by the presence of resin beads in the blood culture medium: some BC bottles contain a proprietary resin that enhances microorganism cultivation by removing antibiotics from the blood that could inhibit growth in the blood bottle.

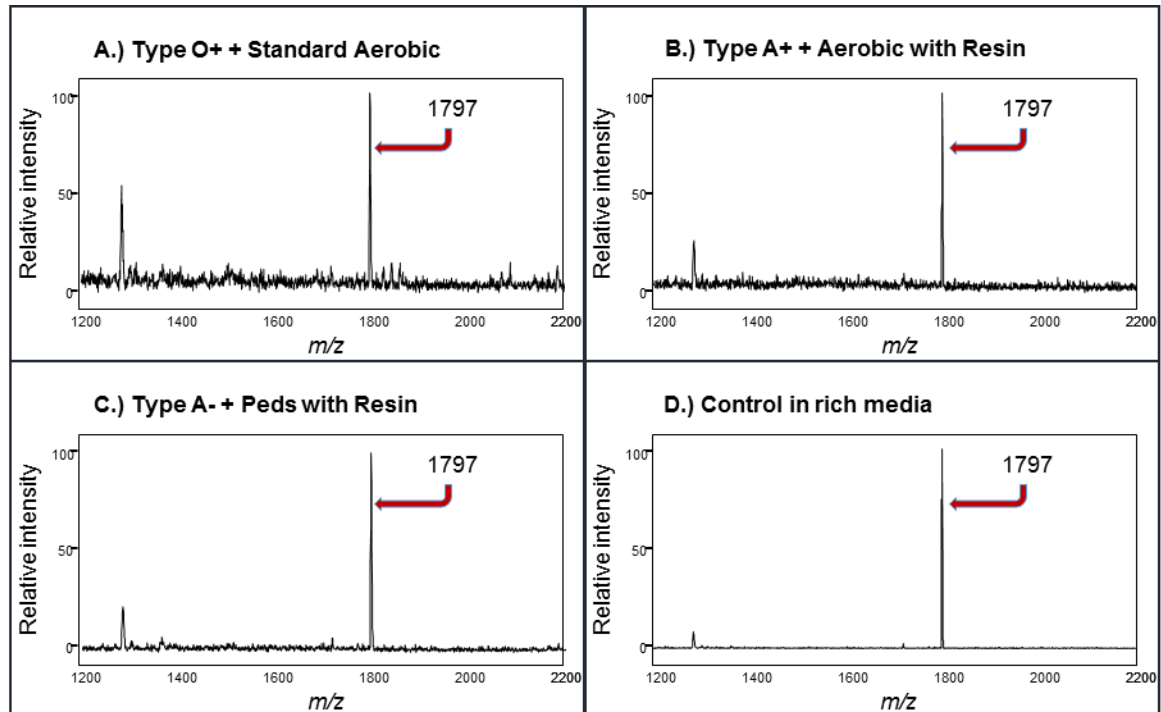


**Figure 6.1. MALDI-TOF MS of *E. coli* W3110 lipid A in different blood types and blood culture bottles. A.) Blood type O positive in Standard Aerobic media; B.) Blood type A positive in Plus Aerobic media containing antibiotic-neutralizing resin; C.) Blood type A negative in Peds Plus media containing antibiotic-neutralizing resin; D.) Control in laboratory rich media.**

*Urine.* Urinary tract infection (UTI) is the most common bacterial infection found in ambulatory care settings in the United States. Uropathogenic *E. coli* is the predominant pathogen in UTIs followed by occurrences of *K. pneumoniae*, Gram-positive Staphylococci and Enterococci, and *Candida* spp. among others. (212) Through collaboration with a clinician at the University of Pittsburgh Medical Center, we obtained 120 clinical isolates collected from 16 UTI patients identified by conventional methods during standard patient care and confirmed by the MALDI Biotyper (MBT). Isolates were cultured, extracted, and analyzed by MS to generate a glycolipid library representing 25 individual species listed in **Table 6.1**. This Biotyper library includes the most prominent pathogens implicated in incidences of UTIs from which *E. coli* (a Gram-negative pathogen), *Enterococcus faecalis* (a Gram-positive pathogen), and *Candida albicans* (a fungal pathogen) were selected for further analysis. Isolates were cultured overnight in rich media and 1 mL aliquots were spiked into sterile urine and processed in the same manner as cultured organisms (cells were harvested by centrifugation and reacted in hot ammonium isobutyrate); additionally, a 10 mL urine specimen from Patient # UR-018 from which multiple *C. albicans* isolates had been identified was centrifuged and directly processed as well. All respective organisms were positively identified from the acquired mass spectra by testing against a Urine library of the 25 organisms built in the MBT (**Figure 6.2**), including the patient specimen that was frozen for over a year before testing.

**Table 6.1. List of species isolated from urine.**

<b>Table 6.1: List of species isolated from urine</b>		
<i>Arthrobacter pigmenti</i>	<i>Micrococcus luteus</i>	<b><i>Staphylococcus aureus</i></b>
<i>Bacillus cereus</i>	<i>Moraxella osloensis</i>	<b><i>Staphylococcus capitis</i></b>
<i>Bacillus pumilus</i>	<i>Paenibacillus lautus</i>	<b><i>Staphylococcus cohnii</i></b>
<i>Brevundimonas diminuta</i>	<i>Pseudomonas oryzihabitans</i>	<b><i>Staphylococcus epidermidis</i></b>
<b><i>Candida albicans</i></b>	<i>Pseudomonas stutzeri</i>	<b><i>Staphylococcus haemolyticus</i></b>
<b><i>Enterococcus faecalis</i></b>	<i>Rhodococcus opacus</i>	<b><i>Staphylococcus hominis</i></b>
<b><i>Escherichia coli</i></b>	<i>Roseomonas mucosa</i>	<b><i>Staphylococcus lugdunensis</i></b>
<i>Exiguobacterium</i>	<i>Rothia amarae</i>	<b><i>Staphylococcus warneri</i></b>
<b><i>Klebsiella pneumoniae</i></b>		

\* Species listed in bold are among the most prevalent pathogens implicated in UTIs.

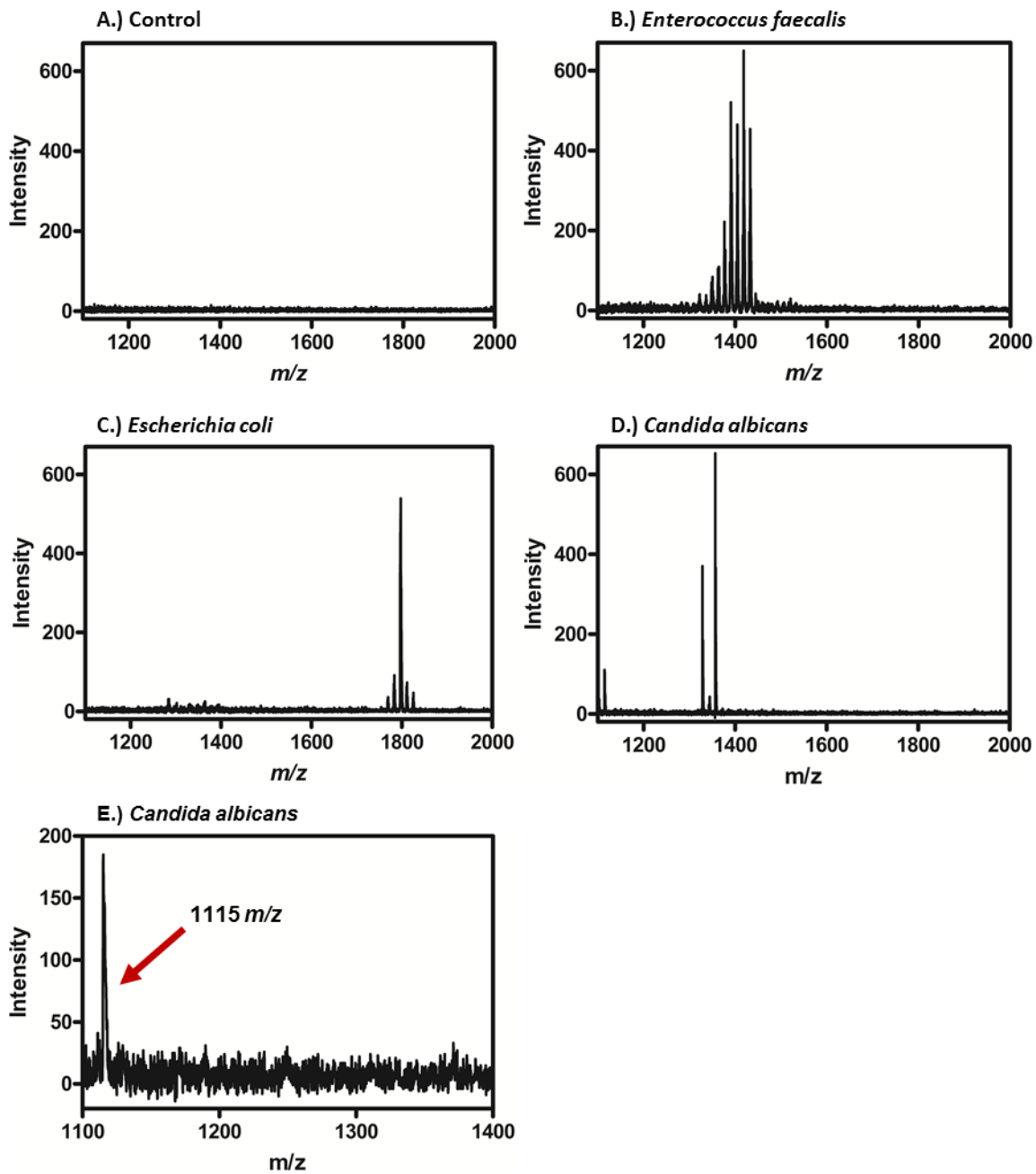


**Figure 6.2. Direct specimen analysis of microbial glycolipids from urine.** Clinical strains isolated from UTI patients were cultured in rich media, seeded into urine, and harvested by centrifugation; lipids were extracted; and, extracts were analyzed by MALDI-TOF MS for **A)** Control containing sterile urine, **B)** Gram-positive *E. faecalis*, **C)** Gram-negative *E. coli*, and **D)** Fungal *C. albicans*. **E)** Extraction and analysis were performed directly on a frozen urine specimen from a patient infected with *C. albicans*.

### **Library module: Fungi**

Fungi have complex and dynamic eukaryotic membranes enclosed by a cell wall. They potentially offer numerous diagnostic lipid biomarkers, notably sphingolipids, consisting of a long-chain base backbone, an amide-linked fatty acyl chain and a polar head group, that have unique chemical structures under the control of fungal-specific enzymes. (213, 214) In evaluating the ESKAPE pathogens, the glycolipid library contained four *Candida* species but no further consideration of the diversity of fungal organisms was done in that study. Incorporation and interrogation of a more comprehensive fungal library would vastly improve the functionality of our glycolipid platform. To date, 43 different yeast and fungi were examined with species and strains listed in **Table 6.2**. To evaluate our fungal library, 14 de-identified samples were analyzed and identified by blinded manual interpretation. Mass spectral analysis resulted in the successful identification at the species level (82%) and at the genus level (92%) using a single acquired spectra for library development, thereby showing the robustness of this fungal library.

Of interest are the various yeast species in the library for which the glycolipid mass spectra distinguish even closely related organisms within the *Candida* genus. In particular, mass spectra from *C. albicans* and *Candida dubliniensis* may permit differentiation overcoming the failures of phenotypic tests to do so with this pair of species, and spectral differences between hyphal (*C. albicans* and *C. dubliniensis*) and non-hyphal forms (*Candida glabrata*) of *Candida* or pathogenic (*Candida*) and non-pathogenic (*Saccharomyces cerevisiae*) yeast species may also offer insight into membrane remodeling or virulence, respectively (**Figure 6.3**).

**Table 6.2. List of fungal species in the glycolipid library.**

<b>Table 6.2: List of fungal species in the glycolipid library</b>		
<i>Aspergillus fumigatus</i>	<i>Candida orthopsilosis</i>	<i>Mucor circinelloides</i>
<i>Bullera alba</i>	<i>Candida parapsilosis</i>	<i>Rhizopus delemar</i>
<i>Candida albicans</i>	<i>Candida quercitrusa</i>	<i>Rhizopus oryzae</i>
<i>Candida beverwijkiae</i>	<i>Candida sojae</i>	<i>Rhodosporeidium toruloides</i>
<i>Candida boidinii</i>	<i>Candida tropicalis</i>	<i>Rhodotorula marina</i>
<i>Candida carpophila</i>	<i>Candida zeylanoides</i>	<i>Rhodotorula mucilaginosa</i>
<i>Candida dubliniensis</i>	<i>Cryptococcus albidosimilis</i>	<i>Rhodotorula slooffiae</i>
<i>Candida fermentati</i>	<i>Cryptococcus curvatus</i>	<i>Rhodotorula taiwanensis</i>
<i>Candida guilliermondii</i>	<i>Cryptococcus flavescens</i>	<i>Saccharomyces cerevisiae</i>
<i>Candida intermedia</i>	<i>Cryptococcus magnus</i>	<i>Sporidiobolus salmonicolor</i>
<i>Candida krusei</i>	<i>Cryptococcus saitoi</i>	<i>Sporobolomyces nylandii</i>
<i>Candida lusitaniae</i>	<i>Cunninghamella bertholletiae</i>	<i>Sporobolomyces pararoseus</i>
<i>Candida metapsilosis</i>	<i>Debaryomyces hansenii</i>	<i>Sporobolomyces ruberrimus</i>
<i>Candida neorugosa</i>	<i>Lictheimia corymbifera</i>	<i>Yarrowia lipolytica</i>
<i>Candida olivae</i>		

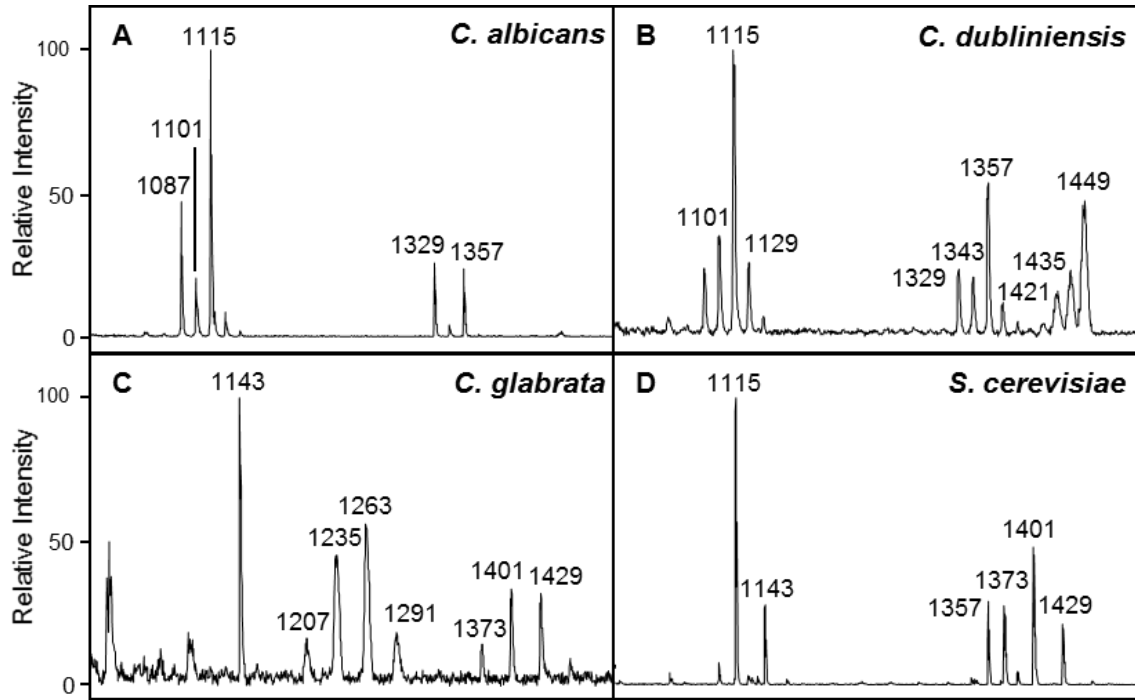


**Figure 6.3. Mass spectra from representative yeast species in the fungal library. A)** *C. albicans*, **B)** non-hyphal *C. glabrata*, **C)** *C. dubliniensis*, and **D)** haploid *S. cerevisiae*.

## **Future directions**

Despite continuing efforts to build and validate our glycolipid platform, much remains to be done. The following section describes work by us and other groups to refine techniques and offer innovative solutions that are essential for the eventual application of this platform.

## **Sample preparation, processing and analysis**

There are many steps along the platform workflow where refinements can be made or are in fact necessary for clinical application. Firstly, sample handling and preparation require the most investment. While our optimized workflow led to the efficient generation of a comprehensive reference database, certain protocols requiring the use of noxious reagents in a chemical hood and multiple centrifugation steps are not amenable for the clinical laboratory. In addition, an overnight lyophilization step is an impediment to reducing time to identification; however, we have dedicated significant effort to address this. Specifically, research on a novel protocol has reduced extraction to less than one hour and a single spin step and eliminated the use of isobutyric acid/ammonium hydroxide and lyophilization with comparable spectral quality to current laboratory protocols (215).

We are also experimenting with sample preparation on the target plate to improve ionization efficiency including varying spotting methods to homogenize crystallization although previous studies have found performance with different spotting methods is highly sample-dependent and varies from organism to organism (216) or varying matrices, including testing of 2-heptyl-3-hydroxy-4-quinolone, a *P. aeruginosa* quorum sensing molecule whose multi-ring structure is similar to many commercial matrices (217). We

have also experimented with matrix additives to permit ionization of glycolipids in positive ion mode. In fact, it has been shown that analysis of an analyte at both ion polarities (positive and negative ion modes) provides more biomarker information for identification (218).

### **Structural analyses**

Sizeable research has been dedicated to MS analyses of Gram-negative bacterial lipid A, specifically following extraction by ammonium isobutyrate reaction. We have incorporated numerous Gram-positive and fungal organisms into our glycolipid library and determined that each produces a unique and reproducible chemical fingerprint, yet little is known about the lipids that comprise these spectral profiles. Thusly, we have begun tandem MS analyses to elucidate these structures; extracts are infused by ESI into a mass spectrometer equipped with a triple quad mass analyzer such that the second quadrupole is a collision cell in which a stream of inert gas is used to fragment molecular ions. Structures were assigned manually by comparison of the experimental  $m/z$  values of fragment ions to the theoretical molecular weights of known lipids. The majority of our efforts to date have been with *S. aureus* strains, and tandem mass spectra have determined the predominant lipid to be cardiolipin (CL), a di-phosphatidylglycerol phospholipid that resides in a variety of microorganisms as well as eukaryotic mitochondrial membranes; all peaks can be assigned with high mass agreement (219). It is unclear at this time why these molecules are the ones presented and why direct analyses of human samples are not complicated by the fact that CL can be found in host cells; however, CL represents an ideal marker that is

abundant in the membrane with species-specific differences in acyl chain length and multiple CL species per organism that offer multiple peaks as identifiers (93, 220, 221).

### **Computational model development**

The MALDI Biotyper was adapted to our glycolipid library and effectively utilized to identify the ESKAPE pathogens both from testing strains grown in laboratory media and extracted from blood culture as well as from representative UTI pathogens in urine. Rates of accuracy were promising and, in some instances, comparable to protein typing; however, the setup is imperfect. The Biotyper's software was designed for the complexity of a protein mass spectrum where up to 100 peaks are considered with the expectation of multiple overlapping peaks as ribosomal proteins are highly conserved. Glycolipid mass spectra, on the other hand, are far sparser where perhaps only a single ion is the determinant of a species. This becomes a problem when there are overlapping peaks between spectra either from shared glycolipid molecules in the membrane or biosynthetic precursors or degraded glycolipid products generating identical ions. Untrained pattern matching as in the Biotyper does not distinguish between a degradation product and a full molecular structure that is characteristic of a particular species, which causes problems when only considering a few peaks. To address this, we are also working towards development of machine learning models that predict ions that are most indicative of a certain species and assign higher weight or importance to those peaks based on their predictive value, which may prove more efficacious when making identifications by glycolipid mass spectra. Additionally, we are exploring integration of an in silico mass spectral library by use of a combinatoric approach in which an algorithm computes all theoretical arrangements of

lipid A based on all possible combinations of modular components of the general structure and predicts structures of the ions in a spectrum (222, 223).

### **Final thoughts**

In conclusion, the work presented in this thesis represents major advancements to the development and validation of a novel diagnostic platform for identification of microbial pathogens via their unique glycolipid mass spectral fingerprint. Additionally, having the ability to detect and identify antimicrobial-resistant bacteria in conjunction with protein MS-technologies has broad implications in the field of diagnostic microbiology with potential for eventual implementation in the clinic.

## REFERENCES

1. Morens DM, Folkers GK, Fauci AS. 2004. The challenge of emerging and re-emerging infectious diseases. *Nature* 430:242–249.
2. Fauci AS, Morens DM. 2012. The Perpetual Challenge of Infectious Diseases. *N Engl J Med* 366:454–461.
3. World Health Organization. 2016. World Health Statistics 2016: monitoring health for the SDGs, sustainable development goals.
4. World Health Organization. 2013. The world health report 2013: research for universal health coverage.
5. Centers for Disease Control and Prevention. 2015. National Center for Health Statistics. Health, United States, 2015: With Special Feature on Racial and Ethnic Health Disparities (Library of Congress Catalog Number 76-641496). Washington, DC: U.S. Government Printing Office.
6. Hall MJ, Williams SN, DeFrances CJ, Golosinskiy A. 2011. Inpatient care for septicemia or sepsis: a challenge for patients and hospitals. *NCHS Data Brief* 62:1–8.
7. Kang CI, Kim SH, Park WB, Lee KD, Kim HB, Kim EC, Oh MD, Choe KW. 2005. Bloodstream infections caused by antibiotic-resistant Gram negative bacilli: risk factors for mortality and impact of inappropriate antimicrobial therapy on outcome. *Antimicrob Agents Chemother* 49:760–766.

8. Kim SH, Park WB, Lee KD, Kang CI, Bang JW, Kim HB, Kim EC, Oh MD, Choe KW. 2004. Outcome of inappropriate initial antimicrobial treatment in patients with methicillin-resistant *Staphylococcus aureus* bacteraemia. *J Antimicrob Chemother* 54:489–497.
9. Centers for Disease Control and Prevention. 2013. Antibiotic resistance threats in the United States, 2013. Washington, DC: U.S. Government Printing Office.
10. World Health Organization. 2014. Antimicrobial resistance: global report on surveillance.
11. Clark AE, Kaleta EJ, Arora A, Wolk DM. 2013. Matrix-assisted laser desorption ionization-time of flight mass spectrometry: a fundamental shift in the routine practice of clinical microbiology. *Clin Microbiol Rev* 26:547–603.
12. Van Belkum A, Durand G, Peyret M, Chatellier S, Zambardi G, Schrenzel J, Shortridge D, Engelhardt A, Dunne WM. 2013. Rapid clinical bacteriology and its future impact. *Ann Lab Med* 33:14–27.
13. Gram C. 1884. The differential staining of Schizomycetes in tissue sections and in dried preparations. *Gen Microbiol* 2:216–218.
14. Jorgenson HJ, Ferraro MJ. 2009. Antimicrobial Susceptibility Testing: A Review of General Principles and Contemporary Practices. *Clin Infect Dis* 7750:1749–1755.
15. Gherardi G, Angeletti S, Panitti M, Pompilio A, Di Bonaventura G, Crea F, Avola A, Fico L, Palazzo C, Sapia GF, Visaggio D, Dicuonzo G. 2012. Comparative evaluation of the Vitek-2 Compact and Phoenix systems for rapid identification and

- antibiotic susceptibility testing directly from blood cultures of Gram-negative and Gram-positive isolates. *Diagn Microbiol Infect Dis* 72:20–31.
16. Fournier PE, Drancourt M, Colson P, Rolain JM, La Scola B, Raoult D. 2013. Modern clinical microbiology: new challenges and solutions. *Nat Rev Microbiol* 11:574–585.
  17. Stender H. 2003. PNA FISH: an intelligent stain for rapid diagnosis of infectious diseases. *Expert Rev Mol Diagn* 3:649–655.
  18. Navarro F, Llovet T, Echeita MA, Coll P, Aladuena A, Usera MA, Prats G. 1996. Molecular typing of *Salmonella enterica* serovar typhi. *J Clin Microbiol* 34:2831–2834.
  19. Petti CA, Polage CR, Schreckenberger P. 2005. The Role of 16S rRNA Gene Sequencing in Identification of Microorganisms Misidentified by Conventional Methods. *J Clin Microbiol* 43:6123–6125.
  20. Clarridge JE. 2004. Impact of 16S rRNA gene sequence analysis for identification of bacteria on clinical microbiology and infectious diseases. *Clin Microbiol Rev* 17:840–862.
  21. Yang S, Rothman RE. 2004. PCR-based diagnostics for infectious diseases: Uses, limitations, and future applications in acute-care settings. *Lancet Infect Dis* 4:337–348.

22. Frye AM, Baker CA, Rustvold DL, Heath KA, Hunt J, Leggett JE, Oethinger M. 2012. Clinical impact of a real-time PCR assay for rapid identification of staphylococcal bacteremia. *J Clin Microbiol* 50:127–133.
23. Maiden MC, Bygraves JA, Feil E, Morelli G, Russell JE, Urwin R, Zhang Q, Zhou J, Zurth K, Caugant DA, Feavers IM, Achtman M, Spratt BG. 1998. Multilocus sequence typing: a portable approach to the identification of clones within populations of pathogenic microorganisms. *Proc Natl Acad Sci* 95:3140–3145.
24. Bertelli C, Greub G. 2013. Rapid bacterial genome sequencing: methods and applications in clinical microbiology. *Clin Microbiol Infect* 19:803–813.
25. Voelkerding KV, Dames SA, Durtschi JD. 2009. Next-generation sequencing: from basic research to diagnostics. *Clin Chem* 55:641–658.
26. Rasko DA, Worsham PL, Abshire TG, Stanley ST, Bannan JD, Wilson MR, Langham RJ, Decker RS, Jiang L, Read TD, Phillippy AM, Salzberg SL, Pop M, Van Ert MN, Kenefic LJ, Keim PS, Fraser-Liggett CM, Ravel J. 2011. *Bacillus anthracis* comparative genome analysis in support of the Amerithrax investigation. *Proc Natl Acad Sci* 108:5027–5032.
27. Rohde H, Qin J, Cui Y, Li D, Loman NJ, Hentschke M, Chen W, Pu F, Peng Y, Li J, Xi F, Li S, Li Y, Zhang Z, Yang X, Zhao M, Wang P, Guan Y, Cen Z, Zhao X, Christner M, Kobbe R, Loos S, Oh J, Yang L, Danchin A, Gao GF, Song Y, Li Y, Yang H, Wang J, Xu J, Pallen MJ, Wang J, Aepfelbacher M, Yang R, the *E. coli* O104:H4 Genome Analysis Crowd-Sourcing Consortium. 2011. Open-Source

- Genomic Analysis of Shiga-Toxin–Producing *E. coli* O104:H4. *N Engl J Med* 365:718–724.
28. Rasko DA, Webster DR, Sahl JW, Bashir A, Boisen N, Scheutz F, Paxinos EE, Sebra R, Chin C-S, Iliopoulos D, Klammer A, Peluso P, Lee L, Kislyuk AO, Bullard J, Kasarskis A, Wang S, Eid J, Rank D, Redman JC, Steyert SR, Frimodt-Møller J, Struve C, Petersen AM, Krogfelt KA, Nataro JP, Schadt EE, Waldor MK. 2011. Origins of the *E. coli* strain causing an outbreak of hemolytic-uremic syndrome in Germany. *N Engl J Med* 365:709–717.
  29. Sherry NL, Porter JL, Seemann T, Watkins A, Stinear TP, Howden BP. 2013. Outbreak investigation using high-throughput genome sequencing within a diagnostic microbiology laboratory. *J Clin Microbiol* 51:1396–1401.
  30. Clerc O, Greub G. 2010. Routine use of point-of-care tests: Usefulness and application in clinical microbiology. *Clin Microbiol Infect* 16:1054-1061.
  31. Rosón B, Fernández-Sabé N, Carratalà J, Verdaguer R, Dorca J, Manresa F, Gudiol F. 2004. Contribution of a Urinary Antigen Assay (Binax NOW) to the Early Diagnosis of Pneumococcal Pneumonia. *Clin Infect Dis* 38:222-226.
  32. Kazandjian D, Chiew R, Gilbert GL. 1997. Rapid Diagnosis of *Legionella pneumophila* Serogroup 1 Infection with the Binax Enzyme Immunoassay Urinary Antigen Test. *J Clin Microbiol* 35:954–956.

33. Wang Y-K, Kuo F-C, Liu C-J, Wu M-C, Shih H-Y, Wang SSW, Wu J-Y, Kuo C-H, Huang Y-K, Wu D-C. 2015. Diagnosis of *Helicobacter pylori* infection: Current options and developments. *World J Gastroenterol* 21:11221–11235.
34. Bergeron MG, Ke D. 2001. New DNA-based PCR approaches for rapid real-time detection and prevention of group B streptococcal infections in newborns and pregnant women. *Expert Rev Mol Med* 3:1–14.
35. Reiner E. 1965. Identification of Bacterial Strains by Pyrolysis Gas-liquid Chromatography. *Nature* 206:1272–1274.
36. Simmonds PG. 1970. Whole Microorganisms Studied by Pyrolysis-Gas Chromatography-Mass Spectrometry: Significance for Extraterrestrial Life Detection Experiments. *Appl Microbiol* 20:567–572.
37. Meuzelaar HLC, Kistemaker PG. 1973. Technique for fast and reproducible fingerprinting of bacteria by pyrolysis mass spectrometry. *Anal Chem* 45:587–590.
38. Schulten HR, Beckey HD, Meuzelaar HLC, Boerboom AJH. 1973. High-resolution field ionization mass spectrometry of bacterial pyrolysis products. *Anal Chem* 45:191–195.
39. Anhalt JP, Fenselau C. 1975. Identification of bacteria using mass spectrometry. *Anal Chem* 47:219–225.
40. Moss CW. 1981. Gas-liquid chromatography as an analytical tool in microbiology. *J Chromatogr A* 203:337–347.

41. Heller DN, Cotter RJ, Fenselau C, Uy OM. 1987. Profiling of bacteria by fast atom bombardment mass spectrometry. *Anal Chem* 59:2806–2809.
42. Heller DN, Murphy CM, Cotter RJ, Fenselau C, Uy OM. 1988. Constant neutral loss scanning for the characterization of bacterial phospholipids desorbed by fast atom bombardment. *Anal Chem* 60:2787–2791.
43. Pramanik BN, Zechman JM, Das PR, Bartner PL. 1990. Bacterial phospholipid analysis by fast atom bombardment mass spectrometry. *Biol Mass Spectrom* 19:164–170.
44. Cole MJ, Enke CG. 1991. Direct determination of phospholipid structures in microorganisms by fast atom bombardment triple quadrupole mass spectrometry. *Anal Chem* 63:1032–1038.
45. Smith PB, Snyder AP, Harden CS. 1995. Characterization of bacterial phospholipids by electrospray ionization tandem mass spectrometry. *Anal Chem* 67:1824–1830.
46. Holland RD, Wilkes JG, Rafii F, Sutherland JB, Persons CC, Voorhees KJ, Lay, Jr JO. 1996. Rapid Identification of Intact Whole Bacteria Based on Spectral Patterns using Matrix-assisted Laser Desorption/Ionization with Time-of-flight Mass Spectrometry. *Rapid Commun Mass Spectrom* 10:1227–1232.
47. Cain TC, Lubman DM, Weber WJ, Vertes A. 1994. Differentiation of bacteria using protein profiles from matrix-assisted laser desorption/ionization time-of-flight mass spectrometry. *Rapid Commun Mass Spectrom* 8:1026–1030.

48. Krishnamurthy T, Ross PL. 1996. Rapid identification of bacteria by direct matrix-assisted laser desorption/ionization mass spectrometric analysis of whole cells. *Rapid Commun Mass Spectrom* 10:1992–1996.
49. Biemann K. 1992. Mass Spectrometry of Peptides and Proteins. *Annu Rev Biochem* 61:977–1010.
50. Elssner T, Kostrzewa M, Maier T, Kruppa G. 2011. Microorganism identification based on MALDI-TOF-MS fingerprints, p. 99–113. *In* NATO Science for Peace and Security Series A: Chemistry and Biology.
51. Karas M, Bachmann D, Bahr U, Hillenkamp F. 1987. Matrix-assisted ultraviolet laser desorption of non-volatile compounds. *Int J Mass Spectrom Ion Process* 78:53–68.
52. Tanaka K, Waki H, Ido Y, Akita S, Yoshida Y, Yoshida T, Matsuo T. 1988. Protein and polymer analyses up to  $m/z$  100 000 by laser ionization time-of-flight mass spectrometry. *Rapid Commun Mass Spectrom* 2:151–153.
53. Muddiman DC, Bakhtiar R, Hofstadler SA, Smith RD. 1997. Matrix-Assisted Laser Desorption/Ionization Mass Spectrometry. Instrumentation and Applications. *J Chem Educ* 74:1288.
54. Guilhaus M, Mlynski V, Selby D. 1997. Perfect Timing: Time-of-flight Mass Spectrometry. *Rapid Commun Mass Spectrom* 11:951–962.

55. Woo PCY, Lau SKP, Teng JLL, Tse H, Yuen K-Y. 2008. Then and now: use of 16S rDNA gene sequencing for bacterial identification and discovery of novel bacteria in clinical microbiology laboratories. *Clin Microbiol Infect* 14:908–934.
56. Ryzhov V, Fenselau C. 2001. Characterization of the protein subset desorbed by MALDI from whole bacterial cells. *Anal Chem* 73:746–750.
57. Fenselau C, Demirev PA. 2001. Characterization of intact microorganisms by MALDI mass spectrometry. *Mass Spectrom Rev* 20:157–171.
58. Patel R, Patel R, Patel R, Anhalt J, Fenselau C, Tanaka K, Karas M, Hillenkamp F, Mellmann A, Cloud J, Maier T, Keckevoet U, Ramminger I, Iwen P, Seng P, Drancourt M, Gouriet F, LaScola B, Fournier P, Rolain J, Raoult D, Cunningham S, Patel R, Branda J, Markham R, Garner C, Rychert J, Ferraro M, Dubois D, Segonds C, Prere M, Marty N, Oswald E, Pavlovic M, Konrad R, Iwobi A, Sing A, Busch U, Huber I, Cunningham S, Mainella J, Patel R, Saffert R, Cunningham S, Ihde S, Jobe K, Mandrekar J, Patel R, Alatoon A, Cunningham S, Ihde S, Mandrekar J, Patel R, Tekippe EM, Shuey S, Winkler D, Butler M, Burnham C, Lau S, Tang B, Teng J, Hsueh P, Lee T, Du S, Teng S, Liao C, Sheng W, Tang L, Schulthess B, Bloemberg G, Zbinden R, Bottger E, Hombach M, Alatoon A, Cazanave C, Cunningham S, Ihde S, Patel R, Richter S, Sercia L, Branda J, Burnham C, Bythrow M, Ferraro M, Manji R, Bythrow M, Branda J, Burnham C, Ferraro M, Garner O, Branda J, Rychert J, Burnham C, Bythrow M, Garner O, Ginocchio C, Rychert J, Burnham C, Bythrow M, Garner O, Ginocchio C, Jennemann R, Karpanoja P, Harju I, Rantakokko-Jalava K, Haanpera M, Sarkkinen H, Jamal W, Shahin M, Rotimi V, Hsu Y, Burnham C,

Schmitt B, Cunningham S, Dailey A, Gustafson D, Patel R, Barreau M, Pagnier I, Scola B La, Garner O, Mochon A, Branda J, Burnham C, Bythrow M, Ferraro M, Teng S, Chen C, Lee M, Lee T, Chien K, Teng L, Hsueh P, Balada-Llasat J, Kamboj K, Pancholi P, Mather C, Rivera S, Butler-Wu S, Theel E, Schmitt B, Hall L, Cunningham S, Walchak R, Patel R, Wengenack N, Dhiman N, Hall L, Wohlfiel S, Buckwalter S, Wengenack N, Lacroix C, Gicquel A, Sendid B, Westblade L, Jennemann R, Branda J, Bythrow M, Ferraro M, Garner O, Pence M, TeKippe EM, Wallace M, Burnham C, Hamprecht A, Christ S, Oestreicher T, Plum G, Kempf V, Gottig S, Carolis E De, Vella A, Vaccaro L, Torelli R, Posteraro P, Ricciardi W, Rosenvinge F, Dzajic E, Knudsen E, Maliq S, Andersen L, Lovig A, Mancini N, Carolis E De, Infurnari L, Vella A, Clementi N, Vaccaro L, Schulthess B, Ledermann R, Mouttet F, Zbinden A, Bloemberg G, Bottger E, Hombach M, Lau A, Drake S, Calhoun L, Henderson C, Zelazny A, Theel E, Hall L, Mandrekar J, Wengenack N, Respinis S de, Tonolla M, Pranghofer S, Petrini L, Petrini O, Bosshard P, Seng P, Abat C, Rolain J, Colson P, Lagier J, Gouriet F, Wang L, Han C, Sui W, Wang M, Lu X, Sparbier K, Schubert S, Weller U, Boogen C, Kostrzewa M, Hoyos-Mallecot Y, Cabrera-Alvargonzalez J, Miranda-Casas C, Rojo-Martin M, Liebana-Martos C, Navarro-Mari J, Alvarez-Buylla A, Picazo J, Culebras E, Jung J, Eberl T, Sparbier K, Lange C, Kostrzewa M, Schubert S, Wieser A, Sparbier K, Lange C, Jung J, Wieser A, Schubert S, Kostrzewa M, Hrabák J, Chudackova E, Walkova R, Sanchez-Juanes F, Ruiz MS, Obregon FM, Gonzalez MC, Equido SH, Serna M de F, Wang X, Zhang G, Fan Y, Yang X, Sui W, Lu X, Rossello GM, Rodriguez MG, Leonardo R de L, Domingo AO, Perez MB, Kohling H, Bittner A,

Muller K, Buer J, Becker M, Rubben H, Demarco M, Burnham C, Hartmeyer GN, Jensen AK, Bocher S, Bartels MD, Pedersen M, Clausen ME, Segawa S, Sawai S, Murata S, Nishimura M, Beppu M, Sogawa K, March Rosselló G, Munoz-Moreno M, Urries MG-L-J de, Bratos-Perez M, Leli C, Cenci E, Cardaccia A, Moretti A, D'Alo F, Pagliochini R, Tadros M, Petrich A, Gray T, Thomas L, Olma T, Iredell J, Chen S, Nonnemann B, Tvede M, Bjarnsholt T, Rodriguez-Sanchez B, Sanchez-Carrillo C, Ruiz A, Marin M, Cercenado E, Rodriguez-Creixems M, Bouza E, Chen J, Ho P, Kwan G, She K, Siu G, Cheng V, Martiny D, Debaugnies F, Gateff D, Gerard M, Aoun M, Martin D, Clerc O, Prod'hom G, Vogne C, Bizzini A, Calandra T, Greub G, Machen A, Drake T, Wang Y, Perez K, Olsen R, Musick W, Cernoch P, David J, Land G, Foster A, Jamal W, Saleem R, Rotimi V, Mencacci A, Monari C, Leli C, Merlini L, Coralís E De, Vella A, Josten M, Reif M, Szekat C, Al-Sabti N, Roemer T, Sparbier K, Gekenidis M, Studer P, Wuthrich S, Brunisholz R, Drissner D, Mutters N, Hodiamont C, Jong M de, Overmeijer H, Boogaard M van den, Visser C, Razavi M, Johnson L, Lum J, Kruppa G, Anderson N, Pearson T. 2015. MALDI-TOF MS for the diagnosis of infectious diseases. *Clin Chem* 61:100–111.

59. Mellmann A, Cloud J, Maier T, Keckevoet U, Ramminger I, Iwen P, Dunn J, Hall G, Wilson D, LaSala P, Kostrzewa M, Harmsen D. 2008. Evaluation of matrix-assisted laser desorption ionization-time-of-flight mass spectrometry in comparison to 16S rRNA gene sequencing for species identification of nonfermenting bacteria. *J Clin Microbiol* 46:1946–1954.

60. Seng P, Drancourt M, Gouriet F, La Scola B, Fournier P-E, Rolain JM, Raoult D. 2009. Ongoing revolution in bacteriology: routine identification of bacteria by matrix-assisted laser desorption ionization time-of-flight mass spectrometry. *Clin Infect Dis* 49:543–551.
61. Hathout Y, Setlow B, Fenselau C, Setlow P. 2003. Small , Acid-Soluble Proteins as Biomarkers in Mass Spectrometry Analysis of *Bacillus* Spores. *Appl Environ Microbiol* 69:1100–1107.
62. March Rosselló GA, Gutiérrez Rodríguez MP, de Lejarazu Leonardo RO, Orduña Domingo A, Bratos Pérez MA. 2014. Procedure for microbial identification based on Matrix-Assisted Laser Desorption/Ionization-Time of Flight Mass Spectrometry from screening-positive urine samples. *APMIS* 122:790–795.
63. Christner M, Rohde H, Wolters M, Sobottka I, Wegscheider K, Aepfelbacher M. 2010. Rapid identification of bacteria from positive blood culture bottles by use of matrix-assisted laser desorption-ionization time of flight mass spectrometry fingerprinting. *J Clin Microbiol* 48:1584–1591.
64. Lévesque S, Dufresne PJ, Soualhine H, Domingo MC, Bekal S, Lefebvre B, Tremblay C. 2015. A Side by Side Comparison of Bruker Biotyper and VITEK MS: Utility of MALDI-TOF MS Technology for Microorganism Identification in a Public Health Reference Laboratory. *PLoS One* 10: e0144878.
65. Deak E, Charlton CL, Bobenchik AM, Miller SA, Pollett S, McHardy IH, Wu MT, Garner OB. 2015. Comparison of the Vitek MS and Bruker Microflex LT MALDI-

- TOF MS platforms for routine identification of commonly isolated bacteria and yeast in the clinical microbiology laboratory. *Diagn Microbiol Infect Dis* 81:27–33.
66. Chen JHK, Ho PL, Kwan GSW, She KKK, Siu GKH, Cheng VCC, Yuen KY, Yam WC. 2013. Direct bacterial identification in positive blood cultures by use of two commercial matrix-assisted laser desorption ionization-time of flight mass spectrometry systems. *J Clin Microbiol* 51:1733–1739.
  67. Leli C, Cenci E, Cardaccia A, Moretti A, D'Alò F, Pagliochini R, Barcaccia M, Farinelli S, Vento S, Bistoni F, Mencacci A. 2013. Rapid identification of bacterial and fungal pathogens from positive blood cultures by MALDI-TOF MS. *Int J Med Microbiol* 303:205–209.
  68. Gray TJ, Thomas L, Olma T, Mitchell DH, Iredell JR, Chen SCA. 2014. Rapid identification of gram negative bacteria from blood culture broth using MALDI-TOF mass spectrometry. *J Vis Exp* 87:1–6.
  69. La Scola B, Raoult D. 2009. Direct identification of bacteria in positive blood culture bottles by matrix-assisted laser desorption ionisation time-of-flight mass spectrometry. *PLoS One* 4:e8041.
  70. Stevenson LG, Drake SK, Murray PR. 2010. Rapid identification of bacteria in positive blood culture broths by matrix-assisted laser desorption ionization-time of flight mass spectrometry. *J Clin Microbiol* 48:444–447.

71. Kok J, Thomas LC, Olma T, Chen SCA, Iredell JR. 2011. Identification of Bacteria in Blood Culture Broths Using Matrix-Assisted Laser Desorption-Ionization Sepsityper and Time of Flight Mass Spectrometry. *PLoS One* 8: e23285.
72. Ferreira L, Sánchez-Juanes F, González-Avila M, Cembrero-Fuciños D, Herrero-Hernández A, González-Buitrago JM, Muñoz-Bellido JL. 2010. Direct identification of urinary tract pathogens from urine samples by matrix-assisted laser desorption ionization-time of flight mass spectrometry. *J Clin Microbiol* 48:2110–2115.
73. Demarco ML, Burnham C-AD. 2014. Diafiltration MALDI-TOF mass spectrometry method for culture-independent detection and identification of pathogens directly from urine specimens. *Am J Clin Pathol* 141:204–212.
74. Pence MA, McElvania TeKippe E, Wallace MA, Burnham CAD. 2014. Comparison and optimization of two MALDI-TOF MS platforms for the identification of medically relevant yeast species. *Eur J Clin Microbiol Infect Dis* 33:1703–1712.
75. Mather CA, Rivera SF, Butler-Wu SM. 2014. Comparison of the Bruker Biotyper and Vitek MS matrix-assisted laser desorption ionization-time of flight mass spectrometry systems for identification of mycobacteria using simplified protein extraction protocols. *J Clin Microbiol* 52:130–138.
76. Zhou M, Yang Q, Kudinha T, Zhang L, Xiao M, Kong F, Zhao Y, Xu YC. 2016. Using matrix-assisted laser desorption ionization-time of flight (MALDI-TOF) complemented with selected 16S rRNA and *gyrB* genes sequencing to practically

- identify clinical important viridans group streptococci (VGS). *Front Microbiol* 7: 1328.
77. McFarland MA, Andrzejewski D, Musser SM, Callahan JH. 2014. Platform for identification of *Salmonella* serovar differentiating bacterial proteins by top-down mass spectrometry: *S. typhimurium* vs *S. heidelberg*. *Anal Chem* 86:6879-6886.
78. Gekenidis MT, Studer P, Wüthrich S, Brunisholz R, Drissner D. 2014. Beyond the matrix-assisted laser desorption ionization (MALDI) biotyping workflow: In search of microorganism-specific tryptic peptides enabling discrimination of subspecies. *Appl Environ Microbiol* 80:4234–4241.
79. Burckhardt I, Zimmermann S. 2011. Using matrix-assisted laser desorption ionization-time of flight mass spectrometry to detect carbapenem resistance within 1 to 2.5 hours. *J Clin Microbiol* 49:3321–3324.
80. Hrabák J, Walková R, Studentová V, Chudácková E, Bergerová T. 2011. Carbapenemase activity detection by matrix-assisted laser desorption ionization-time of flight mass spectrometry. *J Clin Microbiol* 49:3222–3227.
81. Sparbier K, Schubert S, Weller U, Boogen C, Kostrzewa M. 2012. Matrix-assisted laser desorption ionization-time of flight mass spectrometry-based functional assay for rapid detection of resistance against  $\beta$ -lactam antibiotics. *J Clin Microbiol* 50:927–937.
82. Hoyos-Mallecot Y, Cabrera-Alvargonzalez JJ, Miranda-Casas C, Rojo-Martín MD, Liebana-Martos C, Navarro-Marí JM. 2014. MALDI-TOF MS, a useful instrument

- for differentiating metallo- $\beta$ -lactamases in Enterobacteriaceae and *Pseudomonas* spp. *Lett Appl Microbiol* 58:325–329.
83. Sparbier K, Lange C, Jung J, Wieser A, Schubert S, Kostrzewa M. 2013. MALDI Biotyper-based rapid resistance detection by stable-isotope labeling. *J Clin Microbiol* 51:3741–3748.
84. Jung JS, Eberl T, Sparbier K, Lange C, Kostrzewa M, Schubert S, Wieser A. 2014. Rapid detection of antibiotic resistance based on mass spectrometry and stable isotopes. *Eur J Clin Microbiol Infect Dis* 33:949–955.
85. Ecker DJ, Sampath R, Massire C, Blyn LB, Hall TA, Eshoo MW, Hofstadler SA. 2008. Ibis T5000: a universal biosensor approach for microbiology. *Nat Rev Microbiol* 6:553–558.
86. Hofstadler SA, Sampath R, Blyn LB, Eshoo MW, Hall TA, Jiang Y, Drader JJ, Hannis JC, Sannes-Lowery KA, Cummins LL, Libby B, Walcott DJ, Schink A, Massire C, Ranken R, Gutierrez J, Manalili S, Ivy C, Melton R, Levene H, Barrett-Wilt G, Li F, Zapp V, White N, Samant V, McNeil JA, Knize D, Robbins D, Rudnick K, Desai A, Moradi E, Ecker DJ. 2005. TIGER: The universal biosensor. *Int J Mass Spectrom* 242:23–41.
87. Ecker DJ, Sampath R, Li H, Massire C, Matthews HE, Toleno D, Hall TA, Blyn LB, Eshoo MW, Ranken R, Hofstadler SA, Tang Y-W. 2010. New technology for rapid molecular diagnosis of bloodstream infections. *Expert Rev Mol Diagn* 10:399–415.

88. Kaleta EJ, Clark AE, Cherkaoui A, Wysocki VH, Ingram EL, Schrenzel J, Wolk DM. 2011. Comparative analysis of PCR - Electrospray ionization/mass spectrometry (MS) and MALDI-TOF/MS for the identification of bacteria and yeast from positive blood culture bottles. *Clin Chem* 57:1057–1067.
89. Silhavy TJ, Kahne D, Walker S. 2010. The bacterial cell envelope. *Cold Spring Harb Perspect Biol* 2:1-16.
90. Whitfield C, Trent MS. 2014. Biosynthesis and Export of Bacterial Lipopolysaccharides. *Annu Rev Biochem* 83:99-128.
91. Heller DN, Cotter RJ, Fenselau C, Uy OM. 1987. Profiling of Bacteria by Fast Atom Bombardment Mass Spectrometry. *Anal Chem* 59:2806–2809.
92. van Meer G, Voelker DR, Feigenson GW. 2008. Membrane lipids: where they are and how they behave. *Nat Rev Mol Cell Biol* 9:112–124.
93. van Meer G, de Kroon AIPM. 2011. Lipid map of the mammalian cell. *J Cell Sci* 124:5–8.
94. Voorhees KJ, Jensen KR, McAlpin CR, Rees JC, Cody R, Ubukata M, Cox CR. 2013. Modified MALDI MS fatty acid profiling for bacterial identification. *J Mass Spectrom* 48:850–855.
95. Cody RB, McAlpin CR, Cox CR, Jensen KR, Voorhees KJ. 2015. Identification of bacteria by fatty acid profiling with direct analysis in real time mass spectrometry. *Rapid Commun Mass Spectrom* 29:2007–2012.

96. Ishida Y, Kitagawa K, Nakayama A, Ohtani H. 2005. On-Probe Sample Pretreatment for Direct Analysis of Lipids in Gram-Positive Bacterial Cells by Matrix-Assisted Laser Desorption Ionization Mass Spectrometry. *Appl Environ Microbiol* 71:7539–7541.
97. Ishida Y, Madonna AJ, Rees JC, Meetani MA, Voorhees KJ. 2002. Rapid analysis of intact phospholipids from whole bacterial cells by matrix-assisted laser desorption/ionization mass spectrometry combined with on-probe sample pretreatment. *Rapid Commun Mass Spectrom* 16:1877–1882.
98. Hamid AM, Jarmusch AK, Pirro V, Pincus DH, Clay BG, Gervasi G, Cooks RG. 2014. Rapid discrimination of bacteria by paper spray mass spectrometry. *Anal Chem* 86:7500–7507.
99. Percy MG, Gründling A. 2014. Lipoteichoic Acid Synthesis and Function in Gram-Positive Bacteria. *Annu Rev Microbiol* 68:81–100.
100. Morath S, von Aulock S, Hartung T. 2005. Structure/function relationships of lipoteichoic acids. *J Endotoxin Res* 11:348–356.
101. Medzhitov R, Preston-Hurlburt P, Janeway Jr CA. 1997. A human homologue of the *Drosophila* Toll protein signals activation of adaptive immunity. *Nature* 388:394–397.
102. Van Amersfoort ES, Van Berkel TJC, Kuiper J. 2003. Receptors, Mediators, and Mechanisms Involved in Bacterial Sepsis and Septic Shock. *Clin Microbiol Rev* 16:379–414.

103. Raetz CR, Whitfield C. 2002. Lipopolysaccharide endotoxins. *Annu Rev Biochem* 71:635–700.
104. Caroff M, Karibian D. 2003. Structure of bacterial lipopolysaccharides. *Carbohydr Res* 338:2431–2447.
105. Needham BD, Trent MS. 2013. Fortifying the barrier: the impact of lipid A remodelling on bacterial pathogenesis. *Nat Rev Microbiol* 11:467–481.
106. Trent MS, Stead CM, Tran AX, Hankins JV. 2006. Diversity of endotoxin and its impact on pathogenesis. *J Endotoxin Res* 12:205–223.
107. Raetz CRH, Reynolds CM, Trent MS, Bishop RE. 2007. Lipid A modification systems in Gram-negative bacteria. *Annu Rev Biochem* 76:295–329.
108. Miller SI, Ernst RK, Bader MW. 2005. LPS, TLR4 and infectious disease diversity. *Nat Rev Microbiol* 3:36–46.
109. Parker JH, Smith GA, Fredrickson HL, Robie Vestal J, White DC. 1982. Sensitive Assay, Based on Hydroxy Fatty Acids from Lipopolysaccharide Lipid A, for Gram-Negative Bacteria in Sediments. *Appl Environ Microbiol* 44:1170–1177.
110. Uhlig S, Negård M, Heldal KK, Straumfors A, Madsø L, Bakke B, Eduard W. 2016. Profiling of 3-hydroxy fatty acids as environmental markers of endotoxin using liquid chromatography coupled to tandem mass spectrometry. *J Chromatogr A* 1434:119–126.

111. Larrouy-Maumus G, Clements A, Filloux A, McCarthy RR, Mostowy S. 2016. Direct detection of lipid A on intact Gram-negative bacteria by MALDI-TOF mass spectrometry. *J Microbiol Methods* 120:68–71.
112. Bolt F, Cameron SJS, Karancsi T, Simon D, Schaffer R, Rickards T, Hardiman K, Burke A, Bodai Z, Perdonés-Montero A, Rebec M, Balog J, Takats Z. 2016. Automated High-Throughput Identification and Characterisation of Clinically Important Bacteria and Fungi using Rapid Evaporative Ionisation Mass Spectrometry (REIMS). *Anal Chem* 88:9419-9426.
113. Strittmatter N, Rebec M, Jones EA, Golf O, Abdolrasouli A, Balog J, Behrends V, Veselkov KA, Takats Z. 2014. Characterization and identification of clinically relevant microorganisms using rapid evaporative ionization mass spectrometry. *Anal Chem* 86:6555–6562.
114. Leung LM, Fondrie WE, Doi Y, Johnson JK, Strickland DK, Goodlett DR, Ernst RK. 2017. Identification of the ESKAPE pathogens by mass spectrometric analysis of microbial membrane glycolipids. *Sci Rep*, in press.
115. Leung LM, Cooper VS, Rasko DA, Guo Q, Pacey MP, McElheny CL, Mettus RT, Yoon SH, Goodlett DR, Ernst RK. 2017. Structural modification of lipopolysaccharide in colistin-resistant, KPC-producing *Klebsiella pneumoniae*. *J Antimicrob Chemother*, in press.

116. Yoon SH, Huang Y, Edgar JS, Ting YS, Heron SR, Kao Y, Li Y, Masselon CD, Ernst RK, Goodlett DR. 2012. Surface acoustic wave nebulization facilitating lipid mass spectrometric analysis. *Anal Chem* 84:6530–6537.
117. Yoon SH, Liang T, Schneider T, Oyler BL, Chandler CE, Ernst RK, Yen GS, Huang Y, Nilsson E, Goodlett DR. 2016. Rapid lipid A structure determination via surface acoustic wave nebulization and hierarchical tandem mass spectrometry algorithm. *Rapid Commun Mass Spectrom* 30:2555–2560.
118. Crittenden CM, Akin LD, Morrison LJ, Trent MS, Brodbelt JS. 2016. Characterization of Lipid A Variants by Energy-Resolved Mass Spectrometry: Impact of Acyl Chains. *J Am Soc Mass Spectrom* 28:1118-1126.
119. O'Brien JP, Needham BD, Henderson JC, Nowicki EM, Trent MS, Brodbelt JS. 2014. 93 nm Ultraviolet Photodissociation Mass Spectrometry for the Structural Elucidation of Lipid A Compounds in Complex Mixtures. *Chem Sci* 5:4291-4301.
120. Morens DM, Fauci AS. 2013. Emerging Infectious Diseases: Threats to Human Health and Global Stability. *PLoS Pathog* 9:e1003467.
121. Silhavy TJ, Kahne D, Walker S. 2010. The bacterial cell envelope. *Cold Spring Harb Perspect Biol* 2:1-16.
122. Anhalt J, Fenselau C. 1975. Identification of bacteria using mass spectrometry. *Anal Chem* 500:219–225.
123. Percy MG, Gründling A. 2014. Lipoteichoic Acid Synthesis and Function in Gram-Positive Bacteria. *Annu Rev Microbiol* 68:81–100.

124. Boucher HW, Talbot GH, Bradley JS, Edwards JE, Gilbert D, Rice LB, Scheld M, Spellberg B, Bartlett J. 2009. Bad bugs, no drugs: no ESKAPE! An update from the Infectious Diseases Society of America. *Clin Infect Dis* 48:1–12.
125. Andersson DI, Hughes D, Kubicek-Sutherland JZ. 2016. Mechanisms and consequences of bacterial resistance to antimicrobial peptides. *Drug Resist Updat* 26:43–57.
126. Helander IM, Kato Y, Kilpelainen I, Kostianen R, Lindner B, Nummila K, Sugiyama T, Yokochi T. 1996. Characterization of Lipopolysaccharides of Polymyxin-Resistant and Polymyxin-Sensitive *Klebsiella pneumoniae* O3. *Eur J Biochem* 237:272–278.
127. Pelletier MR, Casella LG, Jones JW, Adams MD, Zurawski DV, Hazlett KRO, Doi Y, Ernst RK. 2013. Unique structural modifications are present in the lipopolysaccharide from colistin-resistant strains of *Acinetobacter baumannii*. *Antimicrob Agents Chemother* 57:4831–4840.
128. Ernst RK, Yi EC, Guo L, Lim KB, Burns JL, Hackett M, Miller SI. 1999. Specific lipopolysaccharide found in cystic fibrosis airway *Pseudomonas aeruginosa*. *Science* 286:1561–1565.
129. El Hamidi A, Tirsoaga A, Novikov A, Hussein A, Caroff M. 2005. Microextraction of bacterial lipid A: easy and rapid method for mass spectrometric characterization. *J Lipid Res* 46:1773–1778.

130. Scott AJ, Flinders B, Cappell J, Liang T, Pelc RS, Tran B, Kilgour DPA, Heeren RMA, Goodlett DR, Ernst RK. 2016. Norharmane matrix enhances detection of endotoxin by MALDI-MS for simultaneous profiling of pathogen, host and vector systems. *Pathog Dis* 74:ftw097.
131. Stein SE, Scott DR. 1994. Optimization and testing of mass spectral library search algorithms for compound identification. *J Am Soc Mass Spectrom* 5:859–866.
132. Velkov T, Soon RL, Chong PL, Huang JX, Cooper MA, Azad MAK, Baker MA, Thompson PE, Roberts K, Nation RL, Clements A, Strugnell RA, Li J. 2013. Molecular basis for the increased polymyxin susceptibility of *Klebsiella pneumoniae* strains with under-acylated lipid A. *Innate Immun* 19:265–277.
133. Clinical and Laboratory Standards Institute. Performance standards for antimicrobial susceptibility testing - twenty-fifth informational supplement. CLSI document M100-S25. Wayne, PA: Clinical and Laboratory Standards Institute ; 2015.
134. Llobet E, Campos MA, Giménez P, Moranta D, Bengoechea JA. 2011. Analysis of the networks controlling the antimicrobial-peptide-dependent induction of *Klebsiella pneumoniae* virulence factors. *Infect Immun* 79:3718–3732.
135. Dowd SE, Sun Y, Secor PR, Rhoads DD, Wolcott BM, James GA, Wolcott RD. 2008. Survey of bacterial diversity in chronic wounds using Pyrosequencing, DGGE, and full ribosome shotgun sequencing. *BMC Microbiol* 8:43.

136. Bizzini A, Durussel C, Bille J, Greub G, Prod'hom G. 2010. Performance of Matrix-Assisted Laser Desorption Ionization–Time of Flight Mass Spectrometry for Identification of Bacterial Strains Routinely Isolated in a Clinical Microbiology Laboratory. *J Clin Microbiol* 48:1549–1554.
137. Patel R. 2013. Matrix-assisted laser desorption ionization-time of flight mass spectrometry in clinical microbiology. *Clin Infect Dis* 57:564–572.
138. Singhal N, Kumar M, Kanaujia PK, Viridi JS. 2015. MALDI-TOF mass spectrometry: An emerging technology for microbial identification and diagnosis. *Front Microbiol* 6:1–16.
139. Gibb, S, Strimmer, K. 2012. MALDIquant: a versatile R package for the analysis of mass spectrometry data. *Bioinformatics*, 28:2270–2271.
140. Savitzky A, Golay MJE. 1964. Smoothing and Differentiation of Data by Simplified Least Squares Procedures. *Anal Chem* 36:1627–1639.
141. Ryan CG, Clayton E, Griffin WL, Sie SH, Cousens DR. 1988. SNIP, a statistics-sensitive background treatment for the quantitative analysis of PIXE spectra in geoscience applications. *Nucl Inst Methods Phys Res B* 34:396–402.
142. Suzuki R, Shimodaira H. 2006. Pvclust: An R package for assessing the uncertainty in hierarchical clustering. *Bioinformatics* 22:1540–1542.
143. Castanheira M, Farrell SE, Krause KM, Jones RN, Sader HS. 2014. Contemporary diversity of  $\beta$ -lactamases among Enterobacteriaceae in the nine U.S. census

- regions and ceftazidime-avibactam activity tested against isolates producing the most prevalent  $\beta$ -lactamase groups. *Antimicrob Agents Chemother* 58:833–838.
144. van Duin D, Doi Y. 2016. The global epidemiology of carbapenemase-producing *Enterobacteriaceae*. *Virulence* 0:1–10.
145. Perez F, El Chakhtoura NG, Papp-Wallace KM, Wilson BM, Bonomo RA. 2016. Treatment options for infections caused by carbapenem-resistant *Enterobacteriaceae* : can we apply “precision medicine” to antimicrobial chemotherapy?. *Expert Opin Pharmacother* 17:761–781.
146. Velkov T, Thompson PE, Nation RL, Li J. 2010. Structure-activity relationships of polymyxin antibiotics. *J Med Chem* 53:1898-1916.
147. Olaitan AO, Morand S, Rolain J-M. 2014. Mechanisms of polymyxin resistance: acquired and intrinsic resistance in bacteria. *Front Microbiol* 5:643.
148. Clements A, Tull D, Jenney AW, Farn JL, Kim SH, Bishop RE, McPhee JB, Hancock REW, Hartland EL, Pearse MJ, Wijburg OLC, Jackson DC, McConville MJ, Strugnell RA. 2007. Secondary acylation of *Klebsiella pneumoniae* lipopolysaccharide contributes to sensitivity to antibacterial peptides. *J Biol Chem* 282:15569–15577.
149. Llobet E, Martínez-Moliner V, Moranta D, Dahlström KM, Regueiro V, Tomás A, Cano V, Pérez-Gutiérrez C, Frank CG, Fernández-Carrasco H, Insua JL, Salminen TA, Garmendia J, Bengoechea JA. 2015. Deciphering tissue-induced *Klebsiella pneumoniae* lipid A structure. *Proc Natl Acad Sci* 112:E6369–E6378.

150. Bogdanovich T, Adams-Haduch JM, Tian GB, Nguyen MH, Kwak EJ, Muto CA, Doi Y. 2011. Colistin-resistant, *Klebsiella pneumoniae* Carbapenemase (KPC)-producing *Klebsiella pneumoniae* belonging to the international epidemic clone ST258. Clin Infect Dis 53:373–376.
151. Giani T, Arena F, Vaggelli G, Conte V, Chiarelli A, De Angelis LH, Fornaini R, Grazzini M, Niccolini F, Pecile P, Rossolini GM. 2015. Large nosocomial outbreak of colistin-resistant, carbapenemase-producing *Klebsiella pneumoniae* traced to clonal expansion of an *mgrB* deletion mutant. J Clin Microbiol 53:3341–3344.
152. Olaitan AO, Diene SM, Kempf M, Berrazeg M, Bakour S, Gupta SK, Thongmalayvong B, Akkhavong K, Somphavong S, Paboriboune P, Chaisiri K, Komalamisra C, Adelowo OO, Fagade OE, Banjo OA, Oke AJ, Adler A, Assous MV, Morand S, Raoult D, Rolain JM. 2014. Worldwide emergence of colistin resistance in *Klebsiella pneumoniae* from healthy humans and patients in Lao PDR, Thailand, Israel, Nigeria and France owing to inactivation of the PhoP/PhoQ regulator *mgrB*: An epidemiological and molecular study. Int J Antimicrob Agents 44:500–507.
153. Poirel L, Jayol A, Bontron S, Villegas MV, Ozdamar M, Türkoglu S, Nordmann P. 2015. The *mgrB* gene as a key target for acquired resistance to colistin in *Klebsiella pneumoniae*. J Antimicrob Chemother 70:75–80.

154. Wright MS, Suzuki Y, Jones MB, Marshall SH, Rudin SD, Van Duin D, Kaye K, Jacobs MR, Bonomo RA, Adamsa MD. 2015. Genomic and transcriptomic analyses of colistin-resistant clinical isolates of *Klebsiella pneumoniae* reveal multiple pathways of resistance. *Antimicrob Agents Chemother* 59:536–543.
155. Cannatelli A, Di Pilato V, Giani T, Arena F, Ambretti S, Gaibani P, D’Andrea MM, Rossolinia GM. 2014. *In vivo* evolution to Colistin resistance by PmrB sensor kinase mutation in KPC-producing *Klebsiella pneumoniae* is associated with low-dosage colistin treatment. *Antimicrob Agents Chemother* 58:4399–4403.
156. European Committee on Antimicrobial Susceptibility Testing. 2016. Recommendations for MIC determination of colistin (polymyxin E) As recommended by the joint CLSI-EUCAST Polymyxin Breakpoints Working Group 2016.
157. Cannatelli A, Giani T, D’Andrea MM, Pilato V Di, Arena F, Conte V, Tryfinopoulou K, Vatopoulos A, Rossolini GM. 2014. MgrB inactivation is a common mechanism of colistin resistance in KPC-producing *Klebsiella pneumoniae* of clinical origin. *Antimicrob Agents Chemother* 58:5696–5703.
158. McKenna A, Hanna M, Banks E, Sivachenko A, Cibulskis K, Kernysky A, Garimella K, Altshuler D, Gabriel S, Daly M, DePristo MA. 2010. The genome analysis toolkit: A MapReduce framework for analyzing next-generation DNA sequencing data. *Genome Res* 20:1297–1303.

159. Mathers AJ, Peirano G, Pitout JD. 2015. The role of epidemic resistance plasmids and international high-risk clones in the spread of multidrug-resistant Enterobacteriaceae. *Clin Microbiol Rev* 28:565–591.
160. Giakkoupi P, Papagiannitsis CC, Miriagou V, Pappa O, Polemis M, Tryfinopoulou K, Tzouvelekis LS, Vatopoulos AC. 2011. An update of the evolving epidemic of blaKPC-2-carrying *Klebsiella pneumoniae* in Greece (2009-10). *J Antimicrob Chemother* 66:1510–1513.
161. Choi MJ, Ko KS. 2014. Mutant prevention concentrations of colistin for *Acinetobacter baumannii*, *Pseudomonas aeruginosa* and *Klebsiella pneumoniae* clinical isolates. *J Antimicrob Chemother* 69:275–277.
162. Lee JY, Ko KS. 2014. Mutations and expression of PmrAB and PhoPQ related with colistin resistance in *Pseudomonas aeruginosa* clinical isolates. *Diagn Microbiol Infect Dis* 78:271–276.
163. Kidd TJ, Mills G, Sá-Pessoa J, Dumigan A, Frank CG, Insua JL, Ingram R, Hogley L, Bengoechea JA. 2017. A *Klebsiella pneumoniae* antibiotic resistance mechanism that subdues host defences and promotes virulence. *EMBO Mol Med* 8:569–585.
164. Cannatelli A, Santos-Lopez A, Giani T, Gonzalez-Zorn B, Rossolini GM. 2015. Polymyxin resistance caused by *mgrB* inactivation is not associated with significant biological cost in *Klebsiella pneumoniae*. *Antimicrob Agents Chemother* 59:2898–2900.

165. Park YK, Choi JY, Shin D, Ko KS. 2011. Correlation between overexpression and amino acid substitution of the PmrAB locus and colistin resistance in *Acinetobacter baumannii*. *Int J Antimicrob Agents* 37:525–530.
166. Li J, Rayner CR, Nation RL, Owen RJ, Spelman D, Tan KE, Liolios L. 2006. Heteroresistance to Colistin in Multidrug-Resistant *Acinetobacter baumannii*. *Antimicrob Agents Chemother* 50:2946–2950.
167. Hermes DM, Pormann Pitt C, Lutz L, Teixeira AB, Ribeiro VB, Netto B, Martins AF, Zavascki AP, Barth AL. 2013. Evaluation of heteroresistance to polymyxin B among carbapenem-susceptible and-resistant *Pseudomonas aeruginosa*. *J Med Microbiol* 62:1184–1189.
168. Liu YY, Wang Y, Walsh TR, Yi LX, Zhang R, Spencer J, Doi Y, Tian G, Dong B, Huang X, Yu LF, Gu D, Ren H, Chen X, Lv L, He D, Zhou H, Liang Z, Liu JH, Shen J. 2016. Emergence of plasmid-mediated colistin resistance mechanism MCR-1 in animals and human beings in China: A microbiological and molecular biological study. *Lancet Infect Dis* 16:161–168.
169. Liu Y-Y, Chandler CE, Leung LM, McElheny CL, Mettus RT, Shanks RMQ, Liu J-H, Goodlett DR, Ernst RK, Doi Y. 2017. Structural Modification of Lipopolysaccharide Conferred by *mcr-1* in Gram-Negative ESKAPE Pathogens. *Antimicrob Agents Chemother* AAC.00580-17.
170. World Health Organization. 2017. Global Priority List of Antibiotic-Resistant Bacteria To Guide Research, Discovery, and Development of New Antibiotics.

171. Nikolaidis I, Favini-Stabile S, Dessen A. 2014. Resistance to antibiotics targeted to the bacterial cell wall. *Protein Sci* 23:243-259.
172. Osei Sekyere J, Govinden U, Bester LA, Essack SY. 2016. Colistin and tigecycline resistance in carbapenemase-producing Gram-negative bacteria: emerging resistance mechanisms and detection methods. *J Appl Microbiol* 121:601–617.
173. Hindler JA, Humphries RM. 2013. Colistin MIC Variability by Method for Contemporary Clinical Isolates of Multidrug-Resistant Gram-Negative Bacilli. *J Clin Microbiol* 51:1678-1684.
174. Dafopoulou K, Zarkotou O, Dimitroulia E, Hadjichristodoulou C, Gennimata V, Pournaras S, Tsakris A. 2015. Comparative evaluation of colistin susceptibility testing methods among carbapenem-nonsusceptible *Klebsiella pneumoniae* and *Acinetobacter baumannii* clinical isolates. *Antimicrob Agents Chemother* 59:4625–4630.
175. Miller AK, Brannon MK, Stevens L, Krogh Johansen H, Selgrade SE, Miller SI, Høiby N, Moskowitz SM. 2011. PhoQ Mutations Promote Lipid A Modification and Polymyxin Resistance of *Pseudomonas aeruginosa* Found in Colistin-Treated Cystic Fibrosis Patients. *Antimicrob Agents Chemother* 55:5761–5769.
176. Toh BEW, Paterson DL, Kamolvit W, Zowawi H, Kvaskoff D, Sidjabat H, Wailan A, Peleg AY, Huber CA. 2015. Species identification within *Acinetobacter calcoaceticus-baumannii* complex using MALDI-TOF MS. *J Microbiol Methods* 118:128–132.

177. Hsueh PR, Kuo LC, Chang TC, Lee TF, Teng SH, Chuang YC, Teng LJ, Sheng WH. 2014. Evaluation of the Bruker Biotyper matrix-assisted laser desorption ionization-time of flight mass spectrometry system for identification of blood isolates of *Acinetobacter* species. *J Clin Microbiol* 52:3095–3100.
178. Sousa C, Botelho J, Silva L, Grosso F, Nemeč A, Lopes J, Peixe L. 2014. MALDI-TOF MS and chemometric based identification of the *Acinetobacter calcoaceticus-Acinetobacter baumannii* complex species. *Int J Med Microbiol* 304:669–677.
179. Espinal P, Seifert H, Dijkshoorn L, Vila J, Roca I. 2012. Rapid and accurate identification of genomic species from the *Acinetobacter baumannii* (Ab) group by MALDI-TOF MS. *Clin Microbiol Infect* 18:1097–1103.
180. Wisplinghoff H, Paulus T, Lugenheim M, Stefanik D, Higgins PG, Edmond MB, Wenzel RP, Seifert H. 2012. Nosocomial bloodstream infections due to *Acinetobacter baumannii*, *Acinetobacter pittii* and *Acinetobacter nosocomialis* in the United States. *J Infect* 64:282–290.
181. Schleicher X, Higgins PG, Wisplinghoff H, Körber-Irrgang B, Kresken M, Seifert H. 2013. Molecular epidemiology of *Acinetobacter baumannii* and *Acinetobacter nosocomialis* in Germany over a 5-year period (2005-2009). *Clin Microbiol Infect* 19:737–742.
182. Wang X, Chen T, Yu R, Lü X, Zong Z. 2013. *Acinetobacter pittii* and *Acinetobacter nosocomialis* among clinical isolates of the *Acinetobacter*

- calcoaceticus-baumannii* complex in Sichuan, China. *Diagn Microbiol Infect Dis* 76:392–395.
183. Chuang YC, Sheng WH, Lauderdale TL, Li SY, Wang JT, Chen YC, Chang SC. 2014. Molecular epidemiology, antimicrobial susceptibility and carbapenemase resistance determinants among *Acinetobacter baumannii* clinical isolates in Taiwan. *J Microbiol Immunol Infect* 47:324–332.
184. Chusri S, Chongsuvivatwong V, Rivera JI, Silpapojakul K, Singkhamanan K, McNeil E, Doi Y. 2014. Clinical outcomes of hospital-acquired infection with *Acinetobacter nosocomialis* and *Acinetobacter pittii*. *Antimicrob Agents Chemother* 58:4172–4179.
185. Bader MW, Sanowar S, Daley ME, Schneider AR, Cho U, Xu W, Klevit RE, Le Moual H, Miller SI. 2005. Recognition of Antimicrobial Peptides by a Bacterial Sensor Kinase. *Cell* 122:461–472.
186. Prost LR, Daley ME, Bader MW, Klevit RE, Miller SI. 2008. The PhoQ histidine kinases of *Salmonella* and *Pseudomonas* spp. are structurally and functionally different: Evidence that pH and antimicrobial peptide sensing contribute to mammalian pathogenesis. *Mol Microbiol* 69:503–519.
187. Cheng YH, Lin TL, Lin YT, Wang JT. 2016. Amino acid substitutions of CrrB responsible for resistance to colistin through CrrC in *Klebsiella pneumoniae*. *Antimicrob Agents Chemother* 60:3709–3716.

188. Falagas ME, Kasiakou SK. 2005. Colistin: the revival of polymyxins for the management of multidrug-resistant gram-negative bacterial infections. *Clin Infect Dis* 40:1333–1341.
189. Poirel L, Jayol A, Nordmann P. 2017. Polymyxins: Antibacterial activity, susceptibility testing and resistance mechanisms encoded by plasmid or chromosomes. *Clin Microbiol Rev* 30:557–596.
190. Moskowitz SM, Ernst RK, Miller SI. 2004. PmrAB, a Two-Component Regulatory System of *Pseudomonas aeruginosa* That Modulates Resistance to Cationic Antimicrobial Peptides and Addition of Aminoarabinose to Lipid A. *J Bacteriol* 186:575–579.
191. Beceiro A, Llobet E, Aranda J, Bengoechea JA, Doumith M, Hornsey M, Dhanji H, Chart H, Bou G, Livermore DM, Woodford N. 2011. Phosphoethanolamine Modification of Lipid A in Colistin-Resistant Variants of *Acinetobacter baumannii* Mediated by the *pmrAB* Two-Component Regulatory System. *Antimicrob Agents Chemother* 55:3370–3379.
192. Liu YY, Wang Y, Walsh TR, Yi LX, Zhang R, Spencer J, Doi Y, Tian G, Dong B, Huang X, Yu LF, Gu D, Ren H, Chen X, Lv L, He D, Zhou H, Liang Z, Liu JH, Shen J. 2016. Emergence of plasmid-mediated colistin resistance mechanism MCR-1 in animals and human beings in China: A microbiological and molecular biological study. *Lancet Infect Dis* 16:161-168.

193. Schwarz S, Johnson AP. 2016. Transferable resistance to colistin: A new but old threat. *J Antimicrob Chemother* 71:2066–2070.
194. Gu D, Huang Y, Ma J, Zhou H, Fang Y, Cai J, Hu Y, Zhang R. 2016. Detection of Colistin Resistance Gene *mcr-1* in Hypervirulent *Klebsiella pneumoniae* and *Escherichia coli* Isolates from an Infant with Diarrhea in China. *Antimicrob Agents Chemother* 60:5099–5100.
195. Rolain JM, Kempf M, Leangapichart T, Chabou S, Olaitan AO, Le Page S, Morand S, Raoult D. 2016. Plasmid-mediated *mcr-1* gene in colistin-resistant clinical isolates of *Klebsiella pneumoniae* in France and Laos. *Antimicrob Agents Chemother* 60:6994-6995.
196. Bishop RE, Gibbons HS, Guina T, Trent MS, Miller SI, Raetz CRH. 2000. Transfer of palmitate from phospholipids to lipid A in outer membranes of Gram-negative bacteria. *EMBO J* 19:5071–5080.
197. MacArthur I, Jones JW, Goodlett DR, Ernst RK, Preston A. 2011. Role of *pagL* and *lpxO* in *Bordetella bronchiseptica* lipid A biosynthesis. *J Bacteriol* 193:4726–4735.
198. Ernst RK, Adams KN, Moskowitz SM, Kraig GM, Kawasaki K, Stead CM, Trent MS, Miller SI. 2006. The *Pseudomonas aeruginosa* Lipid A Deacylase: Selection for Expression and Loss within the Cystic Fibrosis Airway. *J Bacteriol* 188:191–201.

199. Paterson DL, Harris PNA. 2016. Colistin resistance: A major breach in our last line of defence. *Lancet Infect Dis* 16:132-133.
200. Monaco M, Giani T, Raffone M, Arena F, Garcia-Fernandez A, Pollini S, Grundmann H, Pantosti A, Rossolini GM, Rossolini GM. 2014. Colistin resistance superimposed to endemic carbapenem-resistant *Klebsiella pneumoniae*: A rapidly evolving problem in Italy, November 2013 to April 2014. *Eurosurveillance* 19:14-18.
201. Xavier B, Lammens C, Ruhel R, Kumar-Singh S, Butaye P, Goossens H, Malhotra-Kumar S. 2016. Identification of a novel plasmid-mediated colistin-resistance gene, *mcr-2*, in *Escherichia coli*, Belgium, June 2016. *Eurosurveillance* 21:6–11.
202. Poirel L, Kieffer N, Brink A, Coetze J, Jayol A, Nordmann P. 2016. Genetic features of MCR-1-producing colistin-resistant *Escherichia coli* isolates in South Africa. *Antimicrob Agents Chemother* 60:4394–4397.
203. Bergen PJ, Landersdorfer CB, Lee HJ, Li J, Nation RL. 2012. “Old” antibiotics for emerging multidrug-resistant bacteria. *Curr Opin Infect Dis* 25:626–633.
204. Shaffer SA, Harvey MD, Goodlett DR, Ernst RK. 2007. Structural heterogeneity and environmentally regulated remodeling of *Francisella tularensis* subspecies *novicida* lipid A characterized by tandem mass spectrometry. *J Am Soc Mass Spectrom* 18:1080–1092.

205. Dixon DR, Darveau RP. 2005. Lipopolysaccharide Heterogeneity: Innate Host Responses to Bacterial Modification of Lipid A Structure. *J Dent Res* 84:584–595.
206. Centers for Disease Control and Prevention. 2013. National Vital Statistics Reports Deaths : Final Data for 2010 (Volume 61, Issue 4). Washington, DC: U.S. Government Printing Office.
207. Angus DC, van der Poll T. 2013. Severe sepsis and septic shock. *N Engl J Med* 369:840–851.
208. Russell JA. 2006. Management of Sepsis. *N Engl J Med* 355:1699–1713.
209. Kumar A, Roberts D, Wood KE, Light B, Parrillo JE, Sharma S, Suppes R, Feinstein D, Zanotti S, Taiberg L, Gurka D, Kumar A, Cheang M. 2006. Duration of hypotension before initiation of effective antimicrobial therapy is the critical determinant of survival in human septic shock. *Crit Care Med* 34:1589–1596.
210. Flores-Mireles AL, Walker JN, Caparon M, Hultgren SJ. 2015. Urinary tract infections: epidemiology, mechanisms of infection and treatment options. *Nat Rev Microbiol* 13:269–284.
211. Singh A, Del Poeta M. 2016. Sphingolipidomics: An Important Mechanistic Tool for Studying Fungal Pathogens. *Front Microbiol* 7:501.
212. Bowman SM, Free SJ. 2006. The structure and synthesis of the fungal cell wall. *Bioessays* 28:799–808.

213. Liang T, Lee YI, Leung LM, Yoon SH, Scott AJ, Ernst RK, Goodlett DR. Ultra-rapid Identification of Bacteria by MALDI-TOF MS. Poster session presented at: The 65<sup>th</sup> ASMS Conference on Mass Spectrometry and Allied Topics; 2017 Jun 4-8; Indianapolis, IN.
214. Nonami H, Tanaka K, Fukuyama Y, Erra-Balsells R. 1998. beta-Carboline alkaloids as matrices for UV-matrix-assisted laser desorption/ionization time-of-flight mass spectrometry in positive and negative ion modes. Analysis of proteins of high molecular mass, and of cyclic and acyclic oligosaccharides. *Rapid Commun Mass Spectrom* 12:285–296.
215. Pesci EC, Milbank JBJ, Pearson JP, McKnight S, Kende AS, Greenberg EP, Iglewski BH. 1999. Quinolone signaling in the cell-to-cell communication system of *Pseudomonas aeruginosa*. 96:11229–11234.
216. Evason DJ, Claydon MA, Gordon DB. 2000. Effects of ion mode and matrix additives in the identification of bacteria by intact cell mass spectrometry. *Rapid Commun Mass Spectrom* 14:669–672.
217. Yoon SH, Oyler BL, Leung LM, Liang T, Lee YI, Ernst RK, Goodlett DR. Molecular structural analysis of the Gram-positive bacterial membrane - *Enterococcus faecium* and *Staphylococcus aureus*. Poster session presented at: The 65<sup>th</sup> ASMS Conference on Mass Spectrometry and Allied Topics; 2017 Jun 4-8; Indianapolis, IN.

218. Gutberlet T, Dietrich U, Bradaczek H, Pohlentz G, Leopold K, Fischer W. 2000. Cardiolipin, alpha-D-glucopyranosyl, and L-lysylcardiolipin from Gram-positive bacteria: FAB MS, monofilm and X-ray powder diffraction studies. *Biochim Biophys Acta* 1463:307–322.
219. Tsai M, Ohniwa RL, Kato Y, Takeshita SL, Ohta T, Saito S, Hayashi H, Morikawa K. 2011. *Staphylococcus aureus* requires cardiolipin for survival under conditions of high salinity. *BMC Microbiol* 11:13.
220. Ting YS, Shaffer SA, Jones JW, Ng WV, Ernst RK, Goodlett DR. 2011. Automated lipid A structure assignment from hierarchical tandem mass spectrometry data. *J Am Soc Mass Spectrom* 22:856–866.
221. Wilson MC, Liang T, Yoon SH, Leung LM, Ernst RK, Goodlett DR. A Cartesian Product Approach To Lipid A Structure Identification. Poster session presented at: The 63<sup>rd</sup> ASMS Conference on Mass Spectrometry and Allied Topics; 2015 May 31-Jun 4; St. Louis, MO.